INTEGRATING BIOMECHANICS, ECOMORPHOLOGY, AND ECOTOXICOLOGY TO CHARACTERIZE THE ROLES OF COASTAL SHARKS FROM SEPARATE ECOLOGICAL NICHES

A Dissertation

by

JOSHUA ALEXANDER CULLEN

Submitted to the Office of Graduate and Professional Studies of
Texas A&M University
in partial fulfillment of the requirements for the degree of

DOCTOR OF PHILOSOPHY

Chair of Committee,	Christopher D. Marshall
Co-Chair of Committee,	David N. Hala
Committee Members,	Jay R. Rooker
	R.J. David Wells
	Kevin W. Conway
Head of Department,	David Caldwell

August 2019

Major Subject: Wildlife and Fisheries Sciences

ABSTRACT

Predators within aquatic environments hold important functional roles that impact the structure and stability of ecosystems. With increasing destabilization caused by climate change, overfishing, habitat degradation, and invasive species, it is critical to comprehensively characterize the functional roles of predators. Sharks are abundant predators in coastal habitats, whose roles can also change over ontogeny. However, the possible mechanisms that drive these shifts in ecological roles have not been directly investigated. This dissertation applies an interdisciplinary approach to discern the ecological roles of bull (*Carcharhinus leucas*), blacktip (*Carcharhinus limbatus*), and bonnethead sharks (*Sphyrna tiburo*) using feeding biomechanics, ecomorphology, and ecotoxicology. Small conspecifics exhibited significant positive allometric scaling of bite force over ontogeny, which was associated with increases in niche breadth and energy-density of prey in bull and bonnethead sharks, respectively. Functional changes in tooth morphology over ontogeny were not found in any of the species, but it appears that the extent of heterodonty may correspond with foraging strategies (generalist versus specialist). The combination of rapid increases in bite force and tooth shape that is best-suited to primary prey items likely improve prey handling efficiency and increase net energy intake. Chronic exposure of sharks to polycyclic aromatic hydrocarbons (PAHs) within the Galveston Bay, TX likely contributed to similar burdens of this contaminant within all three species. Polychlorinated biphenyls (PCBs) showed a pattern of biomagnification, where high trophic position bull and blacktip sharks accumulated

greater burdens than the lower trophic position bonnethead sharks. PCB burdens in these sharks also appeared to accumulate at concentrations above which fish and aquatic mammals experience physiological impacts, suggesting that these species are experiencing deleterious health effects. Overall, these findings suggest that bull sharks change roles from mesopredators as juveniles to top predators as adults, whereas blacktip and bonnethead sharks remain mesopredators across ontogeny. Differences in habitat and diet also differentially expose all species to certain contaminants, which could be at concentrations that impact shark health in Galveston Bay, TX.

DEDICATION

For my brother, Ethan.

ACKNOWLEDGMENTS

I would first like to thank Dr. Christopher Marshall, my committee chair, for the opportunity to pursue my interests and for following through on his promise to provide me with a wide variety of research experiences. I never expected to be performing turtle rodeo in the Middle East, analyzing satellite telemetry data, or measuring contaminant accumulation in sharks, but I am very grateful for your support. Thank you for your guidance and encouragement throughout this entire process and helping me develop personally and professionally.

I would also like to thank Dr. David Hala, my committee co-chair, for giving me a home to conduct my toxicology studies. I did not know if I would be able to pursue this field as part of my research, but appreciate the time and resources you provided to make this possible. I am grateful for your generosity, guidance, and support in completing my research and collaboration on other projects.

I am grateful for all of the other members of my committee: Dr. Jay Rooker, Dr. David Wells, and Dr. Kevin Conway. Thank you for your continued support and guidance during my research. I am also thankful for Dr. Blair Sterba-Boatwright, who provided valuable assistance in fine-tuning the Baysesian model of bite force scaling.

I am indebted to all of the other graduate and undergraduate students that made this research possible. Without the samples or data they collected, I would not have been able to complete this research. I would like to thank Tom TinHan, Jeff Plumlee, Pat Faulkner, Emily Williams, Katie Adams, Nicole Glenn, and Aubree Jones for collecting

and providing samples that were used in all aspects of this research. For assisting with the measurement of theoretical estimates of shark bite force, I would like to thank Daniel Gutierrez, Kendal Clark, Aubree Jones, Sarah Hoskinson, Lexi Hornsby, and Erica Atkins. For the cleaning of shark teeth and pictures taken for further analysis, I would like to thank Mackenzie Merrill, Lexi Hornsby, and Cody Cumba.

Finally, I would like to thank my family and Erica Atkins for their unconditional support, encouragement, and love throughout this entire process. Thank you Mom and Dad for providing financial support when money was tight, emotional support when times seemed tough, and fostering my creativity and work ethic to pursue my passion. Thank you Hannah for supporting me and being with me every step of the way the past 28 years. Thank you Erica for your patience with my long work hours and occasional desire to act irritable, as well as providing love and encouragement when I needed it most.

CONTRIBUTORS AND FUNDING SOURCES

Contributors

This work was supervised by a dissertation committee consisting of Dr. Christopher Marshall (Chair), Dr. Jay Rooker, and Dr. David Wells of both the Department of Marine Biology and Department of Wildlife and Fisheries Sciences, as well as Dr. David Hala (Co-Chair) of the Department of Marine Biology and Dr. Kevin Conway of the Department of Wildlife and Fisheries Sciences.

The data analyzed for Chapter 2 were collected in part by Daniel Gutierrez, Kendal Clark, Aubree Jones, Alexis Hornsby, Sarah Hoskinson, and Erica Atkins of the Department of Marine Biology. Dr. Blair-Sterba Boatwright of the Department of Mathematics and Statistics at Texas A&M University – Corpus Christi assisted in the development of the Bayesian regression model for bite force data. The data analyzed for Chapter 3 were collected in part by Alexis Hornsby, Mackenzie Merrill, and Cody Cumba of the Department of Marine Biology. All work conducted for Chapter 4 of the dissertation was completed independently.

Funding Sources

Graduate study was supported by a Merit Fellowship from Texas A&M University, an Excellence Fellowship from the College of Agriculture and Life Sciences, a Graduate Boost Fellowship from the Research and Graduate Studies Office at Texas

A&M University at Galveston, and Graduate Teaching Assistantships in the Department of Marine Biology.

This work was also made possible in part by Texas Sea Grant Grants-in-Aid of Graduate Research, Erma Lee and Luke Mooney Graduate Travel Grants, and Department of Marine Biology Mini Grants. The contents of this dissertation are solely the responsibility of the author and do not necessarily represent the official views of Texas Sea Grant or Texas A&M University.

TABLE OF CONTENTS

Page

LIST OF FIGURES

Page

LIST OF TABLES

Page

CHAPTER I

INTRODUCTION

Predator-prey interactions are major components of food webs and are used to evaluate ecosystem processes and function over space and time. The prey and habitat resources that a species uses comprise its ecological niche, which dictates the species' role within an ecosystem (Elton 1927; Hutchinson 1957; Leibold 1995). The ecological roles of organisms are critical to evaluate since they can dictate the function, biodiversity, and stability of an ecosystem (Duffy 2002; Lotze et al. 2006; Waycott et al. 2009; Britten et al. 2014; Ellingsen et al. 2015). Predators can impose top-down control on lower trophic level species, which may promote trophic cascades (Heithaus et al. 2008; Estes et al. 2011; Heithaus et al. 2012; Burkholder et al. 2013; Ford et al. 2014; Ripple et al. 2014). Additionally, these predators may connect multiple distinct habitats and energy pathways by redistributing nutrients (Polis et al. 1997; Schmitz et al. 2010; Holtgrieve and Schindler 2011; Rosenblatt et al. 2013). Many organisms exhibit ontogenetic niche shifts in habitat and diet, further complicating the characterization of species roles (Werner and Gilliam 1984; Mittelbach et al. 1988; Snover 2008). One of the mechanisms by which the ecological niche of a species can be shaped includes feeding performance and its changes over ontogeny.

Sharks are an interesting model system to assess feeding biomechanics and trophic ecology since they often undergo one or more ontogenetic dietary shifts towards functionally challenging prey that require increased handling effort (Lowe et al. 1996;

McElroy et al. 2006; Kolmann and Huber 2009; Werry et al. 2011; Motta and Huber 2012). Ontogenetic changes in bite performance and size (through growth) of the feeding apparatus are important considerations for understanding these dietary shifts because such factors can constrain prey choice and influence energetics (Emlen 1966; Schoener 1971; Wainwright 1994; Wainwright and Richard 1995; Motta et al. 2008; Marshall et al. 2012). Constraints on prey selection have the greatest effect on early life stages and will require sharks to feed on small, low trophic level prey due to small gapes and low bite forces of young individuals (Wainwright 1994; Huber et al. 2009; Motta and Huber 2012). Therefore, trophic position is likely limited by performance and morphology of the feeding apparatus at early life stages until ontogenetic shifts in size and growth release these constraints.

Another important consideration that can influence a species' prey selection and ontogenetic dietary shifts is the morphology of the teeth, which transmit force from the jaw adductor musculature during prey capture, retention, and processing. Much less is known about changes in tooth morphology and function over ontogeny than changes in diet and bite force in elasmobranchs. While the size and material properties of the teeth are important factors in prey capture and processing (Whitenack et al. 2010; Whitenack et al. 2011), it would be expected that a shift in diet would be accompanied by a concomitant change in tooth morphology that is best suited to capture and process the prey of choice. Tooth shape and size should be suitable for efficient prey handling, thereby increasing net energy intake. Although many studies have characterized teeth from only a single position in the jaws (Huber et al. 2009; Whitenack and Motta 2010;

Bergman et al. 2017), this does not provide a full perspective of shark tooth morphology since many sharks exhibit heterodonty. Tooth morphology should therefore be evaluated over ontogeny as well at multiple positions along the jaws to determine how teeth of different shapes may contribute to prey acquisition.

Coastal and estuarine habitats are a major sink for anthropogenic contamination, which can be transferred throughout food webs by multiple pathways (van der Oost et al. 2003; Borgå et al. 2004; Islam and Tanaka 2004; Le Croizier et al. 2016). Differences in the habitat and trophic position of an organism can influence the exposure to and bioaccumulation of certain contaminants that may cause toxicity (Borgå et al. 2004; Le Croizier et al. 2016). While there are a large number of environmental contaminants that sharks may be exposed to in estuarine and coastal habitats, assessments of polychlorinated biphenyls (PCBs) are among the most common (Gelsleichter and Walker 2010). Despite the fewer studies on polycyclic aromatic hydrocarbons (PAHs; Al-Hassan et al. 2000; Marsili et al. 2016), these are another important classes of contaminants that are ubiquitous in aquatic ecosystems through both point and non-point sources (van der Oost et al. 2003; Gelsleichter and Walker 2010). High concentrations of organic pollutants are frequently found in estuarine and coastal environments where many petrochemical and industrial facilities meet nursery grounds and primary habitat for many sharks (Gelsleichter and Walker 2010), placing them at risk. Estuaries are particularly vulnerable to increased contaminant loading since these compounds are known to enter as runoff from urban and agricultural areas, as well as wastewater and industrial effluent (Loganathan and Kannan 1994; Yunker et al. 2002; Storelli et al.

2005). The uptake and bioaccumulation of these pollutants in sharks is affected by age, habitat, sex, diet, metabolic rate, and growth rate, among other variables (Gelsleichter and Walker 2010; Lyons et al. 2013). Organic pollutants preferentially partition into lipid-rich tissue due to their high hydrophobicity, which is of concern for sharks since their livers can be comprised of up to 80% lipids and can represent up to 20% body mass (Serrano et al. 2000; Hussey et al. 2010). Highly persistent, lipophilic contaminants can biomagnify up the food web and result in the greatest concentrations being found in high trophic position predators. In addition, mobilization of the lipids containing these contaminants during starvation periods and reproduction can make them bioavailable through catabolism, potentially harming the organism and/or their progeny (Kelly et al. 2011; Lyons et al. 2013; Daley et al. 2014). Due to the ubiquity of PAHs and PCBs as well as the susceptibility of sharks to become exposed to and accumulate high burdens of organic pollutants, bioaccumulation of these contaminants should be further evaluated and related to ecological niche for possible sources of exposure.

Despite the number of studies on elasmobranch feeding that apply either an ecological or biomechanical approach, there is a lack of research that integrates functional measures with empirical dietary data to explain dietary shifts and trophic position over the entire ontogeny of a species. Additionally, few studies have correlated the induction of biomarkers of exposure to tissue-based burdens of contaminants as well as relating these burdens to exposure via habitat and trophic position (Fisk et al. 2002; Lyons et al. 2014; Beaudry et al. 2015; Kiszka et al. 2015; McMeans et al. 2015; Alves et al. 2016). This dissertation will focus on three species of sharks found along the Texas

coast: bull (*Carcharhinus leucas*), blacktip (*Carcharhinus limbatus*), and bonnethead (*Sphyrna tiburo*) sharks. Although these species co-occur in this region, they differ widely in their foraging ecology as they approach adult age classes (Bethea et al. 2007; Barry et al. 2008; Werry et al. 2011). Bull sharks are considered dietary generalists (Snelson et al. 1984; Cliff and Dudley 1991; Werry et al. 2011; but see Matich et al. 2011), whereas blacktips target increasingly larger fish over their ontogeny (Bethea et al. 2004; Barry et al. 2008) and bonnetheads preferentially consume crustaceans at all life stages (Cortés et al. 1996; Bethea et al. 2007). It is expected that differences in bite force and tooth morphology among species contribute to their distinct niches, which impacts their accumulation of contaminants. The overall objective of this dissertation is to integrate measurements of bite force, tooth morphology, and tissue-based burdens of contaminants to comprehensively characterize the ecological niches of these co-occurring species and their roles over ontogeny.

In Chapter 2, I calculate theoretical estimates of bite force in bull, blacktip, and bonnethead sharks and evaluate scaling patterns over ontogeny in separate small and large size classes within each species. Additionally, I relate species-specific changes in scaling pattern of bite force with ontogenetic dietary shifts using a combination of data from previous studies and this dissertation. I evaluate changes in niche variability over ontogeny using stable isotope analysis of $\delta^{13}C$ and $\delta^{15}N$. I also use $\delta^{13}C$ and $\delta^{15}N$ to calculate six ecological niche metrics to measure and compare niche breadth among species, as well as to estimate niche overlap.

In Chapter 3, I use elliptic Fourier analysis to characterize the shape of teeth from bull, blacktip, and bonnethead sharks. These data are quantified for six tooth positions (three each from the upper and lower jaws) that represent the change in morphology from anterior to posterior along the tooth row. I investigate changes in tooth morphology over ontogeny at each of the six tooth positions and I also characterize the extent of heterodonty within each species by comparing tooth morphology among all six positions. I also make interspecific comparisons in tooth morphology at each of the six measured tooth positions and relate these relationships to diet and feeding behavior.

In Chapter 4, I quantify burdens of PAHs and PCBs in muscle and liver tissue of bull, blacktip, and bonnethead sharks and evaluate ontogenetic trends of contaminant accumulation. I compare congener profiles of both contaminant classes (PAHs and PCBs) to determine potential differences in ecological niche and metabolic capability. I measure and compare biomarkers of exposure among species to determine which sharks may be most susceptible to negative health effects. I directly integrate burdens of PAHs and PCBs with biomarker activity to determine which individual PAH or PCB congeners are associated with biotransformation enzyme induction. I also include dioxin-like PAH and PCB congeners within a risk assessment framework to determine if these sharks may be experiencing physiological impacts due to these contaminants.

In my concluding chapter (Chapter 5), I integrate bite force and tooth morphology to describe the ecological roles of each species and their changes over ontogeny. I also discuss the implications of shifts in habitat and diet on the accumulation of organic contaminants within each species and the potential for negative health

outcomes that may result from these burdens. Broader impacts of this research are discussed with respect to the evaluation of ecological roles of species and the potential impacts of habitat degradation on resource use.

References

Al-Hassan JM, Afzal M, Rao CVN, Fayad S. 2000. Petroleum hydrocarbon pollution in sharks in the Arabian Gulf. *Bull. Environ. Contam. Toxicol.* 65:391–398. doi:10.1007/s001280000140.

Alves LMF, Nunes M, Marchand P, Le Bizec B, Mendes S, Correia JPS, Lemos MFL, Novais SC. 2016. Blue sharks (Prionace glauca) as bioindicators of pollution and health in the Atlantic Ocean: Contamination levels and biochemical stress responses. *Sci. Total Environ.* 563–564:282–292. doi:10.1016/j.scitotenv.2016.04.085.

Barry K, Condrey R, Driggers W, Jones C. 2008. Feeding ecology and growth of neonate and juvenile blacktip sharks Carcharhinus limbatus in the Timbalier-Terrebone Bay complex, LA, U.S.A. *J. Fish Biol.* 73:650–662. doi:10.1111/j.1095-8649.2008.01963.x.

Beaudry MC, Hussey NE, McMeans BC, McLeod AM, Wintner SP, Cliff G, Dudley SFJ, Fisk AT. 2015. Comparative organochlorine accumulation in two ecologically similar shark species (Carcharodon carcharias and Carcharhinus obscurus) with divergent uptake based on different life history. *Environ. Toxicol. Chem.* 34:2051–2060. doi:10.1002/etc.3029.

Bergman J, Lajeunesse M, Motta P. 2017. Teeth penetration force of the tiger shark Galeocerdo cuvier and sandbar shark Carcharhinus plumbeus. *J. Fish Biol.* 91:460–472. doi:10.1111/jfb.13351.

Bethea D, Buckel J, Carlson J. 2004. Foraging ecology of the early life stages of four

sympatric shark species. *Mar. Ecol. Prog. Ser.* 268:245–264. doi:10.3354/meps268245.

Bethea DM, Hale L, Carlson JK, Cortés E, Manire CA, Gelsleichter J. 2007. Geographic and ontogenetic variation in the diet and daily ration of the bonnethead shark, Sphyrna tiburo, from the eastern Gulf of Mexico. *Mar. Biol.* 152:1009–1020. doi:10.1007/s00227-007-0728-7.

Borgå K, Fisk AT, Hoekstra PE, Muir DCG. 2004. Biological and chemical factors of importance in the bioaccumulation and trophic transfer of persistent organochlorine contaminants in Arctic marine food webs. *Environ. Toxicol. Chem.* 23:2367–2385. doi:10.1897/03-518.

Britten GL, Dowd M, Minto C, Ferretti F, Boero F, Lotze HK. 2014. Predator decline leads to decreased stability in a coastal fish community. *Ecol. Lett.* 17:1518–1525. doi:10.1111/ele.12354.

Burkholder DA, Heithaus MR, Fourqurean JW, Wirsing A, Dill LM. 2013. Patterns of top-down control in a seagrass ecosystem: could a roving apex predator induce a behaviour-mediated trophic cascade? *J. Anim. Ecol.* 82:1192–202. doi:10.1111/1365-2656.12097.

Cliff G, Dudley SF. 1991. Sharks caught in the protective gill nets off Natal, South Africa. 4. The bull shark Carcharhinus leucas Valenciennes. *South African J. Mar. Sci.* 10:253–270. doi:10.2989/02577619109504636.

Cortés E, Manire CA, Hueter RE. 1996. Diet, feeding habits, and diel feeding chronology of the bonnethead shark, Sphyrna tiburo, in southwest Florida. *Bull.*

Mar. Sci. 58:353–367. doi:10.1007/s00227-006-0325-1.

Le Croizier G, Schaal G, Gallon R, Fall M, Le Grand F, Munaron JM, Rouget ML, Machu E, Le Loc'h F, Laë R, et al. 2016. Trophic ecology influence on metal bioaccumulation in marine fish: Inference from stable isotope and fatty acid analyses. *Sci. Total Environ.* 573:83–95. doi:10.1016/j.scitotenv.2016.08.035.

Daley JM, Paterson G, Drouillard KG. 2014. Bioamplification as a bioaccumulation mechanism for persistent organic pollutants (POPs) in wildlife. In: Whitacre DM, editor. Reviews of Environmental Contamination and Toxicology, Volume 227. Cham: Springer. p. 107–155.

Duffy JE. 2002. Biodiversity and ecosystem function: the consumer connection. *Oikos* 99:201–219. doi:10.1034/j.1600-0706.2002.990201.x.

Ellingsen KE, Anderson MJ, Shackell NL, Tveraa T, Yoccoz NG, Frank KT. 2015. The role of a dominant predator in shaping biodiversity over space and time in a marine ecosystem. *J. Anim. Ecol.* 84:1242–1252. doi:10.1111/1365-2656.12396.

Elton CS. 1927. Animal ecology. Chicago: University of Chicago Press.

Emlen J. 1966. The role of time and energy in food preference. *Am. Nat.* 100:611–617.

Estes JA, Terborgh J, Brashares JS, Power ME, Berger J, Bond WJ, Carpenter SR, Essington TE, Holt RD, Jackson JBC, et al. 2011. Trophic downgrading of planet earth. *Science* 333:301–306. doi:10.1126/science.1205106.

Fisk AT, Tittlemier SA, Pranschke JL, Norstrom RJ. 2002. Using anthropogenic contaminants and stable isotopes to asses the feeding ecology of Greenland sharks. *Ecology* 83:2162–2172.

Ford AT, Goheen JR, Otieno TO, Bidner L, Isbell LA, Palmer TM, Ward D, Woodroffe R, Pringle RM. 2014. Large carnivores make savanna tree communities less thorny. *Science* 346:346–349. doi:10.1126/science.1252753.

Gelsleichter J, Walker CJ. 2010. Pollutant exposure and effects in sharks and their relatives. In: Carrier J, Musick J, Heithaus M, editors. Sharks And Their Relatives II: Biodiversity, Adaptive Physiology, And Conservation. Boca Raton: CRC Press. p. 491–537.

Heithaus MR, Frid A, Wirsing AJ, Worm B. 2008. Predicting ecological consequences of marine top predator declines. *Trends Ecol. Evol.* 23:202–210. doi:10.1016/j.tree.2008.01.003.

Heithaus MR, Wirsing AJ, Dill LM. 2012. The ecological importance of intact top-predator populations: a synthesis of 15 years of research in a seagrass ecosystem. *Mar. Freshw. Res.* 63:1039–1050. doi:10.1071/MF12024.

Holtgrieve GW, Schindler DE. 2011. Marine-derived nutrients, bioturbation, and ecosystem metabolism: Reconsidering the role of salmon in streams. *Ecology* 92:373–385. doi:10.1890/09-1694.1.

Huber DR, Claes JM, Mallefet J, Herrel A. 2009. Is extreme bite performance associated with extreme morphologies in sharks? *Physiol. Biochem. Zool.* 82:20–28. doi:10.1086/588177.

Hussey NE, Wintner SP, Dudley S, Cliff G, Cocks DT, Aaron MacNeil M. 2010. Maternal investment and size-specific reproductive output in carcharhinid sharks. *J. Anim. Ecol.* 79:184–193. doi:10.1111/j.1365-2656.2009.01623.x.

Hutchinson GE. 1957. Concluding Remarks. *Cold Spring Harb. Symp. Quant. Biol.* 22:415–427. doi:10.1101/SQB.1957.022.01.039.

Islam MS, Tanaka M. 2004. Impacts of pollution on coastal and marine ecosystems including coastal and marine fisheries and approach for management: A review and synthesis. *Mar. Pollut. Bull.* 48:624–649. doi:10.1016/j.marpolbul.2003.12.004.

Kelly BC, Ikonomou MG, MacPherson N, Sampson T, Patterson DA, Dubetz C. 2011. Tissue residue concentrations of organohalogens and trace elements in adult Pacific salmon returning to the Fraser River, British Columbia, Canada. *Environ. Toxicol. Chem.* 30:367–376. doi:10.1002/etc.410.

Kiszka JJ, Aubail A, Hussey NE, Heithaus MR, Caurant F, Bustamante P. 2015. Plasticity of trophic interactions among sharks from the oceanic south-western Indian Ocean revealed by stable isotope and mercury analyses. *Deep Sea Res. Part I Oceanogr. Res. Pap.* 96:49–58. doi:10.1016/j.dsr.2014.11.006.

Kolmann MA, Huber DR. 2009. Scaling of feeding biomechanics in the horn shark Heterodontus francisci: ontogenetic constraints on durophagy. *Zoology* 112:351–361. doi:10.1016/j.zool.2008.11.002.

Leibold MA. 1995. The niche concept revisited: Mechanistic models and community context. *Ecology* 76:1371–1382. doi:10.1007/s.

Loganathan B, Kannan K. 1994. Global organochiorine contamination trends: An overview. *Ambio* 23:187–191.

Lotze HK, Lenihan HS, Bourque BJ, Bradbury RH, Cooke RG, Kay MC, Kidwell SM, Kirby MX, Peterson CH, Jackson JBC. 2006. Depletion, degradation, and recovery

potential of estuaries and coastal seas. *Science* 312:1806–1809. doi:10.1126/science.1128035.

Lowe C, Wetherbee B, Crow G, Tester A. 1996. Ontogenetic dietary shifts and feeding behavior of the tiger shark, Galeocerdo cuvier, in Hawaiian waters. *Environ. Biol. Fishes* 47:203–211.

Lyons K, Carlisle A, Preti A, Mull C, Blasius M, O'Sullivan J, Winkler C, Lowe CG. 2013. Effects of trophic ecology and habitat use on maternal transfer of contaminants in four species of young of the year lamniform sharks. *Mar. Environ. Res.* 90:27–38. doi:10.1016/j.marenvres.2013.05.009.

Lyons K, Lavado R, Schlenk D, Lowe CG. 2014. Bioaccumulation of organochlorine contaminants and ethoxyresorufin-o-deethylase activity in southern California round stingrays (Urobatis halleri) exposed to planar aromatic compounds. *Environ. Toxicol. Chem.* 33:1380–1390. doi:10.1002/etc.2564.

Marshall CD, Guzman A, Narazaki T, Sato K, Kane EA, Sterba-Boatwright BD. 2012. The ontogenetic scaling of bite force and head size in loggerhead sea turtles (Caretta caretta): implications for durophagy in neritic, benthic habitats. *J. Exp. Biol.* 215:4166–4174. doi:10.1242/jeb.074385.

Marsili L, Coppola D, Giannetti M, Casini S, Fossi M, van Wyk J, Sperone E, Tripepi S, Micarelli P, Rizzuto S. 2016. Skin biopsies as a sensitive non-lethal technique for the ecotoxicological studies of great white shark (Carcharodon carcharias) sampled in South Africa. *Expert Opin. Environ. Biol.* 4:1–8. doi:10.4172/2325-9655.1000126.

Matich P, Heithaus MR, Layman CA. 2011. Contrasting patterns of individual specialization and trophic coupling in two marine apex predators. *J. Anim. Ecol.* 80:294–305. doi:10.1111/j.1365-2656.2010.01753.x.

McElroy WD, Wetherbee BM, Mostello CS, Lowe CG, Crow GL, Wass RC. 2006. Food habits and ontogenetic changes in the diet of the sandbar shark, Carcharhinus plumbeus, in Hawaii. *Environ. Biol. Fishes* 76:81–92. doi:10.1007/s10641-006-9010-y.

McMeans BC, Arts MT, Fisk AT. 2015. Impacts of food web structure and feeding behavior on mercury exposure in Greenland Sharks (Somniosus microcephalus). *Sci. Total Environ.* 509:216–225. doi:10.1016/j.scitotenv.2014.01.128.

Mittelbach GG, Osenberg CW, Leibold MA. 1988. Trophic relations and ontogenetic niche shifts in aquatic organisms. In: Ebenman B, Persson L, editors. Size-Structured Populations. Berlin, Heidelberg: Springer. p. 219–235.

Motta P, Huber D. 2012. Prey capture behavior and feeding mechanics of elasmobranchs. In: Carrier JC, Musick JA, Heithaus MR, editors. Biology of Sharks and Their Relatives. 2nd ed. Boca Raton: CRC Press. p. 153–210.

Motta PJ, Hueter RE, Tricas TC, Summers AP, Huber DR, Lowry D, Mara KR, Matott MP, Whitenack LB, Wintzer AP. 2008. Functional morphology of the feeding apparatus, feeding constraints, and suction performance in the nurse shark Ginglymostoma cirratum. *J. Morphol.* 269:1041–1055. doi:10.1002/jmor.10626.

van der Oost R, Beyer J, Vermeulen NPE. 2003. Fish bioaccumulation and biomarkers in environmental risk assessment: A review. *Environ. Toxicol. Pharmacol.* 13:57–

149. doi:10.1016/S1382-6689(02)00126-6.

Polis GA, Anderson WB, Holt RD. 1997. Toward an integration of landscape and food web ecology: The dynamics of spatially subsidized food webs. *Annu. Rev. Ecol. Syst.* 28:289–316. doi:10.1146/annurev.ecolsys.28.1.289.

Ripple WJ, Estes JA, Beschta RL, Wilmers CC, Ritchie EG, Hebblewhite M, Berger J, Elmhagen B, Letnic M, Nelson MP, et al. 2014. Status and ecological effects of the world' s largest carnivores. *Science* 343:1241484. doi:10.1126/science.1241484.

Rosenblatt A, Heithaus M, Mather M, Matich P, Nifong J, Ripple W, Silliman B. 2013. The roles of large top predators in coastal ecosystems: New insights from long term ecological research. *Oceanography* 26:156–167. doi:10.5670/oceanog.2013.59.

Schmitz OJ, Hawlena D, Trussell GC. 2010. Predator control of ecosystem nutrient dynamics. *Ecol. Lett.* 13:1199–1209. doi:10.1111/j.1461-0248.2010.01511.x.

Schoener TW. 1971. Theory of feeding strategies. *Annu. Rev. Ecol. Syst.* 2:369–404.

Serrano R, Fernández M, Rabanal R, Hernández M, Gonzalez MJ. 2000. Congener-specific determination of polychlorinated biphenyls in shark and grouper livers from the northwest African Atlantic Ocean. *Arch. Environ. Contam. Toxicol.* 38:217–224. doi:10.1007/s002449910029.

Snelson FF, Mulligan TJ, Williams SE. 1984. Food habits, occurrence, and population structure of the bull shark, Carcharhinus leucas, in Florida coastal lagoons. *Bull. Mar. Sci.* 34:71–80.

Snover ML. 2008. Ontogenetic habitat shifts in marine organisms: Influencing factors and the impact of climate variability. *Bull. Mar. Sci.* 83:53–67.

Storelli MM, Storelli A, Marcotrigiano GO. 2005. Concentrations and hazard assessment of polychlorinated biphenyls and organochlorine pesticides in shark liver from the Mediterranean Sea. *Mar. Pollut. Bull.* 50:850–855. doi:10.1016/j.marpolbul.2005.02.023.

Wainwright PC. 1994. Functional morphology as a tool in ecological research. In: Wainwright P, Reilly S, editors. Ecological Morphology: Integrative Organismal Biology. Chicago: University of Chicago Press. p. 42–59.

Wainwright PC, Richard BA. 1995. Predicting patterns of prey use from morphology of fishes. *Environ. Biol. Fishes* 44:97–113. doi:10.1007/BF00005909.

Waycott M, Duarte CM, Carruthers TJB, Orth RJ, Dennison WC, Olyarnik S, Calladine A, Fourqurean JW, Heck KL, Hughes AR, et al. 2009. Accelerating loss of seagrasses across the globe threatens coastal ecosystems. *Proc. Natl. Acad. Sci.* 106:12377–12381. doi:10.1073/pnas.0905620106.

Werner EE, Gilliam JF. 1984. The ontogenetic niche and species interactions in size-structured populations. *Annu. Rev. Ecol. Syst.* 15:393–425.

Werry J, Lee S, Otway N, Hu Y, Sumpton W. 2011. A multi-faceted approach for quantifying the estuarine-nearshore transition in the life cycle of the bull shark, Carcharhinus leucas. *Mar. Freshw. Res.* 62:1421–1431. doi:10.1071/MF11136.

Whitenack L, Motta P. 2010. Performance of shark teeth during puncture and draw: implications for the mechanics of cutting. *Biol. J. Linn. Soc.* 100:271–286.

Whitenack LB, Simkins DC, Motta PJ. 2011. Biology meets engineering: the structural mechanics of fossil and extant shark teeth. *J. Morphol.* 272:169–179.

doi:10.1002/jmor.10903.

Whitenack LB, Simkins DC, Motta PJ, Hirai M, Kumar A. 2010. Young's modulus and hardness of shark tooth biomaterials. *Arch. Oral Biol.* 55:203–209. doi:10.1016/j.archoralbio.2010.01.001.

Yunker MB, Backus SM, Graf Pannatier E, Jeffries DS, Macdonald RW. 2002. Sources and significance of alkane and PAH hydrocarbons in Canadian Arctic Rivers. *Estuar. Coast. Shelf Sci.* 55:1–31. doi:10.1006/ecss.2001.0880.

CHAPTER II

ECOMECHANICS OF ELASMOBRANCH FORAGING: INTEGRATING THEORETICAL ESTIMATES OF BITE FORCE AND FEEDING ECOLOGY USING STABLE ISOTOPES

Introduction

Bite force is an ecologically relevant metric of feeding performance that has been associated with niche diversification and partitioning in terrestrial and aquatic taxa (Kiltie 1982; Hernandez and Motta 1997; Aguirre et al. 2002; Anderson et al. 2008; Huber et al. 2009; Santana et al. 2010). An organism's feeding performance is often associated with its ecological role, which can dramatically change during ontogeny (Erickson et al. 2003; Herrel and O'Reilly 2006; Habegger et al. 2012). Juveniles are often at a disadvantage in gaining access to dietary resources due to smaller gapes and lower bite forces compared to adults (Schmidt-Nielsen 1984; Werner and Gilliam 1984; Herrel and Gibb 2006; Herrel and O'Reilly 2006). Many species respond to this selection pressure by targeted increased growth of the muscle cross-sectional area and/or mechanical advantage of the jaw lever system, resulting in significant positive allometric scaling of bite force (Hernandez and Motta 1997; Binder and Van Valkenburgh 2000; Erickson et al. 2003; Huber et al. 2006). Upon reaching large body sizes, selection pressure to continue significant positive allometric scaling typically relaxes because high absolute bite forces of larger individuals are capable of handling most prey items (Aguirre et al. 2003; Herrel and Gibb 2006; Huber et al. 2009; Habegger et al. 2012).

Therefore, the timing of a possible change in the scaling of bite force is likely of ecological significance.

The relationship between bite force and the mechanical demands of dietary resources typically reflects accessibility to food items, resulting in adaptations for resource partitioning within or among species (Kiltie 1982; Aguirre et al. 2003; Santana et al. 2010; Marshall et al. 2012). The critical period where constraint and selective pressure on bite force is released in large conspecifics often corresponds with a dietary shift in prey size, diversity, or material properties (Wainwright 1988; Clifton and Motta 1998; Scharf et al. 2000; Aguirre et al. 2003; Bethea et al. 2004). Ontogenetic dietary shifts associated with changes in bite force have been empirically investigated in a variety of species (Hernandez and Motta 1997; Herrel and O'Reilly 2006; Pfaller et al. 2011), but these changes have yet to be thoroughly evaluated in elasmobranchs (but see Kolmann and Huber 2009).

Elasmobranchs (sharks, skates, and rays) perform a variety of ecological roles within estuarine, coastal, and oceanic food webs, which change over ontogeny (Heithaus et al. 2008; Kinney et al. 2011; Navia et al. 2016). Many sharks undergo ontogenetic niche shifts that impact their trophic position, dietary breadth (Lowe et al. 1996; Estrada et al. 2006; Bethea et al. 2007; Werry et al. 2011) and likely contributes to intra- and interspecific resource partitioning (Papastamatiou et al. 2006; Kinney et al. 2011; Heithaus et al. 2013; Navia et al. 2016). For some large-bodied sharks, this results in a role change from a mesopredator to a top predator (Daly et al. 2013; Heupel et al. 2014; Navia et al. 2016). A powerful time-integrated method to discern the ecological niche

and trophic relationships of these species includes the use of biochemical tracers such as stable isotopes (SIs).

Stomach content analyses have traditionally been the most common method to determine the feeding ecology of sharks, which imposes limitations on the interpretations of diet because this measure only provides a snapshot of resource use. More recently, the application of SIs in ecological studies have become increasingly common since they can be performed non-lethally and generally do not require as large a sample size as does stomach content analysis (Shiffman et al. 2012; Pethybridge et al. 2018). Carbon ($\delta^{13}C$) and nitrogen ($\delta^{15}N$) SIs are useful to characterize general niche metrics, such as basal carbon sources of food webs and trophic position, respectively (Peterson and Fry 1987). Since $\delta^{13}C$ typically varies along depth and nearshore salinity gradients and is minimally altered with each successive trophic level, it often serves as a proxy for the carbon source(s) used by a consumer (Peterson and Fry 1987; Garcia et al. 2007; Pethybridge et al. 2018). Trophic position can be assessed using $\delta^{15}N$ since it becomes more enriched from prey to predator due to trophic fractionation, which is considerably larger than that of $\delta^{13}C$ (Vander Zanden et al. 1997; Post 2002; Hussey et al. 2011). The use of $\delta^{13}C$ and $\delta^{15}N$ in combination can also be used to estimate niche breadth and its changes over ontogeny using a variety of metrics (Layman et al. 2007; Jackson et al. 2011; Matich et al. 2019).

Several sharks use estuarine and coastal habitats throughout their ontogeny and are common to the Gulf of Mexico, including bull (*Carcharhinus leucas*), blacktip (*Carcharhinus limbatus*), and bonnethead sharks (*Sphyrna tiburo*) (Carlson et al. 2010;

Drymon et al. 2010; Froeschke et al. 2010; Bethea et al. 2015). These species exhibit different life history characteristics (maximum body size, age at maturity, fecundity) and ecological niches, which is supported by differences in observed dietary breadth and trophic position (Branstetter 1987; Branstetter and Stiles 1987; Cliff and Dudley 1991; Castro 1996; Cortés et al. 1996; Cortés 1999; Cortés 2000; Lombardi-Carlson et al. 2003). All species purportedly undergo ontogenetic shifts in diet, but only bull and bonnethead sharks appear to consume increasingly greater proportions of potentially difficult-to-handle prey (Cliff and Dudley 1991; Castro 1996; Cortés et al. 1996; Bethea et al. 2007; Barry et al. 2008; Werry et al. 2011). Previous studies have measured significant positive allometry of bite force in blacktip (Huber et al. 2006) and juvenile bull sharks, but only isometry in adult bull sharks (Habegger et al. 2012). Only general bite force data are available for juvenile bonnethead sharks (Mara et al. 2010). Although these studies have quantified bite force and/or its scaling pattern over ontogeny, the present study will directly incorporate ecological data and build upon the change in scaling pattern that was observed by Habegger et al. (2012).

This study seeks to evaluate the use of biomechanical models of theoretical bite force to discern relationships with ecological niche shifts over ontogeny. To accomplish this overall goal, the present study will (i) estimate theoretical bite force and measure scaling patterns over ontogeny in small versus large conspecifics, (ii) discern the relationship between ecological niche shifts and changes in bite force over ontogeny, (iii) evaluate changes in niche breadth over ontogeny, and (iv) quantify niche breadth and overlap among species. I hypothesize that bite force of small conspecifics of each

species will scale with significant positive allometry, whereas bite force of large individuals will scale isometrically. This incorporates the recommendation of Habegger et al. (2012) that juvenile and adult conspecifics be evaluated separately for scaling of bite force. I also hypothesize that rapid increases in bite force (during positive allometric scaling) will precede ecological transitions, which may facilitate the widening of niche breadth or the inclusion of greater proportions of energetically-dense prey. Isotopic niche breadth (using $\delta^{13}C$ and $\delta^{15}N$) is expected to increase over ontogeny in the generalist bull shark, but to decrease in the specialist blacktip and bonnethead sharks. Last, I predict that bull sharks will display the greatest niche breadth and will largely overlap with blacktip sharks, which are also piscivorous, but will minimally overlap with bonnethead sharks that primarily consume benthic invertebrates.

Materials and Methods

Sample collection

Bull (N = 31), blacktip (N = 42), and bonnethead sharks (N = 41) were opportunistically sampled from fishing charters or from routine long-line surveys conducted by the Texas Parks and Wildlife Department in Galveston, Texas in March through October from 2013 to 2016. Of these 114 sharks, 82 were used to estimate theoretical bite force (bull: N = 24; blacktip: N = 30; bonnethead: N = 28) and 86 were used to analyze $\delta^{13}C$ and $\delta^{15}N$ stable isotopes (bull: N = 25; blacktip: N = 27; bonnethead: N = 34). Sample sizes varied between these analyses due to the availability of intact shark heads (for theoretical bite force measurements) across all age classes of

each species. Sex was identified for each shark and measurements of total (TL; cm) and fork length (FL; cm) were recorded (Table 2-1). Age classes for each species were distinguished based upon previous studies from Texas or from a nearby location at a similar latitude, which has been shown to affect growth rates in bonnethead sharks (Lombardi-Carlson et al. 2003). Four age classes were delineated in bull sharks: young-of-the-year (YoY; TL < 90.0 cm), juvenile (90.0 < TL < 160.0 cm), sub-adult (160.0 < TL < 210.0 cm), and adult (TL > 210.0 cm) (Branstetter and Stiles 1987). Four age classes were also delineated in blacktip sharks: YoY (TL < 83.0 cm), juvenile (83.0 < TL < 111.5 cm), sub-adult (111.5 < TL < 140.0 cm), and adult (TL > 140.0 cm) (Branstetter 1987). Only three age classes were defined for bonnethead sharks (YoY, juvenile, adult) since this species reaches maturity much earlier (3-4 years; Lombardi-Carlson et al. 2003) than bull (14-18 years; Branstetter and Stiles 1987) and blacktip sharks (4-8 years; Branstetter 1987). Due to a latitudinal gradient in growth rate, age-growth curves of bonnethead sharks from northwest Florida were used to develop age classes for individuals sampled from Galveston, TX since these locations share a similar latitude (Lombardi-Carlson et al. 2003). These age classes were delineated as YoY (TL < 70.0 cm), juvenile (70.0 < TL < 88.5 cm), and adult (TL > 88.5 cm). Muscle tissue samples (~ 5 g) were taken from the epaxial region near the anterior dorsal fin. Shark heads and muscle tissue samples were transported on ice for up to 30 minutes before storage at -20°C for further analysis.

Table 2-1. Summary of sample sizes (N), sex ratio of females (F) to males (M), mean TL (min – max), mean FL (min – max), and polynomial regression inflection point of ABF ~ FL (small/large size class cutoffs) for each shark species

Species	N	Sex (F/M)	TL (cm)	FL (cm)	Inflection Point (cm)
Bull	31	6/25	115.1 (69.9 – 215.0)	91.6 (54.9 – 174.5)	120.9 (125.9/115.9)
Blacktip	42	23/19	123.9 (66.9 – 171.1)	99.0 (52.7 – 135.6)	99.2 (104.2/94.2)
Bonnethead	41	30/11	89.7 (51.7 – 125.4)	71.2 (40.8 – 99.8)	82.1 (87.1/77.1)

Theoretical modeling of bite force

Unilateral dissections of the adductor mandibulae complex were performed on each specimen and individual muscles were identified following Motta and Wilga (1995). These jaw adductor muscles included the preorbitalis dorsalis (POD), preorbitalis ventralis (POV), quadratomandibularis dorsal divisions 1 – 4 (QD 1, QD 2, QD 3, QD 4), and quadratomandibularis ventral division (QV). All subdivisions were measured separately except for the QD 2 and QD 3 subdivisions in bonnethead sharks because the small size of the QD 3 muscle made it difficult to isolate and measure without being damaged. Three-dimensional coordinates of the origin and insertion of each muscle subdivision, a single bite point (the anterior margin of the functional tooth row on the lower jaw), and the jaw joint were recorded with a three-dimensional Patriot digitizer (Polhemus, Colchester, VT, USA) while the jaws were completely adducted. The tip of the snout was treated as the center of this coordinate system. Although measurements with the jaws fully-adducted may slightly underestimate maximal bite force (Ferrara et al. 2011), previous studies have found no significant difference between

this theoretical method of estimation and *in vivo* bite force measured from sharks under tetanic stimulation (Huber and Motta 2004; Huber et al. 2005; Mara et al. 2010). Subsequently, each muscle subdivision was excised and sectioned through the center of mass perpendicular to the principal fiber direction. The center of mass was determined by freely suspending each muscle from a pin at different points with a plumb line. These lines were traced, and their point of intersection denoted the center of mass for a given muscle (Huber and Motta 2004; Habegger et al. 2012). Cross-sections of each muscle were photographed with a Fujifilm FinePix XP70 digital camera and the anatomical cross-sectional area (CSA; cm^2) was measured using ImageJ (version 1.46; National Institutes of Health, Bethesda, MD, USA). To calculate the maximal force production or theoretical maximum tetanic tension (P_O; N) of each muscle (Powell et al. 1984), CSAs of the POD, POV, QD 1, QD 2, QD 3, and QV were multiplied by the specific tension (T_S; N/cm^2) of shark white muscle (28.9 N/cm^2), whereas the CSA of the QD 4 subdivision was multiplied by the T_S of shark red muscle (14.2 N/cm^2; Lou et al. 2002):

$$P_O = CSA * T_S \quad (1)$$

Three-dimensional force vectors were created using the coordinates of the origin and insertion points of each muscle and P_O. In-lever (L_I) distances were calculated as the distance between the insertion of each muscle subdivision and the jaw joint. A resolved in-lever (RL_I) was calculated by using a weighted average of all individual L_I based upon the proportional contribution of each muscle to total force production (Huber et al. 2005). Out-lever (L_O) distance was calculated as the distance between the anterior bite

point (ABP) and the jaw joint. Mechanical advantage (MA) for the ABP was therefore calculated as the ratio of the RL_I to the L_O. Based upon a previously implemented theoretical bite force model used in multiple studies of elasmobranchs (Huber et al. 2005; Huber et al. 2006; Kolmann and Huber 2009; Mara et al. 2010; Habegger et al. 2012), the present study developed a similar model in the R statistical software (R Core Team 2018):

$$\mathrm{ABF} = \mathrm{F_{POD}} + \mathrm{F_{POV}} + \mathrm{F_{QD1}} + \mathrm{F_{QD2}} + \mathrm{F_{QD3}} + \mathrm{F_{QD4}} + \mathrm{F_{QV}}\,, \quad (2)$$

where ABF is the anterior bite force and F_{POD}, F_{POV}, F_{QD1}, F_{QD2}, F_{QD3}, F_{QD4}, F_{QV}, are the forces generated by each subdivision of the adductor mandibulae complex. To achieve a measurement of ABF in the direction perpendicular to the jaws, a plane was created using the ABP and both jaw joint positions to generate orthogonal unit vectors. This was conducted by taking the cross product of unit vectors for the ABP and the jaw joint divided by the magnitude. New force vectors in the plane orthogonal to the ABP and jaw joint were generated by taking the dot product of the orthogonal unit vectors and the original force vectors for each muscle subdivision. This total unilateral force production was multiplied by the MA to account for the lever mechanics of the system and doubled to account for bilateral force production of the adductor mandibulae complex.

Stable isotope analysis

Muscle tissue samples were dried in an oven at 60°C for 72 h. Since lipids and nitrogenous compounds (urea and trimethylamine oxide) are known to alter both $\delta^{13}C$

and $\delta^{15}N$ values in elasmobranch muscle (Post et al. 2007; Logan and Lutcavage 2010; Hussey et al. 2012; Kim and Koch 2012), these compounds were extracted following the general recommendations of Carlisle et al. (2017). Lipids were extracted from muscle tissue samples by rinsing with petroleum ether in a Dionex Accelerated Solvent Extractor, followed by rinsing the samples with deionized water to remove nitrogenous compounds (Kim and Koch 2012). Samples were subsequently dried in an oven for 24 h at 60°C to remove any residual solvent and then homogenized using a mortar and pestle.

Approximately 600 μg of each homogenized muscle tissue sample was weighed and packed into tin capsules and then sent to the Light Stable Isotope Mass Spectrometry Lab at the University of Florida (Gainesville, FL, USA) for analysis. Carbon and nitrogen isotope composition was analyzed using a Carlo Erba NA 1500 elemental analyzer (Thermo Scientific, Waltham, MA, USA) coupled to a Thermo Delta V Advantage continuous flow isotope ratio mass spectrometer (Thermo Electron, Waltham, MA, USA). Stable isotope ratios are expressed in δ-notation as per mil (‰) using the following equation: $\delta X = [(R_{sample}/R_{standard}) - 1)] \times 1000$, where X is ^{13}C or ^{15}N and R is $^{13}C/^{12}C$ or $^{15}N/^{14}N$. The standard reference material for $\delta^{13}C$ was carbonate from Vienna Peedee Belemnite (VPDB) and atmospheric nitrogen (AIR) for $\delta^{15}N$. Analytical precision for instrumentation was ± 0.10 and ± 0.08 ‰ for $\delta^{13}C$ and $\delta^{15}N$, respectively. Instrumentation accuracy was determined based upon a USGS40 standard (L-glutamic acid), where mean (± SD) differences from certified values were 0.16 ± 0.09 ‰ for $\delta^{13}C$ and 0.20 ± 0.20 ‰ for $\delta^{15}N$ (n = 22 replicates).

Statistical analyses

All statistical analyses were performed in R ver. 3.5.1 (R Core Team 2018) and the level of significance was set at $\alpha = 0.05$. Sharks within each species were separated into small and large size classes to determine scaling relationships of bite force over ontogeny, which differed from the defined age classes for each species. Previous studies have shown that there is the potential for smaller individuals to exhibit positive allometric scaling of bite force, whereas adults may exhibit isometry (Herrel et al. 2005a; Habegger et al. 2012). To determine a threshold for where this change was likely to occur, the root of the second derivative (inflection point) was determined from the best fitting regression line of ABF versus FL. This relationship was evaluated using FL since it has been found to be a more precise measurement than TL (Kohler et al. 1996). Model selection was based upon Akaike information criterion corrected for small sample size (AIC_C) of first- through fourth-order regressions. To extend the trend that was evaluated for scaling relationships, species size thresholds were expanded by 5 cm for small and large classes of bull and blacktip sharks and by 1 cm for bonnetheads; this process included an additional two data points at most per size class.

Scaling relationships of ABF over body size (FL) were evaluated for small and large classes of individuals within each species using the allometric power function $Y = aX^b$, where a represents the y-intercept and b is the slope. This regression was fit using two different methods: reduced major axis regression (RMA) and Bayesian regression. Both methods were performed to determine if Bayesian regression may provide better or comparable estimates of scaling coefficients (especially with small sample sizes)

compared to the traditional method of RMA regression based on the variance explained by the regressions. In RMA regression, ABF and FL were log-transformed and analyzed by linear regression using the 'smatr' package (ver. 3.4-8; Warton et al. 2012) in R. The Bayesian regressions were fit using a Gaussian distribution with vague priors (on the scaling coefficients and standard deviation) on log-transformed data using the 'R2jags' package (ver. 0.5-7; Su and Yajima 2015) in R to interface with JAGS (Just Another Gibbs Sampler; Plummer 2003). Convergence of Bayesian models was assessed by chain mixing in trace plots of Markov chain Monte Carlo (MCMC), Gelman-Rubin diagnostics (potential scale reduction factors (PSRF); Gelman and Rubin 1992), and posterior predictive checks (Gelman 2004) on 30,000 draws from the posterior distribution. The pattern of scaling was determined by comparing the 95% confidence or credible intervals of the slopes obtained by RMA and Bayesian regression to the predicted slope based upon Euclidean geometry (CSAs and forces = 2; Hill 1950). Relationships were determined to be isometric if the expected slope fell within the confidence/credible intervals of the regression slope, whereas regression slope confidence/credible intervals above or below the expected slope indicated significant positive and negative allometry, respectively. Since the coefficient of determination (R^2) can exceed a value of 1.00 in Bayesian modeling due to greater variance of the predicted values compared to variance of the data, I applied the alternative method proposed by Gelman et al. (2018) to calculate R^2 for the Bayesian regressions.

Changes in $\delta^{13}C$ and $\delta^{15}N$ over FL within each species were analyzed by ordinary least squares (OLS) regression after testing for potential differences by

sampling year and between sexes; sex differences were not evaluated within bull sharks since only two females were evaluated for stable isotope analysis (SIA). Since sample sizes were unequal among sampling years, a weighted generalized least squares (GLS) ANOVA was performed. Normality and homogeneity of variance were assessed by quantile – quantile plots and plots of residuals against fitted values, respectively. A weighted GLS ANCOVA was performed on bonnethead sharks to test for differences between sexes while also accounting for body size (FL), whereas an OLS ANCOVA was performed on blacktip sharks.

Models of $\delta^{13}C$ or $\delta^{15}N$ versus FL for each species were fit by linear and polynomial regression to characterize patterns of niche shifts over ontogeny. Polynomial regressions were only selected if they exhibited significant improvements in R^2 and F values (Matich et al. 2019). Normality was assessed by quantile – quantile plots, but homogeneity of variance was not directly tested since patterns in the residuals could inform changes in niche breadth over ontogeny (Matich et al. 2019). To evaluate potential differences in niche breadth over ontogeny, absolute values of residuals from the best-fit regression model were evaluated against FL by both linear and polynomial regression; model selection followed the same process as previously described. Interpretations of these results follow Matich et al. (2019), where (1) small residuals represent limited isotopic niche breadth and large residuals indicate large niche breadth, (2) a non-significant slope represents no difference in niche breadth over ontogeny, (3) a significant negative slope indicates a decrease in niche breadth over ontogeny, and (4) a significant positive slope signifies an increase in niche breadth over ontogeny.

I also examined isotopic niche breadth of all conspecifics for each shark species using multiple niche metrics in the 'SIBER' package (ver. 2.1.3.9; Jackson et al. 2011) in R. These metrics included four of the six niche metrics recommended by Layman et al. (2007): $\delta^{13}C$ (CR) and $\delta^{15}N$ ranges (NR), total area of the convex hull (TA), and mean distance to the centroid (CD). Additionally, standard ellipse area corrected for small sample size (SEA_C) and standard ellipse area estimated via Bayesian inference (SEA_B) were also calculated as additional measures of isotopic niche breadth (Jackson et al. 2011). The SEA is the bivariate equivalent of the standard deviation for univariate data and represents *c.* 40% of the data regardless of sample size (Batschelet 1981; Jackson et al. 2011). Since TA continues to increase with growing sample sizes and therefore biases interpretations, measures of SEA were calculated to provide a more reliable comparison of a species' core isotopic niche (Jackson et al. 2011; Syväranta et al. 2013). However, TA was still calculated to provide a conservative estimate of niche breadth (Layman et al. 2012; Every et al. 2017). The SEA_B of each species was estimated using 20,000 iterations, a burn-in of 1,000 iterations, and thinned by 10 iterations for two MCMC chains, resulting in 4,000 draws from the posterior distribution for each of the parameters (covariance matrix, mean $\delta^{13}C$, mean $\delta^{15}N$). Convergence of MCMC chains was evaluated by observing trace plots and implementing the Gelman-Rubin diagnostic using the 'coda' package (ver. 0.19-1; Plummer et al. 2006) in R. To make pairwise comparisons of isotopic niche breadth between species, I calculated the percentage of draws from the posterior distribution in the species with greater mean SEA_B that were larger than the draws from the posterior distribution of the species with

lower mean SEA_B relative to the total number of draws from the posterior distribution (4,000; Daly et al. 2013; Yurkowski et al. 2018). Additionally, mean values of $\delta^{13}C$ and $\delta^{15}N$ were compared among species using weighted GLS ANOVA, which accounted for differences in sample size.

Isotopic niche overlap was evaluated using TA, SEA_C, and SEA_B to compare how each of these metrics may affect the interpretation of niche-partitioning among co-occurring species. Niche overlap of TA and SEA_C were calculated as the proportion of intersection between niche *A* and niche *B* over the total area of niche *B* (or *A*; Swanson et al. 2015). Overlap of Bayesian niche estimates (SEA_B) were calculated using the 'nicheROVER' package (ver. 1.0; Lysy et al., 2014) in R, which avoids potential problems arising from a purely geometric calculation of overlap (Swanson et al. 2015). Per the recommendation of Swanson et al. (2015), I estimated overlap of Bayesian estimated SEA using 95% ($SEA_{B(0.95)}$) and 40% (SEA_B or $SEA_{B(0.40)}$) probability niche regions since the size of the niche region will affect the probability of overlap. Although the $SEA_{B(0.95)}$ is the suggested niche size for this analysis, $SEA_{B(0.40)}$ was also assessed since this estimate had already been calculated and is the SEA proposed by Jackson et al. (2011). These measures of overlap were calculated with directionality, as was performed for TA and SEA_C.

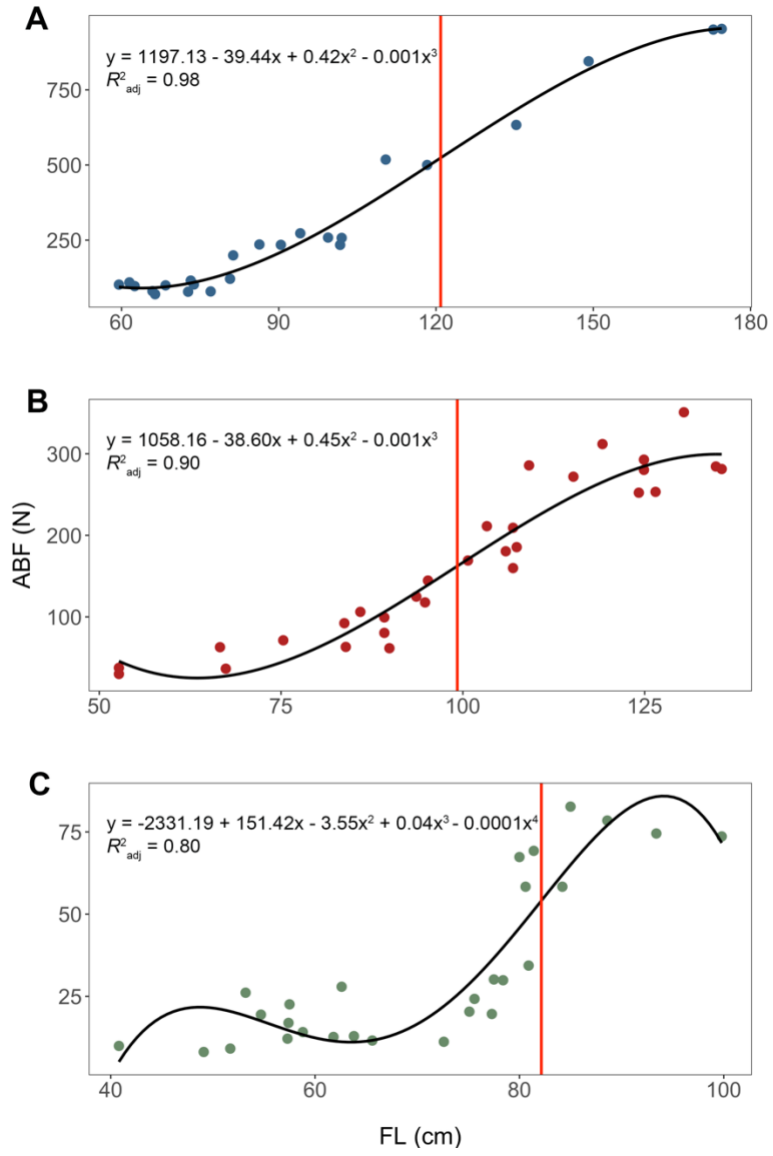

Figure 2-1. Polynomial regressions were fit to the relationship between anterior bite force (ABF) and fork length (FL) within (**A**) bull, (**B**) blacktip, and (**C**) bonnethead sharks. The best-fitting regressions were used to determine the root of the second derivative (inflection point) for each species (vertical red lines), which would dictate the threshold of small and large size classes for the analysis of scaling relationships of ABF over ontogeny.

Results

Scaling of bite force

Theoretical measures of bite force displayed prominent sigmoid patterns over ontogeny within all three species, with greater than 10-fold increases in bite force across all species. For a given body size, bite force was greatest in bull sharks, followed by blacktip and bonnethead sharks. Bite force values ranged from 70.22 to 952.97 N in bull sharks, 29.96 to 350.86 N in blacktip sharks, and 8.10 to 82.69 N in bonnethead sharks (Figure 2-1).

Table 2-2. Summary information for model selection among linear and polynomial regressions for bull shark anterior bite force (ABF) versus fork length (FL)

Model	K	Log-likelihood	AIC_C	ΔAIC_C	R^2_{adj}
$ABF \sim FL + FL^2 + FL^3$	5	-122.71	258.76	0	0.98
$ABF \sim FL + FL^2 + FL^3 + FL^4$	6	-122.70	262.35	3.59	0.97
$ABF \sim FL + FL^2$	4	-129.48	269.06	10.30	0.96
$ABF \sim FL$	3	-131.77	270.75	11.99	0.95

Table 2-3. Summary information for model selection among linear and polynomial regressions for blacktip shark anterior bite force (ABF) versus fork length (FL)

Model	K	Log-likelihood	AIC_C	ΔAIC_C	R^2_{adj}
$ABF \sim FL + FL^2 + FL^3 + FL^4$	6	-140.47	296.59	0	0.91
$ABF \sim FL + FL^2 + FL^3$	5	-142.50	297.51	0.92	0.90
$ABF \sim FL + FL^2$	4	-147.79	305.17	8.59	0.87
$ABF \sim FL$	3	-149.98	306.89	10.31	0.85

Table 2-4. Summary information for model selection among linear and polynomial regressions for bonnethead shark anterior bite force (ABF) versus fork length (FL)

Model	K	Log-likelihood	AIC_C	ΔAIC_C	R^2_{adj}
$ABF \sim FL + FL^2 + FL^3 + FL^4$	6	-105.00	225.99	0	0.80
$ABF \sim FL + FL^2$	4	-111.63	233.00	7.00	0.70
$ABF \sim FL + FL^2 + FL^3$	5	-111.08	234.89	8.90	0.70
$ABF \sim FL$	3	-114.69	236.38	10.38	0.64

Among the four regression models (first- through fourth-order) fitted to the relationship between ABF and FL used to determine the threshold for small/large size classes, higher-order models exhibited the best fit for all three species. The third-order polynomial regression fit best for the relationship in bull sharks based upon AIC_C values, whereas the fourth-order models fit best for blacktip and bonnethead sharks (Tables 2-2 – 2-4). However, the third-order model in blacktip sharks was used to derive the inflection point since it was comparable to the fourth-order model ($\Delta AIC_C = 0.92$), but more parsimonious as a result of fewer explanatory variables (Table 2-3). The root of the second derivative (inflection point) for each of the polynomial models were 120.9, 99.2, and 82.1 cm FL for bull, blacktip, and bonnethead sharks, respectively (Table 2-1; Figure 2-1).

Scaling relationships of bite force over increasing body length were generally the same when comparing among species of the same size class (small/large) but differed between these groups within each species. In small bull sharks (n = 20; 59.5 – 118.3 cm FL), ABF scaled with significant positive allometry for both RMA (slope = 3.00) and Bayesian methods (slope = 3.16; Table 2-5), but scaled with isometry (RMA: slope =

Table 2-5. Scaling relationships of anterior bite force (ABF) over fork length (FL) for small individuals of each species. Slopes calculated from reduced major axis regression (RMA) and Bayesian regression (mean) were compared against isometric relationships to determine if slopes exhibited positive allometry (P), negative allometry (N), or isometry (I) using 95% confidence intervals (CI)

Species	Method	Isometric slope	Slope (*b*)	Intercept (*a*)	R^2	95% CI	Scaling Pattern
Bull	RMA	2	3.00	-3.52	0.81	2.43 – 3.70	P
	Bayesian	2	3.16	-3.84	0.83	2.51 – 3.87	P
Blacktip	RMA	2	2.90	-3.62	0.80	2.15 – 3.90	P
	Bayesian	2	3.87	-5.54	0.80	2.47 – 5.52	P
Bonnethead	RMA	2	3.20	-4.48	0.48	2.32 – 4.41	P
	Bayesian	2	4.32	-6.56	0.62	1.83 – 9.29	I

Table 2-6. Scaling relationships of anterior bite force (ABF) over fork length (FL) for large individuals of each species. Slopes calculated from reduced major axis regression (RMA) and Bayesian regression (mean) were compared against isometric relationships to determine if slopes exhibited positive allometry (P), negative allometry (N), or isometry (I) using 95% confidence intervals (CI)

Species	Method	Isometric slope	Slope (*b*)	Intercept (*a*)	R^2	95% CI	Scaling Pattern
Bull	RMA	2	1.68	-0.78	0.95	1.33 – 2.12	I
	Bayesian	2	1.59	-0.58	0.88	0.77 – 2.55	I
Blacktip	RMA	2	2.64	-3.07	0.73	2.01 – 3.45	P
	Bayesian	2	1.95	-1.64	0.63	1.20 – 2.70	I
Bonnethead	RMA	2	1.61	-1.28	0.08	0.54 – 4.83	I
	Bayesian	2	0.72	0.46	0.17	0.04 – 1.92	N

1.68; Bayesian: slope = 1.59) for large bull sharks (n = 5; 118.3 – 174.5 cm FL; Table 2-6; Figure 2-2). Similar to small bull sharks, ABF of small blacktips (n = 16; 52.7 – 103.3 cm FL) also scaled with significant positive allometry based on both the RMA (slope =

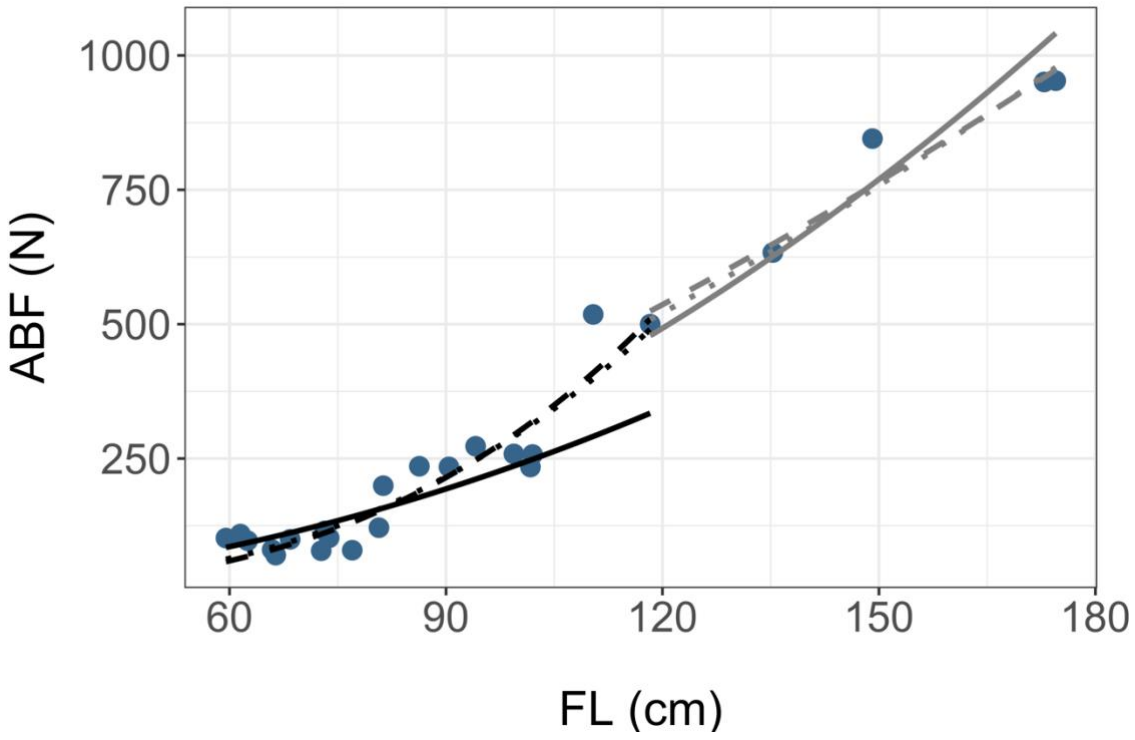

Figure 2-2. Values of anterior bite force (ABF) regressed against fork length (FL) for small (black lines) and large (gray lines) bull sharks. Solid lines denote scaling predictions based on isometric growth, dotted lines denote RMA regression estimates, and dashed lines denote Bayesian regression estimates.

2.90) and Bayesian methods (slope = 3.87; Table 2-5; Figure 2-3). Discrepancies between models were found in the scaling of ABF in large blacktip sharks (n = 18; 94.8 – 135.6 cm FL), where RMA regression indicated significant positive allometry (slope = 2.64) but Bayesian regression suggested isometry (slope = 1.95; Table 2-6; Figure 2-3). However, the 95% confidence interval for the slope of the RMA regression nearly included the isometric slope (95% CI: 2.01 – 3.45), which suggests that the scaling of ABF in large blacktips is likely isometric. Conflicting results were also found for the

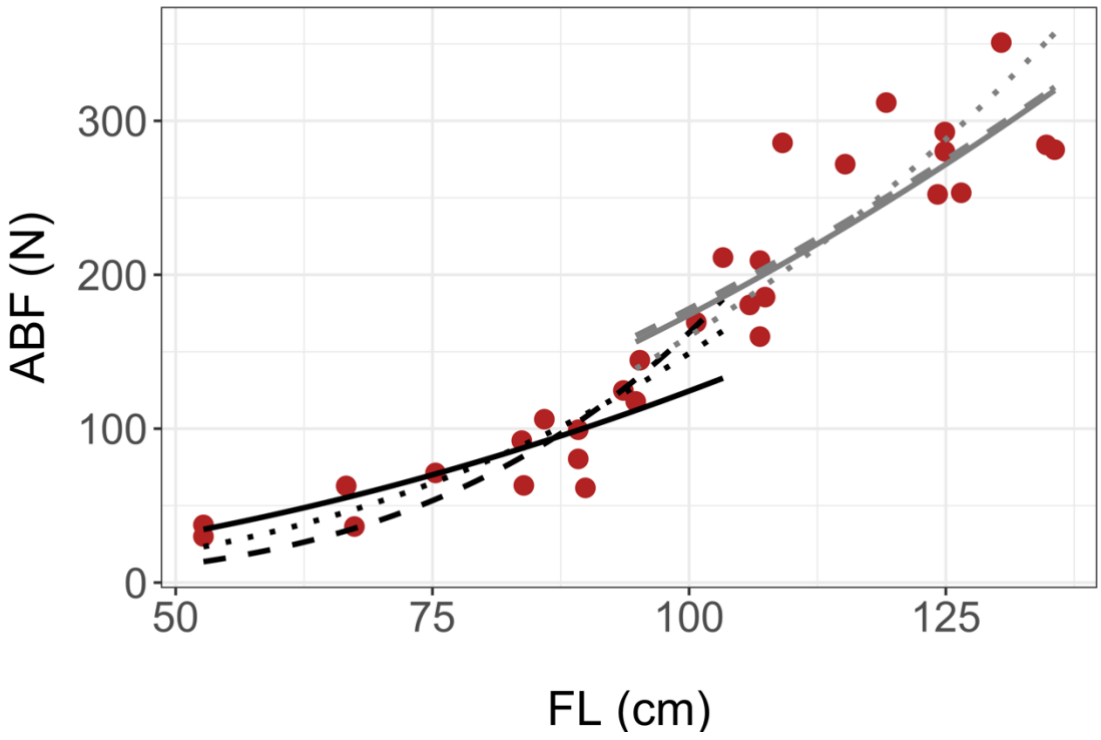

Figure 2-3. Values of anterior bite force (ABF) regressed against fork length (FL) for small (black lines) and large (gray lines) blacktip sharks. Solid lines denote scaling predictions based on isometric growth, dotted lines denote RMA regression estimates, and dashed lines denote Bayesian regression estimates.

scaling of ABF in small bonnetheads (n = 23; 40.8 – 81.4 cm FL), where RMA regression suggested significant positive allometry (slope = 3.20) but Bayesian regression suggested isometry (slope = 4.32; Table 2-5; Figure 2-4). This is due to the very wide credible interval for the slope of the Bayesian regression (95% CI: 1.83 – 9.29), which barely included the isometric slope. Therefore, it is likely that this scaling pattern exhibits significant positive allometry rather than isometry, although this may vary at an individual-level due to phenotypic plasticity (Gould 1966; Pélabon et al. 2014;

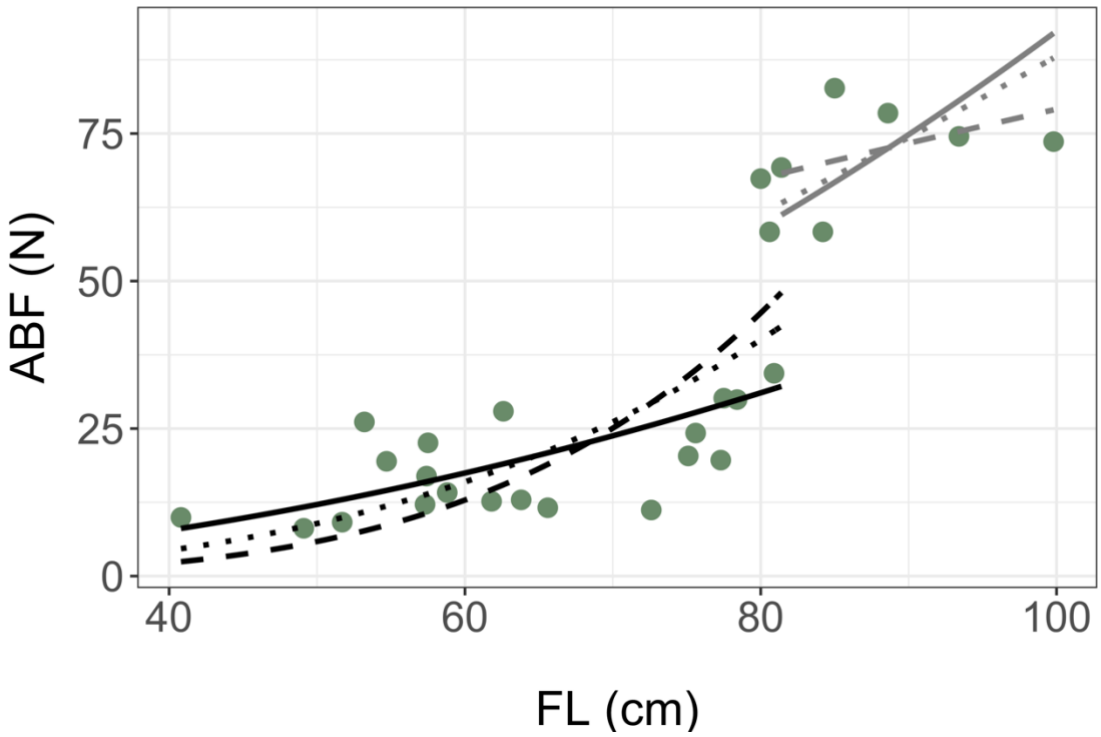

Figure 2-4. Values of anterior bite force (ABF) regressed against fork length (FL) for small (black lines) and large (gray lines) bonnethead sharks. Solid lines denote scaling predictions based on isometric growth, dotted lines denote RMA regression estimates, and dashed lines denote Bayesian regression estimates.

Araya-Ajoy et al. 2019). In large bonnethead sharks (n = 6; 81.4 – 99.8 cm FL) however, RMA regression indicated isometry (slope = 1.61) but Bayesian regression suggested negative allometry (slope = 0.72; Table 2-6; Figure 2-4). Since the credible interval for the Bayesian regression nearly included the isometric slope (95% CI: 0.04 – 1.92), large bonnetheads likely exhibit isometric scaling of ABF. Visual inspection of trace plots and posterior predictive checks indicated convergence of the MCMC chains on the posterior distribution for bite force scaling coefficients, which was corroborated by the low PSRFs

from the Gelman-Rubin diagnostic (all < 1.01).

Patterns of $\delta^{13}C$ and $\delta^{15}N$ over ontogeny

All prepared muscle samples had C:N ratios below the recommended value of 3.5 (mean ± SD: 3.2 ± 0.1), indicating that lipids were not interfering with interpretation of $\delta^{13}C$ values (Post et al. 2007). No significant differences in $\delta^{13}C$ or $\delta^{15}N$ were found among sampling years for bull ($\delta^{13}C$: $F_{3,21} = 2.36$, $p = 0.10$; $\delta^{15}N$: $F_{3,21} = 1.33$, $p = 0.29$), blacktip ($\delta^{13}C$: $F_{2,24} = 0.78$, $p = 0.47$; $\delta^{15}N$: $F_{2,24} = 0.93$, $p = 0.41$), or bonnethead sharks ($\delta^{13}C$: $F_{2,32} = 0.96$, $p = 0.39$; $\delta^{15}N$: $F_{2,32} = 1.42$, $p = 0.26$) following weighted GLS ANOVA. Additionally, no significant differences in $\delta^{13}C$ or $\delta^{15}N$ were found between sexes in blacktip ($\delta^{13}C$: $p = 0.25$; $\delta^{15}N$: $p = 0.10$) and bonnethead sharks ($\delta^{13}C$: $p = 0.84$; $\delta^{15}N$: $p = 0.34$) following OLS ANCOVA and weighted GLS ANCOVA, respectively. Differences between sexes were not tested in bull sharks due to the presence of only two females in the dataset. Since the effects of sampling year and sex were not significant, all subsequent analyses were performed on pooled samples by species.

No significant relationships of $\delta^{13}C$ ($F_{2,22} = 1.68$, $p = 0.21$) and $\delta^{15}N$ ($F_{2,22} = 3.33$, $p = 0.054$) were found over ontogeny in bull sharks. However, it appears that $\delta^{13}C$ may become depleted and then enriched over ontogeny, while $\delta^{15}N$ may become enriched until reaching an asymptote (Figure 2-5A,D). These possible isotopic patterns occur before the inflection of the ABF versus FL trend in bull sharks (Figure 2-5G). Blacktip sharks displayed slight, but significant enrichment in $\delta^{13}C$ ($F_{1,25} = 18.35$, $p = 0.0002$) and

$\delta^{15}N$ ($F_{2,24} = 6.84$, $p = 0.004$) over ontogeny (Figure 2-5B,E); however, it appears that $\delta^{15}N$ becomes depleted before increasing. Compared to the trend of ABF over increasing FL and the associated inflection point (Figure 2-5H), there did not appear to be a corresponding change in the rate of isotopic enrichment for $\delta^{13}C$ or $\delta^{15}N$ in blacktip sharks. Significant enrichment of $\delta^{13}C$ was also detected in bonnethead sharks ($F_{2,32} = 19.09$, $p < 0.0001$), which rapidly increased and appeared to reach an asymptote (Figure 2-5C). This asymptote approximately begins at the start of the rapid increase in ABF versus FL in bonnetheads (Figure 2-5I). A clear pattern was not found for $\delta^{15}N$ ($F_{1,33} = 2.68$, $p = 0.11$) in bonnethead sharks (Figure 2-5F).

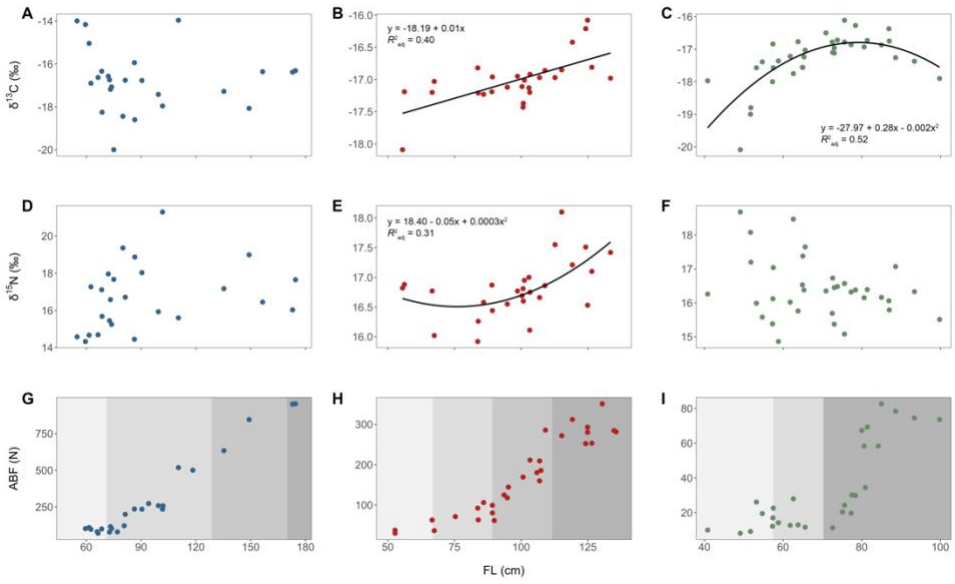

Figure 2-5. Relationships between fork length (FL) and (**A-C**) $\delta^{13}C$, (**D-F**) $\delta^{15}N$, and (**G-I**) anterior bite force (ABF) in (**A**,**D**,**G**) bull, (**B**,**E**,**H**) blacktip, and (**C**,**F**,**I**) bonnethead sharks. Only significant linear or polynomial regressions are shown for relationships between FL and stable isotopes ($\delta^{13}C$ and $\delta^{15}N$). Increasingly darker gray shading of background indicates age classes for each species; light = young-of-the-year (YoY); medium-light = juvenile; medium-dark = sub-adult; dark = adult.

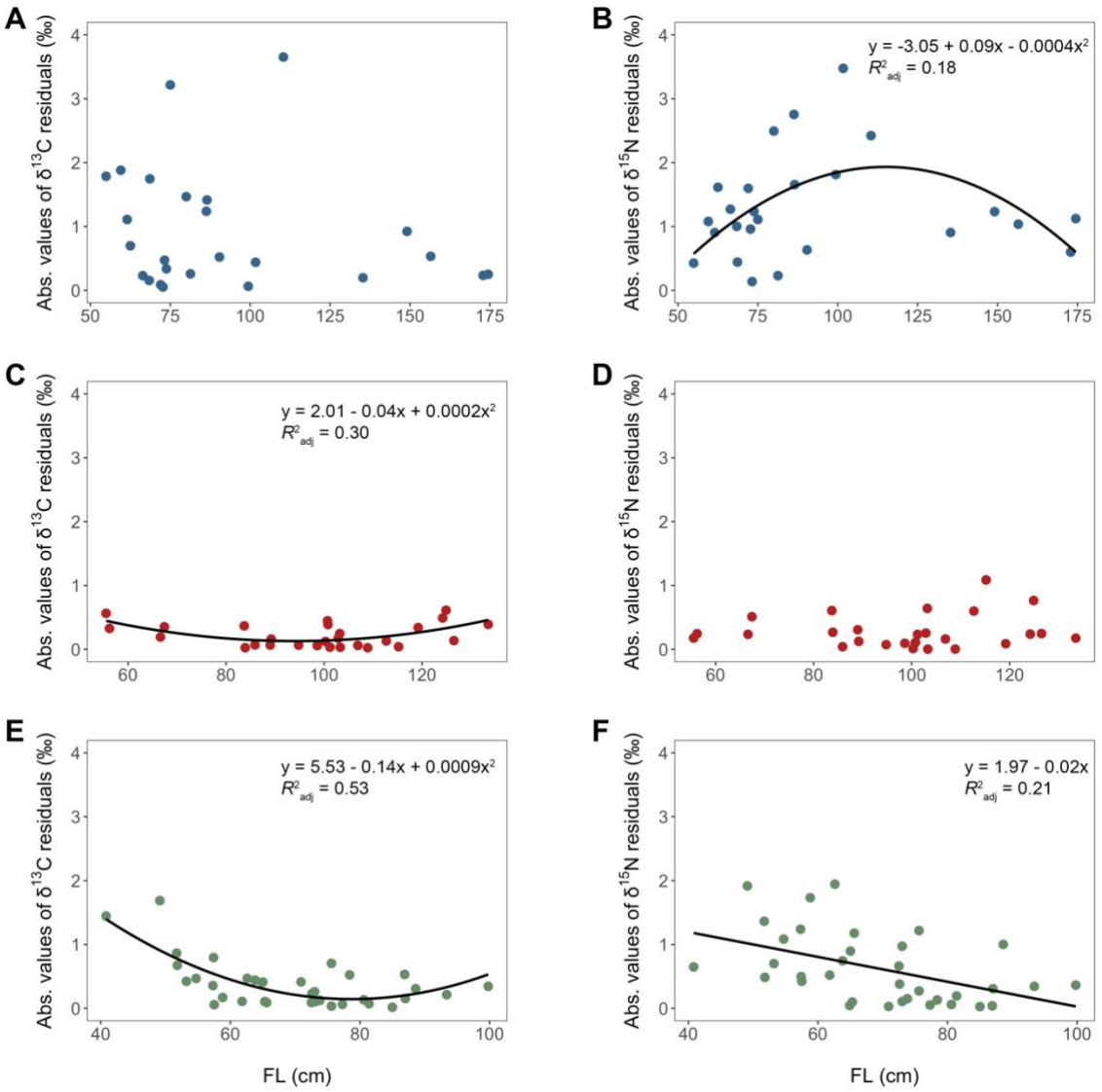

Figure 2-6. Relationships between fork length (FL) and absolute values of (**A**,**C**,**E**) $\delta^{13}C$ residuals and (**B**,**D**,**F**) $\delta^{15}N$ residuals in (**A**,**B**) bull, (**C**,**D**) blacktip, and (**E**,**F**) bonnethead sharks to evaluate ontogenetic changes in isotopic niche breadth. Only significant regressions are shown for relationships between FL and absolute values of $\delta^{13}C$ and $\delta^{15}N$ residuals.

Ontogenetic changes in isotopic niche breadth were prevalent among all species, as indicated by the residuals of the regressions for $\delta^{13}C$ and $\delta^{15}N$ against FL. Residuals of $\delta^{13}C$ did not display a significant pattern over ontogeny in bull sharks ($F_{1,23} = 0.93$, $p = 0.34$; Figure 2-6A), but showed a possible negative relationship with the exception of an outlier. However, residuals of $\delta^{15}N$ did exhibit a significant parabolic trend, where niche breadth was greatest within juveniles ($F_{2,22} = 3.64$, $p = 0.043$; Figure 2-6B). Likewise, a significant pattern in $\delta^{13}C$ residuals of blacktip sharks over ontogeny was found ($F_{2,24} = 6.49$, $p = 0.006$; Figure 2-6C), where niche breadth was highest at YoY and adult size classes. Residuals of $\delta^{15}N$ did not display a significant shift over ontogeny in blacktip sharks ($F_{1,25} = 0.36$, $p = 0.56$; Figure 2-6D). Bonnethead sharks displayed significant decreases in residuals of $\delta^{13}C$ ($F_{2,32} = 19.97$, $p < 0.0001$) and $\delta^{15}N$ ($F_{1,33} = 9.80$, $p = 0.004$) over ontogeny (Figure 2-6E,F), where the lowest $\delta^{13}C$ residuals were measured at the same body size as the rapid increase in bonnethead shark ABF (Figure 2-5I). By comparison, the extent of variability in the residuals for both isotopes was much lower in blacktip sharks than bonnethead sharks and bull sharks.

Isotopic niche breadth and overlap

No significant differences in $\delta^{13}C$ ($F_{2,84} = 2.19$, $p = 0.12$) or $\delta^{15}N$ ($F_{2,84} = 2.59$, $p = 0.081$) were found among these three shark species in Galveston Bay, TX. Additionally, the CR and NR were nearly identical to one another on a per species basis, where isotopic ranges were greatest in bull sharks and smallest in blacktip sharks (Table 2-7; Figure 2-7). Bull sharks also had the greatest CD, TA, SEA_C, and SEA_B, followed

Table 2-7. Summary of $\delta^{13}C$ and $\delta^{15}N$ (mean ± SD), $\delta^{13}C$ (CR) and $\delta^{15}N$ ranges (NR), mean distance to centroid (CD), total area of the convex hull (TA), standard ellipse area corrected for small sample size (SEA_C), and mean standard ellipse area from Bayesian estimation (SEA_B) for all shark species sampled from Galveston Bay, Texas, USA

Species	$\delta^{13}C$ (‰)	$\delta^{15}N$ (‰)	CR (‰)	NR (‰)	CD (‰)	TA ($‰^2$)	SEA_C ($‰^2$)	SEA_B ($‰^2$)
Bull	-16.76 ± 1.44	16.71 ± 1.76	6.04	6.96	1.86	21.16	6.47	6.61
Blacktip	-17.01 ± 0.38	16.80 ± 0.48	2.01	2.18	0.49	2.51	0.58	0.58
Bonnethead	-17.29 ± 0.79	16.41 ± 0.88	3.98	3.82	0.93	7.93	1.86	1.88

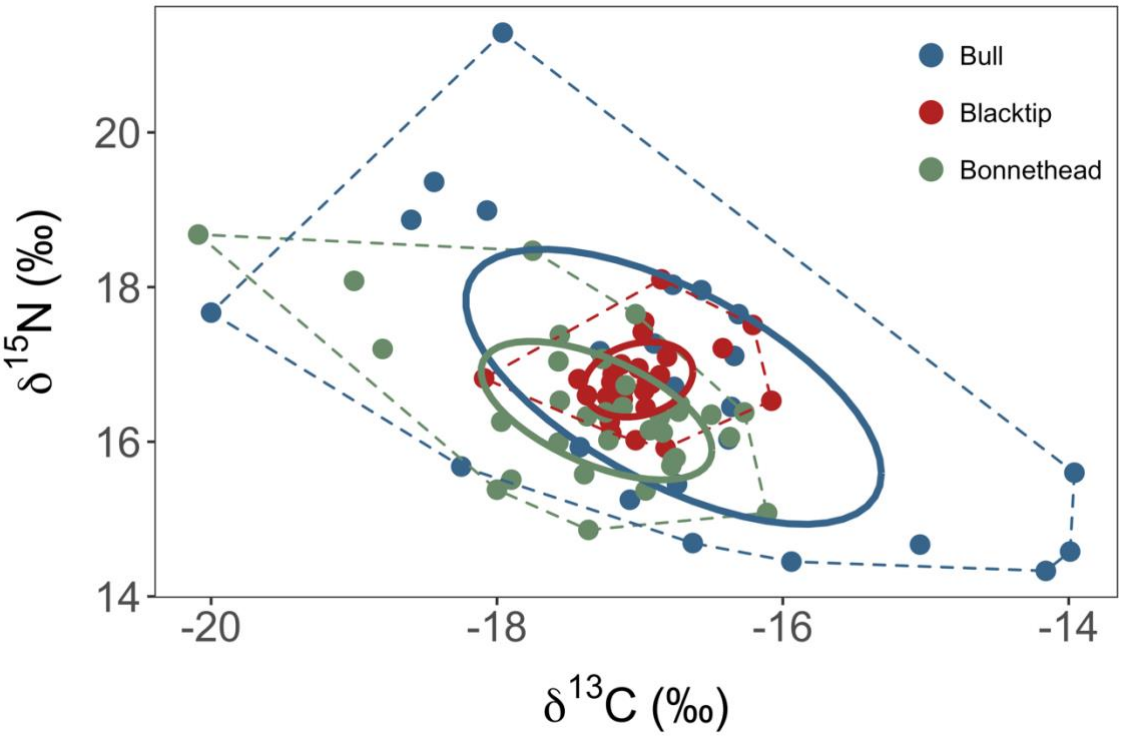

Figure 2-7. Isotopic biplot of niche space occupied by bull, blacktip, and bonnethead sharks using $\delta^{13}C$ and $\delta^{15}N$. Total area (TA) of convex hulls that enclose the maximum extent of niche space are identified by dashed lines. Standard ellipse areas (SEAs) that represent *c*. 40% of core niche area are denoted by solid lines.

by bonnethead and then blacktip sharks (Table 2-7; Figure 2-7; Figure 2-8). Visual inspection of trace plots and low PSRFs from the Gelman-Rubin diagnostic (all ≤ 1.01) indicated that MCMC chains converged for SEA_B estimates of each species. The probability that SEA_B size was greater in bull sharks (mean SEA_B = 6.63 ‰^{2}) was 100.00% compared to blacktip sharks (mean SEA_B = 0.58 ‰^{2}) and 99.83% compared to bonnethead sharks (mean SEA_B = 1.87 ‰^{2}; Figure 2-8). There was a 98.2% probability that bonnethead shark SEA_B size was greater than the niche size of blacktip sharks.

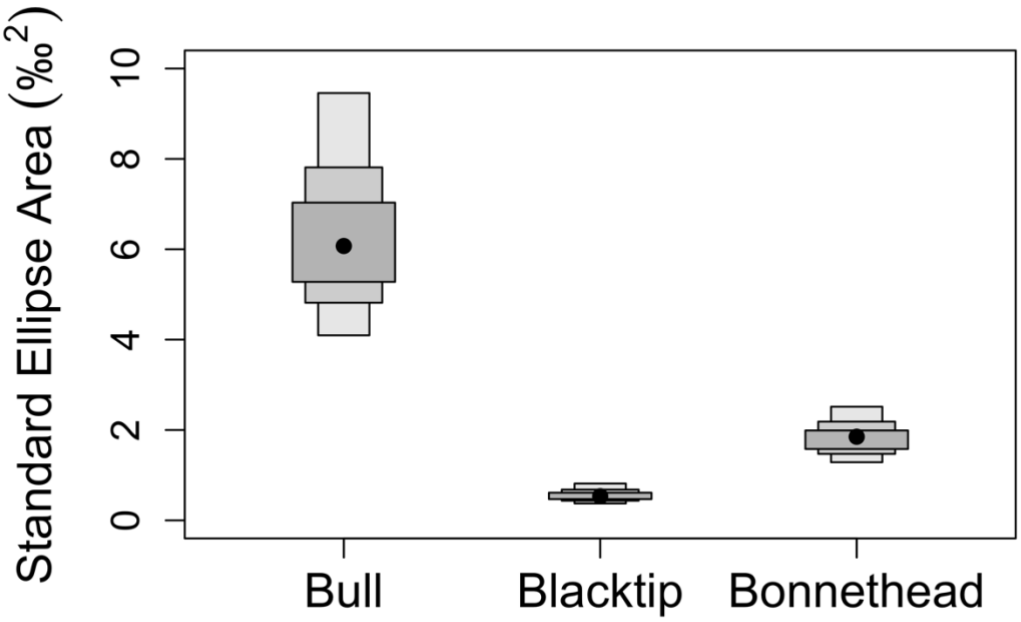

Figure 2-8. Estimates of standard ellipse area via Bayesian inference (SEA_B) for each species based upon $\delta^{13}C$ and $\delta^{15}N$. Shaded boxes represent 50, 75, and 95% Bayesian credible intervals from dark to light gray and black dots represent the mode of the posterior distributions.

The extent of niche overlap varied widely among pairwise species comparisons and also varied based upon the niche metric used. The greatest levels of overlap were measured using the $SEA_{B(0.95)}$ metric, followed by TA, SEA_C, and $SEA_{B(0.40)}$ (Table 2-8). The overlap of blacktip shark niche area onto bull shark niche area was consistently the highest extent of overlap measured for all metrics used and ranged from 89.40 to 100.00%. This was followed closely by the overlap of bonnethead shark niche area onto bull shark niche area, which ranged from 57.38 to 99.10%. Overlap of blacktip shark niche area onto bonnethead shark niche area (range: 48.12 – 94.44%) was much greater than bonnethead shark niche area onto blacktip shark niche area (range: 9.96 – 45.98%). Bull sharks displayed the lowest levels of niche area overlap onto blacktip shark niche area (range: 4.29 – 21.54%), whereas overlap onto bonnethead shark niche area ranged from 11.08 to 49.65%).

Table 2-8. Isotopic overlap (%) of convex hull total areas (TA), standard ellipse areas corrected for small sample size (SEA_C), and mean standard ellipse areas (95% credible interval) estimated with Bayesian inference for 40% ($SEA_{B(0.40)}$) and 95% niche regions ($SEA_{B(0.95)}$) among shark species. Overlap is represented as the percentage of the isotopic niche of species *a* within the isotopic niche of species *b*

Species comparison (*a* × *b*)	TA	SEA_C	$SEA_{B(0.40)}$	$SEA_{B(0.95)}$
Bull × Blacktip	11.88	8.99	4.29 (2.40 – 6.97)	21.54 (13.29 – 32.67)
Bull × Bonnethead	35.81	24.88	11.08 (6.34 – 17.70)	49.65 (32.85 – 68.50)
Blacktip × Bull	100.00	100.00	89.40 (71.72 – 98.91)	99.98 (99.79 – 100.00)
Blacktip × Bonnethead	67.85	59.54	48.12 (28.16 – 69.88)	94.44 (81.84 – 99.79)
Bonnethead × Bull	95.49	86.37	57.38 (31.92 – 83.52)	99.10 (94.95 – 100.00)
Bonnethead × Blacktip	21.49	18.58	9.96 (5.35 – 16.48)	45.98 (30.64 – 63.18)

Discussion

This study demonstrates that scaling patterns of bite force differ between small and large size classes of bull, blacktip, and bonnethead sharks, which supports the findings of Habegger et al. (2012). Smaller sharks exhibited significant positive allometric scaling, whereas larger sharks displayed isometric scaling of bite force. This suggests that rapid increases in ABF are especially important at small sizes, which could allow greater access to dietary resources compared to co-occurring predators that experience isometric ontogenetic trajectories (Hernandez and Motta 1997; Kolmann and Huber 2009; Habegger et al. 2012). Once sharks attain large body sizes, selection pressure on maximal bite force is likely relaxed due to the ability of these predators to puncture or crush most prey items (Aguirre et al. 2003; Herrel and Gibb 2006; Huber et al. 2009). However, this may not necessarily be the case for durophagous bonnethead sharks, which do not necessarily crush the carapace of large crab prey before consumption and may rely more heavily on chemical digestion (Myrberg and Gruber 1974; Wilga and Motta 2000; Mara et al. 2010; Jhaveri et al. 2015). This pattern of positive allometric scaling followed by isometric scaling of bite force differs from the majority of other studies that have evaluated fishes (Huber et al. 2005; Huber et al. 2006; Huber et al. 2008; Habegger et al. 2011; Grubich et al. 2012; but see Herrel et al. 2005a and Habegger et al. 2012), reptiles (Meyers et al. 2002; Erickson et al. 2003; Jones and Lappin 2009; Marshall et al. 2012; Erickson et al. 2014; Marshall et al. 2014; but see Herrel and O'Reilly 2006), birds (van der Meij and Bout 2004; Herrel et al. 2005b), and mammals (Binder and Van Valkenburgh 2000; Thompson et al. 2003; Becerra et al.

2011; Law et al. 2016; Santana and Miller 2016). Since most of these other studies have evaluated all conspecifics together, any potential size-specific differences in scaling patterns have been obscured (Habegger et al. 2012). Therefore, future studies should evaluate juveniles and adults separately before pooling together in the analysis of ontogenetic scaling patterns.

For bull and blacktip sharks, the mean maximum force required by their teeth to puncture teleost or elasmobranch prey was 40.93 N and 17.08 N, respectively (Whitenack and Motta 2010). Since these forces are achieved by even the smallest conspecifics measured in the present study (bull: 70.22 N, blacktip: 29.96 N), other contributing factors likely influence the ability of these sharks to consume potential prey. These factors may include greater forces required to fracture skeletal elements of prey, as well as the capability to maintain a firm grip on large prey during lateral head-shaking behavior for the removal of smaller-sized pieces (Huber et al. 2006; Habegger et al. 2012). High bite forces in lacertid lizards corresponded with increased prey handling efficiency (Herrel et al. 2001; Verwaijen et al. 2002). A similar pattern was found in finches with respect to seed husking time (van der Meij and Bout 2006). This would result in an increase in net energy intake for an individual and would likely enhance fitness (Emerson et al. 1994; Anderson et al. 2008; Pfaller et al. 2011; Timm 2013). Some sharks may also exhibit this relationship, but this has yet to be directly tested.

The change in ABF scaling occurred at different relative age classes in each species, which may indicate that age or maturity status are not driving this transition. Based on von Bertalanffy growth curves for each species, the estimated age where this

change in ABF occurred was approximately 7+ years in bull sharks (Branstetter and Stiles 1987), 3+ years in blacktip sharks (Branstetter 1987), and 5.5+ years in bonnethead sharks (Lombardi-Carlson et al. 2003). In bull and blacktip sharks, this change occurs at approximately the transition from juvenile to sub-adult age classes (Branstetter 1987; Branstetter and Stiles 1987), but occurs after all individuals have likely matured in bonnethead sharks (Lombardi-Carlson et al. 2003). Therefore, age and maturity status do not appear to be major drivers of the shift in bite force scaling. Instead, a relationship between bite force and ecological transitions (i.e. habitat and diet shifts) over the ontogeny of each species may be present.

Multiple sources of ecological data for bull sharks from the present study and prior studies strongly support a shift in habitat and diet prior to the change in bite force scaling pattern from positive allometry to isometry. YoY bull sharks use the freshwater-influenced upper reaches of bays and estuaries as nursery habitats and move progressively towards marine environments as they get larger (Werry et al. 2011). Sub-adult bull sharks commonly occupy the lower reaches of bays and estuaries as well as coastal habitats, whereas adult bull sharks are found predominantly in marine habitats, although gravid females may enter bays and estuaries before parturition (Werry et al. 2011). This freshwater to marine transition was observed by shifts in both $\delta^{13}C$ and trace elements in their vertebrae, with a rapid transition occurring at approximately 130 cm TL (~ 104 cm FL; Werry et al. 2011). The transition measured by Werry et al. (2011) occurs towards the end of the positive allometric scaling phase of ABF in bull sharks found in the present study. This may facilitate the shift in habitat and diet of bull sharks

by allowing them to consume prey in new habitats that are larger or more difficult to process (e.g., puncture), but also provide a greater source of energy for growth and development (Snover 2008; Habegger et al. 2012; Hussey et al. 2017). Similarly, the present study showed a similar pattern over ontogeny where the $\delta^{13}C$ values were highly enriched at the neonate stage, rapidly depleted during the YoY stage, and increased again in juveniles, sub-adults, and adults. Enriched $\delta^{13}C$ in neonates is likely a result of a maternal isotopic signal that could interfere with the ecological interpretation of these data (McMeans et al. 2009; Matich et al. 2010; Olin et al. 2011; Belicka et al. 2012). The isotopic turnover rate of elasmobranch muscle has been measured on the scale of months (MacNeil et al. 2006; Kim et al. 2012; Malpica-Cruz et al. 2012; Caut et al. 2013), but this is assumed to be more rapid in young, fast-growing conspecifics (Malpica-Cruz et al. 2012; Vander Zanden et al. 2015). Therefore, a lag between the diet and isotopic signal should be considered in these interpretations. Similar to the pattern in $\delta^{15}N$ measured by Werry et al. (2011), the present study also found a curvilinear trend of increasingly enriched $\delta^{15}N$ over ontogeny that reached an asymptote. This pattern is likely a result of bull sharks reaching their highest trophic position in the food web (Werry et al. 2011; Daly et al. 2013). This trend differed from measurements in other studies that showed slight parabolic patterns (Matich et al. 2010; Gallagher et al. 2017) but were both measured in bull sharks from the same locale (Everglades National Park, Florida Bay). No maternal isotopic signal was observed in the $\delta^{15}N$ measurements in YoY individuals, which may result from these young sharks feeding from an equivalent $\delta^{15}N$ baseline compared to the habitat of their mothers (Olin et al. 2011). Werry et al.

(2011) also found that bull sharks larger than 120 cm TL (~ 96 cm FL) displayed an increase in their dietary breadth that included the consumption of larger prey, including greater proportions of elasmobranchs, reptiles, and birds. The inclusion of a greater proportion of functionally difficult prey may be facilitated by the positive allometric scaling of bite force, allowing smaller sharks to potentially consume these prey years sooner than if bite force scaled isometrically (Habegger et al. 2012).

Unlike bull sharks, blacktip sharks did not appear to demonstrate major shifts in habitat or diet in association with bite force. No changes in isotopic patterns were found to precede or follow the change in scaling pattern of ABF in blacktip sharks, where only a slight change in habitat and diet was found. This aligns with numerous studies in vertebrates, where there is a lack of association between diet and changes in bite force (Huber et al. 2006; Fry et al. 2009; Habegger et al. 2011; Ferguson et al. 2015; Habegger et al. 2017). YoY and juvenile blacktip sharks are typically found in the brackish waters of estuaries and bays as part of their nursery habitat before moving into nearshore coastal habitats as sub-adults and adults (Castro 1996; Heupel and Hueter 2002; Hoffmayer and Parsons 2003; Bethea et al. 2004; Froeschke et al. 2010). No maternal signal was observed for $\delta^{13}C$ in this species in the present study, where the range in observed values was ~2 ‰. The increase in $\delta^{13}C$ over ontogeny is likely a result of moving from estuarine nursery habitats to coastal areas as well as an increase in trophic position, which are both expected to be result in a more enriched $\delta^{13}C$ signal (Peterson and Fry 1987; Garcia et al. 2007; Pethybridge et al. 2018). A significant quadratic relationship in $\delta^{15}N$ over ontogeny displayed the loss of a maternal isotopic signature in

YoY blacktips, which then became more enriched in juvenile through adult stages. Similar to $\delta^{13}C$, there was only a small difference (~2 ‰) between the minimum and maximum $\delta^{15}N$ values measured. This may also indicate a slight dietary shift, or possibly a shift in baseline $\delta^{15}N$ in the diet of these age classes. Previous studies of blacktip shark stomach contents found only minor changes in prey composition of their diet over ontogeny, which did not necessarily result in a change in the material properties of their primarily sciaenid and clupeid prey (Castro 1996; Hoffmayer and Parsons 2003; Bethea et al. 2004; Barry et al. 2008). Despite not including a greater proportion of functionally difficult prey over ontogeny, blacktip sharks consume increasingly larger prey (> 20% FL) that may require greater force to maintain a firm grasp prior to consumption (Bethea et al. 2004). This also includes the occasional inclusion of elasmobranchs in the diet of large adults (3-4% occurrence in stomachs; Castro 1996; Hoffmayer and Parsons 2003). It is possible that the change in scaling of ABF over ontogeny may be a phylogenetically-constrained pattern that this species only rarely takes advantage (Gould 1966; Pélabon et al. 2013, 2014; Araya-Ajoy et al. 2019).

A shift in the habitat of bonnethead sharks appeared to precede the change in the pattern of ABF scaling, but did not show a clear change with diet. Similar to the space use of blacktip sharks, bonnethead sharks also grow and develop in brackish estuaries and bays before moving into coastal marine habitats (Froeschke et al. 2010; Bethea et al. 2015). This habitat shift is also associated with an increasing reliance on benthic prey species as adults, including blue crabs (*Callinectes sapidus*) and other crustaceans (Cortés et al. 1996; Bethea et al. 2007; Plumlee and Wells 2016). The trend of

decreasing $\delta^{13}C$ in the largest bonnethead sharks in the present study may be the result of a seasonal movement offshore to follow migrating blue crabs during spawning periods (Heupel et al. 2006; Driggers et al. 2014; Plumlee and Wells 2016). Bonnethead sharks include an increasing proportion of blue crabs in their diet over ontogeny, and this is best characterized as a quadratic relationship between predator and prey body size (Cortés et al. 1996). Carapace length of consumed crabs began to rapidly increase at approximately 60 cm pre-caudal length (~65 cm FL) of shark body size, which precedes the rapid increase in ABF of bonnethead sharks. However, a large increase in bite force may not be necessary to consume all crab prey because approximately 20% of crabs found in the stomachs of juvenile bonnetheads (~60 – 75 cm FL) could not be crushed by sharks in this size range (Mara et al. 2010). Therefore, this large increase in ABF may only occur in adult bonnethead sharks to provide greater access to much larger crabs than could be consumed by YoY and juveniles due to bite force or gape limitations. This may be an additional source of resource partitioning within this species, as well as with other durophagous competitors.

Isotopic niche breadth differed over ontogeny but did not necessarily follow the hypothesized patterns by species. Although the relationship between absolute values of $\delta^{13}C$ residuals and FL was not significant in bull sharks, a noticeable pattern did appear to emerge. With the exception of an outlier, the data suggest a negative quadratic relationship of niche breadth (via $\delta^{13}C$ residuals) over FL in bull sharks similar to that found by Matich et al. (2019). This pattern also appeared in blacktip sharks and bonnethead sharks, and these relationships were significant for both species. Rather than

a true change in niche breadth (of carbon sources) over ontogeny, this relationship may reflect the loss of the maternal isotopic signal in YoY individuals. Unlike the trend for residuals of $\delta^{13}C$, true changes in niche breadth may be present in the absolute residuals of $\delta^{15}N$ over ontogeny. A significant parabolic relationship was found in bull sharks, where isotopic niche breadth of $\delta^{15}N$ was lowest in YoY and sub-adult/adult conspecifics and was greatest in juveniles. Matich et al. (2019) reported a negative relationship for $\delta^{15}N$-derived niche breadth over ontogeny in bull sharks, which may reflect differences in resource availability between Galveston Bay, TX and Shark River Estuary, FL. The high $\delta^{15}N$-derived niche breadth of juveniles in the present study may be due to specialization at the individual level (Bolnick et al. 2003; Svanbäck and Bolnick 2007; Araújo et al. 2011; Matich et al. 2011). Positive allometric scaling of bite force may facilitate this divergence in dietary specialization by providing these conspecifics access to a greater diversity of potential prey items. There is also the possibility that this pattern could be a result of a shift in habitat from the upper to lower reaches of Galveston Bay as part of their life history, which exhibit different $\delta^{15}N$ baselines (Holt and Ingall 2000; Barcenas 2013). Decreasing $\delta^{15}N$-derived niche breadth over the ontogeny of bonnethead sharks is likely the result of specialization on crabs (e.g. *C. sapidus*). Young sharks are unskilled foragers that rely upon intrinsic energy stores (maternal resource dependency) and opportunistically feed upon available prey that they can capture (Belicka et al. 2012; Newman et al. 2012). Once they become more proficient foragers, sharks are expected to become more selective in their prey choice (Belicka et al. 2012; Newman et al. 2012). Unlike YoY conspecifics, juvenile and adult

bonnetheads do consume greater proportions of crabs and some other crustaceans (Cortés et al. 1996; Bethea et al. 2007). No ontogenetic patterns in $\delta^{15}N$-derived niche breadth were found in blacktip sharks in the present study, which may reflect their consistent piscivory on species such as Atlantic croaker (*Micropogonias undulates*) and gulf menhaden (*Brevoortia patronus*; Hoffmayer and Parsons 2003; Bethea et al. 2004; Barry et al. 2008; Plumlee and Wells 2016).

Bull sharks occupied the greatest niche breadth among the shark species investigated, which was contrasted by the narrow niche breadth of blacktip and bonnethead sharks. Bull sharks are well-documented generalists at the population level (Snelson et al. 1984; Cliff and Dudley 1991; Werry et al. 2011), which was supported by the high values calculated for CR, NR, CD, TA, SEA_C, and SEA_B. Previous studies measuring the isotopic niche of bull sharks did not necessarily share similar values for the same niche metrics, but they did observe large niche breadths in this species across different life stages (Daly et al. 2013; Every et al. 2017; Gallagher et al. 2017). Bonnethead sharks possessed the next greatest niche breadth as supported by all six niche metrics, but these values were closer to those measured in blacktips than bull sharks. This corroborated the results of Gallagher et al. (2017), which measured significantly smaller niche width in blacktips compared to bull sharks. Although measures of SEA_C and SEA_B likely provide more robust estimates compared to the other metrics, it appears that any of these metrics would be suitable for general comparisons in niche breadth among species.

The generalist diet of bull sharks may be supported by the large bite forces they achieve, which is much greater than the force required to puncture their putative prey even after one year of growth. The tooth morphology of this species also suggests a generalist diet, where the high extent of heterodonty in bull sharks can be used to shear pieces of tissue from large prey items or prey that are otherwise functionally difficult to consume (Cullen and Marshall 2019). By comparison, the smaller niche breadth of bonnethead sharks appears much more similar in size to blacktip sharks, especially when not including the outlier YoY bonnethead sharks. This finding supports natural history data that blacktip sharks and bonnethead sharks specialize in piscivory and durophagy, respectively (Barry et al. 2008; Plumlee and Wells 2016). Both of these species also possessed a dentition that is expected to be best-suited to their dietary preferences, with gracile teeth present in blacktip sharks and molariform teeth found in bonnethead sharks (Cullen and Marshall 2019). However, the relationship between absolute bite force and diet is not as clear. A phylogenetically-informed regression conducted by Habegger et al. (2012) found that chondrichthyans with greater body mass consumed a lower percentage of decapod crustaceans and occupied high trophic positions. Therefore, traits that separate dietary generalists from specialists needs to be investigated further, particularly with respect to bite force capability.

The extent of isotopic niche overlap varied by niche metric, but generally showed a pattern of bull sharks largely overlapping with niche space of both blacktip sharks and bonnethead sharks. The percentage of overlap was greatest when measured using the TA or $SEA_{B(0.95)}$ metrics, which were also the most conservative estimates of niche breadth.

The extent of overlap was similar when using SEA_C or $SEA_{B(0.40)}$, which both represented the core niche of each species and estimated lower levels of overlap between species. Since teleost prey represent a major prey item of both bull and blacktip sharks, it is not surprising that the entire isotopic niche of blacktip sharks is within that of bull sharks since the latter species is a generalist. Despite the small proportion of benthic invertebrates consumed by bull sharks (Snelson et al. 1984; Cliff and Dudley 1991), the isotopic niche of this species exhibited a high level of overlap with bonnethead sharks. Since the isotopic niches of these species are only measured in two dimensions, this is likely an artifact of not including a more discriminating isotopic marker (i.e. $\delta^{34}S$) for differentiating prey from benthic environments relative to water column species (Plumlee and Wells 2016; Rossman et al. 2016). The moderate level of overlap of bonnethead sharks onto blacktip sharks is likely reflective of the same issues faced when comparing the former against bull sharks. Plumlee and Wells (2016) found a significant difference in $\delta^{34}S$ between blacktip sharks and bonnethead sharks, where $\delta^{34}S$ was more depleted in bonnethead sharks than blacktip sharks. This is indicative of bonnethead sharks primarily foraging on epibenthic prey, whereas blacktip sharks forage higher in the water column (Peterson and Fry 1987; Plumlee and Wells 2016). While the present study did not measure $\delta^{34}S$, this evidence supports the premise that niche overlap is lower than calculated between the epipelagic (bull and blacktip sharks) and demersal species (bonnethead sharks).

Scaling patterns of bite force in bull, blacktip, and bonnethead sharks were consistent across species and were also used to characterize ontogenetic niche shifts.

Scaling coefficients of bite force over ontogeny were mostly consistent between both methods that were used (RMA and Bayesian regression), but instances where they differed show that interpretation of these data may benefit from using multiple approaches to weigh the uncertainty of these estimates. Associations between bite force and ontogenetic niche shifts in habitat and diet were found in bull and bonnethead sharks, but not in blacktip sharks. The lack of major changes in habitat or diet in blacktips with significant positive allometry of bite force may be the result of a phylogenetically-constrained process, which warrants further investigation. All three species appeared to exhibit a habitat shift from nurseries within Galveston Bay to coastal habitats in the Gulf of Mexico based upon changes in $\delta^{13}C$, which occurred concurrently with increases in trophic position in bull and blacktip sharks and a specialization of bonnetheads on low trophic level crustaceans. Additionally, maternal isotopic signals were observed in the YoY of all three species, which precluded the characterization of resource use from stable isotopes alone. The variability of $\delta^{13}C$ and $\delta^{15}N$ residuals provided useful indicators of niche breadth over ontogeny, particularly if sample sizes of separate age classes are too small to compare niche breadth. All six quantified metrics of niche breadth of all species confirmed the generalist strategy of bull sharks and specialization of blacktip and bonnethead sharks, where estimates using SEA_C or SEA_B provided similar and robust measurements compared to the other metrics. Niche overlap between bonnethead sharks and the other two species was higher than expected using $\delta^{13}C$ and $\delta^{15}N$ isotopes, but this finding would likely be lower if a more discriminating biochemical tracer such as $\delta^{34}S$ (Plumlee and Wells 2016) was used. Future studies

should evaluate net energy intake of primary prey items within each species to determine if changes in energetic requirements over ontogeny (with changes in body size and metabolic state) are important drivers of bite force scaling and ontogenetic niche shifts. The present study benefited from an ecomechanics perspective that is rare in the literature and made connections between feeding performance and trophic ecology.

References

Aguirre LF, Herrel A, Van Damme R, Matthysen E. 2002. Ecomorphological analysis of trophic niche partitioning in a tropical savannah bat community. *Proc. R. Soc. B Biol. Sci.* 269:1271–1278. doi:10.1098/rspb.2002.2011.

Aguirre LF, Herrel A, Van Damme R, Matthysen E. 2003. The implications of food hardness for diet in bats. *Funct. Ecol.* 17:201–212.

Anderson RA, Mcbrayer LD, Herrel A. 2008. Bite force in vertebrates: opportunities and caveats for use of a nonpareil whole-animal performance measure. *Biol. J. Linn. Soc.* 93:709–720. doi:10.1111/j.1095-8312.2007.00905.x.

Araújo MS, Bolnick DI, Layman CA. 2011. The ecological causes of individual specialisation. *Ecol. Lett.* 14:948–958. doi:10.1111/j.1461-0248.2011.01662.x.

Araya-Ajoy YG, Ranke PS, Kvalnes T, Rønning B, Holand H, Myhre AM, Pärn H, Jensen H, Ringsby TH, Sæther BE, et al. 2019. Characterizing morphological (co)variation using structural equation models: Body size, allometric relationships and evolvability in a house sparrow metapopulation. *Evolution (N. Y).* 73:452–466. doi:10.1111/evo.13668.

Barcenas DL. 2013. Use of stable isotope analyses to describe trophic dynamics of aquatic ecosystems in Galveston Bay, Texas. MS Thesis. University of Houston Clear Lake, Clear Lake, TX.

Barry K, Condrey R, Driggers W, Jones C. 2008. Feeding ecology and growth of neonate and juvenile blacktip sharks Carcharhinus limbatus in the Timbalier-Terrebone Bay complex, LA, U.S.A. *J. Fish Biol.* 73:650–662. doi:10.1111/j.1095-

8649.2008.01963.x.

Batschelet E. 1981. Circular Statistics in Biology. London: Academic Press.

Becerra F, Echeverría A, Vassallo AI, Casinos A. 2011. Bite force and jaw biomechanics in the subterranean rodent Talas tuco-tuco (Ctenomys talarum) (Caviomorpha: Octodontoidea). *Can. J. Zool.* 89:334–342. doi:10.1139/z11-007.

Belicka L, Matich P, Jaffé R, Heithaus M. 2012. Fatty acids and stable isotopes as indicators of early-life feeding and potential maternal resource dependency in the bull shark Carcharhinus leucas. *Mar. Ecol. Prog. Ser.* 455:245–256. doi:10.3354/meps09674.

Bethea D, Buckel J, Carlson J. 2004. Foraging ecology of the early life stages of four sympatric shark species. *Mar. Ecol. Prog. Ser.* 268:245–264. doi:10.3354/meps268245.

Bethea DM, Ajemian MJ, Carlson JK, Hoffmayer ER, Imhoff JL, Grubbs RD, Peterson CT, Burgess GH. 2015. Distribution and community structure of coastal sharks in the northeastern Gulf of Mexico. *Environ. Biol. Fishes* 98:1233–1254. doi:10.1007/s10641-014-0355-3.

Bethea DM, Hale L, Carlson JK, Cortés E, Manire CA, Gelsleichter J. 2007. Geographic and ontogenetic variation in the diet and daily ration of the bonnethead shark, Sphyrna tiburo, from the eastern Gulf of Mexico. *Mar. Biol.* 152:1009–1020. doi:10.1007/s00227-007-0728-7.

Binder WJ, Van Valkenburgh B. 2000. Development of bite strength and feeding behaviour in juvenile spotted hyenas (Crocuta crocuta). *J. Zool.* 252:273–283.

doi:10.1017/S0952836900000017.

Bolnick DI, Svanbäck R, Fordyce JA, Yang LH, Davis JM, Hulsey CD, Forister ML. 2003. The ecology of individuals: Incidence and implications of individual specialization. *Am. Nat.* 161:1–28. doi:10.1086/343878.

Branstetter S. 1987. Age and growth estimates for blacktip, Carcharhinus limbatus, and spinner, C. brevipinna, sharks from the northwestern Gulf of Mexico. *Copeia* 1987:964–974.

Branstetter S, Stiles R. 1987. Age and growth estimates of the bull shark, Carcharhinus leucas, from the northern Gulf of Mexico. *Environ. Biol. Fishes* 20:169–181.

Carlisle AB, Litvin SY, Madigan DJ, Lyons K, Bigman JS, Ibarra M, Bizzarro JJ. 2017. Interactive effects of urea and lipid content confound stable isotope analysis in elasmobranch fishes. *Can. J. Fish. Aquat. Sci.* 74:419–428.

Carlson J, Ribera M, Conrath C, Heupel M, Burgess G. 2010. Habitat use and movement patterns of bull sharks Carcharhinus leucas determined using pop-up satellite archival tags. *J. Fish Biol.* 77:661–675. doi:10.1111/j.1095-8649.2010.02707.x.

Castro JI. 1996. Biology of the blacktip shark, Carcharhinus limbatus, off the southeastern United States. *Bull. Mar. Sci.* 59:508–522.

Caut S, Jowers MJ, Michel L, Lepoint G, Fisk AT. 2013. Diet-and tissue-specific incorporation of isotopes in the shark Scyliorhinus stellaris, a North Sea mesopredator. *Mar. Ecol. Prog. Ser.* 492:185–198. doi:10.3354/meps10478.

Cliff G, Dudley SF. 1991. Sharks caught in the protective gill nets off Natal, South Africa. 4. The bull shark Carcharhinus leucas Valenciennes. *South African J. Mar.*

Sci. 10:253–270. doi:10.2989/02577619109504636.

Clifton KB, Motta PJ. 1998. Feeding morphology, diet, and ecomorphological relationships among five Caribbean labrids (Teleostei, Labridae). *Copeia* 1998:953–966.

Cortés E. 1999. Standardized diet compositions and trophic levels of sharks. *ICES J. Mar. Sci.* 56:707–717. doi:10.1006/jmsc.1999.0489.

Cortés E. 2000. Life history patterns and correlations in sharks. *Rev. Fish. Sci.* 8:299–344. doi:10.1080/10408340308951115.

Cortés E, Manire CA, Hueter RE. 1996. Diet, feeding habits, and diel feeding chronology of the bonnethead shark, Sphyrna tiburo, in southwest Florida. *Bull. Mar. Sci.* 58:353–367. doi:10.1007/s00227-006-0325-1.

Cullen JA, Marshall CD. 2019. Do sharks exhibit heterodonty by tooth position and over ontogeny? A comparison using elliptic Fourier analysis. *J. Morphol.* 280:687–700. doi:10.1002/jmor.20975.

Daly R, Froneman PW, Smale MJ. 2013. Comparative feeding ecology of bull sharks (Carcharhinus leucas) in the coastal waters of the southwest Indian Ocean inferred from stable isotope analysis. *PLoS One* 8:e78229. doi:10.1371/journal.pone.0078229.

Driggers WB, Frazier BS, Adams DH, Ulrich GF, Jones CM, Hoffmayer ER, Campbell MD. 2014. Site fidelity of migratory bonnethead sharks Sphyrna tiburo (L. 1758) to specific estuaries in South Carolina, USA. *J. Exp. Mar. Bio. Ecol.* 459:61–69. doi:10.1016/j.jembe.2014.05.006.

Drymon JM, Powers SP, Dindo J, Dzwonkowski B, Henwood TA. 2010. Distributions of sharks across a continental shelf in the northern Gulf of Mexico. *Mar. Coast. Fish.* 2:440–450. doi:10.1577/C09-061.1.

Emerson SB, Greene HW, Charnov EL. 1994. Allometric aspects of predator-prey interactions. In: Ecological Morphology: Integrative Organismal Biology. Chicago: University of Chicago Press. p. 123–139.

Erickson GM, Gignac PM, Lappin AK, Vliet KA, Brueggen JD, Webb GJW. 2014. A comparative analysis of ontogenetic bite-force scaling among Crocodylia. *J. Zool.* 292:48–55. doi:10.1111/jzo.12081.

Erickson GM, Lappin AK, Vliet KA. 2003. The ontogeny of bite-force performance in American alligator (Alligator mississippiensis). *J. Zool.* 260-:317–327. doi:10.1017/S0952836903003819.

Estrada JA, Rice AN, Natanson LJ, Skomal GB. 2006. Use of isotopic analysis of vertebrae in reconstructiong ontogenetic feeding ecology in white sharks. *Ecology* 87:829–834. doi:10.1890/0012-9658(2006)87[829:UOIAOV]2.0.CO;2.

Every SL, Pethybridge HR, Fulton CJ, Kyne PM, Crook DA. 2017. Niche metrics suggest euryhaline and coastal elasmobranchs provide trophic connections among marine and freshwater biomes in northern Australia. *Mar. Ecol. Prog. Ser.* 565:181–196. doi:10.3354/meps11995.

Ferguson AR, Huber DR, Lajeunesse MJ, Motta PJ. 2015. Feeding performance of king mackerel, Scomberomorus cavalla. J. Exp. Zool. Part A Ecol. Genet. Physiol. 323:399–413. doi:10.1002/jez.1933.

Ferrara T, Clausen P, Huber D, McHenry C, Peddemors V, Wroe S. 2011. Mechanics of biting in great white and sandtiger sharks. *J. Biomech.* 44:430–435. doi:10.1016/j.jbiomech.2010.09.028.

Froeschke J, Stunz GW, Wildhaber ML. 2010. Environmental influences on the occurrence of coastal sharks in estuarine waters. *Mar. Ecol. Prog. Ser.* 407:279–292. doi:10.3354/meps08546.

Fry BG, Wroe S, Teeuwisse W, van Osch MJP, Moreno K, Ingle J, McHenry C, Ferrara T, Clausen P, Scheib H, et al. 2009. A central role for venom in predation by Varanus komodoensis (Komodo Dragon) and the extinct giant Varanus (Megalania) priscus. Proc. Natl. Acad. Sci. U. S. A. 106:8969–8974. doi:10.1073/pnas.0810883106.

Gallagher AJ, Shiffman DS, Byrnes EE, Hammerschlag-Peyer CM, Hammerschlag N. 2017. Patterns of resource use and isotopic niche overlap among three species of sharks occurring within a protected subtropical estuary. *Aquat. Ecol.* 51:435–448. doi:10.1007/s10452-017-9627-2.

Garcia AM, Hoeinghaus DJ, Vieira JP, Winemiller KO. 2007. Isotopic variation of fishes in freshwater and estuarine zones of a large subtropical coastal lagoon. *Estuar. Coast. Shelf Sci.* 73:399–408. doi:10.1016/j.ecss.2007.02.003.

Gelman A. 2004. Exploratory data analysis for complex models. *J. Comput. Graph. Stat.* 13:755–779. doi:10.1198/106186004X11435.

Gelman A, Goodrich B, Gabry J, Vehtari A. 2018. R-squared for Bayesian regression models. *Am. Stat.* doi:10.1080/00031305.2018.1549100.

Gelman A, Rubin DB. 1992. Inference from iterative simulation using multiple sequences. *Stat. Sci.* 7:457–511.

Gould SJ. 1966. Allometry and size in ontogeny and phylogeny. *Biol. Rev.* 41:587–640.

Grubich JR, Huskey S, Crofts S, Orti G, Porto J. 2012. Mega-Bites: Extreme jaw forces of living and extinct piranhas (Serrasalmidae). *Sci. Rep.* 2:1009. doi:10.1038/srep01009.

Habegger ML, Huber DH, Lajeunesse MJ, Motta PJ. 2017. Theoretical calculations of bite force in billfishes. J. Zool. 303:15–26. doi:10.1111/jzo.12465.

Habegger ML, Motta PJ, Huber DR, Dean MN. 2012. Feeding biomechanics and theoretical calculations of bite force in bull sharks (Carcharhinus leucas) during ontogeny. *Zoology* 115:354–364. doi:10.1016/j.zool.2012.04.007.

Habegger ML, Motta PJ, Huber DR, Deban SM. 2011. Feeding biomechanics in the Great Barracuda during ontogeny. *J. Zool.* 283:63–72. doi:10.1111/j.1469-7998.2010.00745.x.

Heithaus MR, Frid A, Wirsing AJ, Worm B. 2008. Predicting ecological consequences of marine top predator declines. *Trends Ecol. Evol.* 23:202–210. doi:10.1016/j.tree.2008.01.003. [accessed 2014 May 23]. http://www.ncbi.nlm.nih.gov/pubmed/18308421.

Heithaus MR, Vaudo JJ, Kreicker S, Layman CA, Krützen M, Burkholder DA, Gastrich K, Bessey C, Sarabia R, Cameron K, et al. 2013. Apparent resource partitioning and trophic structure of large-bodied marine predators in a relatively pristine seagrass ecosystem. *Mar. Ecol. Prog. Ser.* 481:225–237. doi:10.3354/meps10235.

Hernandez LP, Motta PJ. 1997. Trophic consequences of differential performance: ontogeny of oral jaw-crushing performance in the sheepshead, Archosargus probatocephalus (Teleostei, Sparidae). *J. Zool.* 243:737–756. doi:10.1111/j.1469-7998.1997.tb01973.x.

Herrel A, Van Damme R, Vanhooydonck B, De Vree F. 2001. The implications of bite performance for diet in two species of lacertid lizards. *Can. J. Zool.* 79:662–670. doi:10.1139/z01-031.

Herrel A, Gibb AC. 2006. Ontogeny of performance in vertebrates. *Physiol. Biochem. Zool.* 79:1–6.

Herrel A, O'Reilly JC. 2006. Ontogenetic scaling of bite force in lizards and turtles. *Physiol. Biochem. Zool.* 79:31–42. doi:10.1086/498193.

Herrel A, Podos J, Huber SK, Hendry AP. 2005b. Bite performance and morphology in a population of Darwin's finches: implications for the evolution of beak shape. *Funct. Ecol.* 19:43–48.

Herrel A, Van Wassenbergh S, Wouters S, Adriaens D, Aerts P. 2005a. A functional morphological approach to the scaling of the feeding system in the African catfish, Clarias gariepinus. *J. Exp. Biol.* 208:2091–2102. doi:10.1242/jeb.01604.

Heupel M, Hueter R. 2002. The importance of prey density in relation to the movement patterns of juvenile blacktip sharks (Carcharhinus limbatus) within a coastal nursery area. *Mar. Freshw. Res.* 53:543–550.

Heupel M, Knip D, Simpfendorfer C, Dulvy N. 2014. Sizing up the ecological role of sharks as predators. *Mar. Ecol. Prog. Ser.* 495:291–298. doi:10.3354/meps10597.

Heupel MR, Simpfendorfer CA, Collins AB, Tyminski JP. 2006. Residency and movement patterns of bonnethead sharks, Sphyrna tiburo, in a large Florida estuary. *Environ. Biol. Fishes* 76:47–67. doi:10.1007/s10641-006-9007-6.

Hill AV. 1950. The dimensions of animals and their muscular dynamics. *Sci. Prog.* 38:209–230.

Hoffmayer ER, Parsons GR. 2003. Food habits of three shark species from the Mississippi Sound in the northern Gulf of Mexico. *Southeast. Nat.* 2:271–280. doi:10.1656/1528-7092(2003)002[0271:fhotss]2.0.co;2.

Holt SA, Ingall ED. 2000. Carbon and nitrogen sources supporting food webs of spotted seatrout (Cynoscion nebulosus) in Galveston Bay and the Laguna Madre:preliminary observations. No. 172. Texas Parks and Wildlife Coastal Fisheries Division, Austin, TX.

Huber DR, Claes JM, Mallefet J, Herrel A. 2009. Is extreme bite performance associated with extreme morphologies in sharks? *Physiol. Biochem. Zool.* 82:20–28. doi:10.1086/588177.

Huber DR, Dean MN, Summers AP. 2008. Hard prey, soft jaws and the ontogeny of feeding mechanics in the spotted ratfish Hydrolagus colliei. *J. R. Soc. Interface* 5:941–952. doi:10.1098/rsif.2007.1325.

Huber DR, Eason TG, Hueter RE, Motta PJ. 2005. Analysis of the bite force and mechanical design of the feeding mechanism of the durophagous horn shark Heterodontus francisci. *J. Exp. Biol.* 208:3553–3571. doi:10.1242/jeb.01816.

Huber DR, Motta PJ. 2004. Comparative analysis of methods for determining bite force

in the spiny dogfish Squalus acanthias. *J. Exp. Zool. Part A Comp. Exp. Biol.* 301:26–37. doi:10.1002/jez.a.20003.

Huber DR, Weggelaar CL, Motta PJ. 2006. Scaling of bite force in the blacktip shark Carcharhinus limbatus. *Zoology* 109:109–119. doi:10.1016/j.zool.2005.12.002.

Hussey NE, DiBattista JD, Moore JW, Ward EJ, Fisk AT, Kessel S, Guttridge TL, Feldheim KA, Franks BR, Gruber SH, et al. 2017. Risky business for a juvenile marine predator? Testing the influence of foraging strategies on size and growth rate under natural conditions. *Proc. R. Soc. B Biol. Sci.* 284:20170166. doi:10.1098/rspb.2017.0166.

Hussey NE, Dudley SFJ, Mccarthy ID, Cliff G, Fisk AT. 2011. Stable isotope profiles of large marine predators: viable indicators of trophic position, diet, and movement in sharks? *Can. J. Fish. Aquat. Sci.* 68:2029–2045. doi:10.1139/F2011-115.

Hussey NE, MacNeil MA, Olin JA, McMeans BC, Kinney MJ, Chapman DD, Fisk AT. 2012. Stable isotopes and elasmobranchs: tissue types, methods, applications and assumptions. *J. Fish Biol.* 80:1449–1484. doi:10.1111/j.1095-8649.2012.03251.x.

Jackson AL, Inger R, Parnell AC, Bearhop S. 2011. Comparing isotopic niche widths among and within communities: SIBER - Stable Isotope Bayesian Ellipses in R. *J. Anim. Ecol.* 80:595–602. doi:10.1111/j.1365-2656.2011.01806.x.

Jhaveri P, Papastamatiou YP, German DP. 2015. Digestive enzyme activities in the guts of bonnethead sharks (Sphyrna tiburo) provide insight into their digestive strategy and evidence for microbial digestion in their hindguts. *Comp. Biochem. Physiol. Part A Mol. Integr. Physiol.* 189:76–83. doi:10.1016/j.cbpa.2015.07.013.

Jones MEH, Lappin KA. 2009. Bite-force performance of the last rhynchocephalian (Lepidosauria: Sphenodon). *J. R. Soc. New Zeal.* 39:71–83. doi:10.1080/03014220909510565.

Kiltie RA. 1982. Bite force as a basis for niche differentiation between rain forest p[eccaries (Tayassu tajacu and T. pecari). *Biotropica* 14:188–195. doi:10.2307/2388025.

Kim SL, Koch PL. 2012. Methods to collect, preserve, and prepare elasmobranch tissues for stable isotope analysis. *Environ. Biol. Fishes* 95:53–63. doi:10.1007/s10641-011-9860-9.

Kim SL, Martinez del Rio C, Casper D, Koch PL. 2012. Isotopic incorporation rates for shark tissues from a long-term captive feeding study. *J. Exp. Biol.* 215:2495–2500. doi:10.1242/jeb.070656.

Kinney M, Hussey N, Fisk A, Tobin A, Simpfendorfer C. 2011. Communal or competitive? Stable isotope analysis provides evidence of resource partitioning within a communal shark nursery. *Mar. Ecol. Prog. Ser.* 439:263–276. doi:10.3354/meps09327.

Kohler NE, Casey JG, Turner PA. 1996. Length-length and length-weight relationships for 13 shark species from the western North Atlantic. NOAA Tech Memo NMFS-NE-110.

Kolmann MA, Huber DR. 2009. Scaling of feeding biomechanics in the horn shark Heterodontus francisci: ontogenetic constraints on durophagy. *Zoology* 112:351–361. doi:10.1016/j.zool.2008.11.002.

Law CJ, Young C, Mehta RS. 2016. Ontogenetic scaling of theoretical bite force in southern sea otters (Enhydra lutris nereis). *Physiol. Biochem. Zool.* 89:347–363. doi:10.1086/688313.

Layman CA, Araujo MS, Boucek R, Hammerschlag-Peyer CM, Harrison E, Jud ZR, Matich P, Rosenblatt AE, Vaudo JJ, Yeager LA, et al. 2012. Applying stable isotopes to examine food-web structure: an overview of analytical tools. *Biol. Rev.* 87:545–562. doi:10.1111/j.1469-185X.2011.00208.x.

Layman CA, Arrington DA, Montaña CG, Post DM. 2007. Can stable isotope ratios provide for community-wide measures of trophic structure? *Ecology* 88:42–48. doi:10.1890/0012-9623(2008)89[5:ESOAPI]2.0.CO;2.

Logan J, Lutcavage M. 2010. Stable isotope dynamics in elasmobranch fishes. *Hydrobiologia* 644:231–244.

Lombardi-Carlson L, Cortés E, Parsons G, Manire C. 2003. Latitudinal variation in life-history traits of bonnethead sharks, Sphyrna tiburo, (Carcharhiniformes : Sphyrnidae) from the eastern Gulf of Mexico. *Mar. Freshw. Res.* 54:875–883.

Lou F, Curtin NA, Woledge RC. 2002. Isometric and isovelocity contractile performance of red musle fibres from the dogfish Scyliorhinus canicula. *J. Exp. Biol.* 205:1585–1595.

Lowe C, Wetherbee B, Crow G, Tester A. 1996. Ontogenetic dietary shifts and feeding behavior of the tiger shark, Galeocerdo cuvier, in Hawaiian waters. *Environ. Biol. Fishes* 47:203–211.

Lysy M, Stasko AD, Swanson HK. 2014. nicheROVER: (Niche) (R)egion and Niche

(Over)lap Metrics for Multidimensional Ecological Niches. R package version 1.0. https://CRAN.R-project.org/package=nicheROVER.

MacNeil MA, Drouillard KG, Fisk AT. 2006. Variable uptake and elimination of stable nitrogen isotopes between tissues in fish. *Can. J. Fish. Aquat. Sci.* 63:345–353. doi:10.1139/f05-219.

Malpica-Cruz L, Herzka SZ, Sosa-Nishizaki O, Lazo JP, Trudel M. 2012. Tissue-specific isotope trophic discrimination factors and turnover rates in a marine elasmobranch: empirical and modeling results. *Can. J. Fish. Aquat. Sci.* 69:551–564. doi:10.1002/art.39222.

Mara KR, Motta PJ, Huber DR. 2010. Bite force and performance in the durophagous bonnethead shark, Sphyrna tiburo. *J. Exp. Zool. Part A Ecol. Genet. Physiol.* 313:95–105. doi:10.1002/jez.576.

Marshall CD, Guzman A, Narazaki T, Sato K, Kane EA, Sterba-Boatwright BD. 2012. The ontogenetic scaling of bite force and head size in loggerhead sea turtles (Caretta caretta): implications for durophagy in neritic, benthic habitats. *J. Exp. Biol.* 215:4166–4174. doi:10.1242/jeb.074385.

Marshall CD, Wang J, Rocha-Olivares A, Godinez-Reyes C, Fisler S, Narazaki T, Sato K, Sterba-Boatwright BD. 2014. Scaling of bite performance with head and carapace morphometrics in green turtles (Chelonia mydas). *J. Exp. Mar. Bio. Ecol.* 451:91–97. doi:10.1016/j.jembe.2013.11.004.

Matich P, Heithaus MR, Layman CA. 2010. Size-based variation in intertissue comparisons of stable carbon and nitrogen isotopic signatures of bull sharks

(Carcharhinus leucas) and tiger sharks (Galeocerdo cuvier). *Can. J. Fish. Aquat. Sci.* 67:877–885. doi:10.1139/F10-037.

Matich P, Heithaus MR, Layman CA. 2011. Contrasting patterns of individual specialization and trophic coupling in two marine apex predators. *J. Anim. Ecol.* 80:294–305. doi:10.1111/j.1365-2656.2010.01753.x.

Matich P, Kiszka JJ, Heithaus MR, Le Bourg B, Mourier J. 2019. Inter-individual differences in ontogenetic trophic shifts among three marine predators. *Oecologia* 189:621–636. doi:10.1007/s00442-019-04357-5.

McClelland JW, Valiela I. 1998. Linking nitrogen in estuarine producers to land-derived sources. *Limnol. Oceanogr.* 43:577–585.

McMeans BC, Olin JA, Benz GW. 2009. Stable-isotope comparisons between embryos and mothers of a placentatrophic shark species. *J. Fish Biol.* 75:2464–2474. doi:10.1111/j.1095-8649.2009.02402.x.

van der Meij MAA, Bout RG. 2004. Scaling of jaw muscle size and maximal bite force in finches. *J. Exp. Biol.* 207:2745–2753. doi:10.1242/jeb.01091.

van der Meij MAA, Bout RG. 2006. Seed husking time and maximal bite force in finches. *J. Exp. Biol.* 209:3329–3335. doi:10.1242/jeb.02379.

Meyers JJ, Herrel Anthony, Birch J. 2002. Scaling of morphology, bite force and feeding kinematics in an iguanian and a scleroglossan lizard. In: Aerts P, D'Août K, Herrel A., Van Damme R, editors. Topics in Functional and Ecological Vertebrate Morphology. Maastricht: Shaker. p. 47–62.

Motta PJ, Wilga CAD. 1995. Anatomy of the feeding apparatus of the lemon shark,

Negaprion brevirostris. *J. Morphol.* 226:309–329.

Myrberg AA, Gruber SH. 1974. The behavior of the bonnethead shark, Sphyrna tiburo. *Copeia* 1974:358–374.

Navia AF, Mejía-Falla PA, López-García J, Giraldo A, Cruz-Escalona VH. 2016. How many trophic roles can elasmobranchs play in a marine tropical network? *Mar. Freshw. Res.* 68:1–12.

Newman SP, Handy RD, Gruber SH. 2012. Ontogenetic diet shifts and prey selection in nursery bound lemon sharks, Negaprion brevirostris, indicate a flexible foraging tactic. *Environ. Biol. Fishes* 95:115–126. doi:10.1007/s10641-011-9828-9.

Olin JA, Hussey NE, Fritts M, Heupel MR, Simpfendorfer CA, Poulakis GR, Fisk AT. 2011. Maternal meddling in neonatal sharks: implications for interpreting stable isotopes in young animals. *Rapid Commun. Mass Spectrom.* 25:1008–1016. doi:10.1002/rcm.4946.

Papastamatiou YP, Wetherbee BM, Lowe CG, Crow GL. 2006. Distribution and diet of four species of carcharhinid shark in the Hawaiian Islands: evidence for resource partitioning and competitive exclusion. *Mar. Ecol. Prog. Ser.* 320:239–251.

Pélabon C, Bolstad GH, Egset CK, Cheverud JM, Pavlicev M, Rosenqvist G. 2013. On the relationship between ontogenetic and static allometry. *Am. Nat.* 181:195–212. doi:10.1086/668820.

Pélabon C, Firmat C, Bolstad GH, Voje KL, Houle D, Cassara J, Rouzic A Le, Hansen TF. 2014. Evolution of morphological allometry. *Ann. N. Y. Acad. Sci.* 1320:58–75. doi:10.1111/nyas.12470.

Peterson BJ, Fry B. 1987. Stable isotopes in ecosystem studies. *Annu. Rev. Ecol. Syst.* 18:293–320. doi:10.1146/annurev.es.18.110187.001453.

Pethybridge HR, Choy CA, Polovina JJ, Fulton EA. 2018. Improving marine ecosystem models with biochemical tracers. *Ann. Rev. Mar. Sci.* 10:199–228. doi:10.1146/annurev-marine-121916-063256.

Pfaller JB, Gignac PM, Erickson GM. 2011. Ontogenetic changes in jaw-muscle architecture facilitate durophagy in the turtle Sternotherus minor. *J. Exp. Biol.* 214:1655–1667. doi:10.1242/jeb.048090.

Plumlee JD, Wells RD. 2016. Feeding ecology of three coastal shark species in the northwest Gulf of Mexico. *Mar. Ecol. Prog. Ser.* 550:163–174. doi:10.3354/meps11723.

Plummer M. 2003. JAGS: A program for analysis of Bayesian graphical models using Gibbs sampling. http://sourceforge.net/projects/mcmc-jags/.

Plummer M, Best N, Cowles K, Vines K. 2006. CODA: Convergence diagnosis and output analysis for MCMC. *R News* 6:7–11.

Post DM. 2002. Using stable isotopes to estimate trophic position: models, methods and assumptions. *Ecology* 83:703–718.

Post DM, Layman CA, Arrington DA, Takimoto G, Quattrochi J, Montaña CG. 2007. Getting to the fat of the matter: models, methods and assumptions for dealing with lipids in stable isotope analyses. *Oecologia* 152:179–189. doi:10.1007/s00442-006-0630-x.

Powell PL, Roy RR, Kanim P, Bello MA, Edgerton VR. 1984. Predictability of skeletal

muscle tension from architectural determinations in guinea pig hindlimbs. *J. Appl. Physiol.* 57:1715–1721. doi:10.1152/jappl.1984.57.6.1715.

R Core Team. 2018. R: A Language and Environment for Statistical Computing.

Rossman S, Ostrom PH, Gordon F, Zipkin EF. 2016. Beyond carbon and nitrogen: guidelines for estimating three-dimensional isotopic niche space. *Ecol. Evol.* 6:2405–2413. doi:10.1002/ece3.2013.

Santana SE, Dumont ER, Davis JL. 2010. Mechanics of bite force production and its relationship to diet in bats. *Funct. Ecol.* 24:776–784. doi:10.1111/j.1365-2435.2010.01703.x.

Santana SE, Miller KE. 2016. Extreme postnatal scaling in bat feeding performance: a view of ecomorphology from ontogenetic and macroevolutionary perspectives. *Integr. Comp. Biol.* 56:459–468. doi:10.1093/icb/icw075.

Scharf FS, Juanes F, Rountree RA. 2000. Predator size - prey size relationships of marine fish predators: Interspecific variation and effects of ontogeny and body size on trophic-niche breadth. *Mar. Ecol. Prog. Ser.* 208:229–248. doi:10.3354/meps208229.

Schmidt-Nielsen K. 1984. Scaling: why is animal size so important? Cambridge: Cambridge University Press.

Shiffman DS, Gallagher AJ, Boyle MD, Hammerschlag-Peyer CM, Hammerschlag N. 2012. Stable isotope analysis as a tool for elasmobranch conservation research: a primer for non-specialists. *Mar. Freshw. Res.* 63:635–643.

Snelson FF, Mulligan TJ, Williams SE. 1984. Food habits, occurrence, and population

structure of the bull shark, Carcharhinus leucas, in Florida coastal lagoons. *Bull. Mar. Sci.* 34:71–80.

Snover ML. 2008. Ontogenetic habitat shifts in marine organisms: Influencing factors and the impact of climate variability. *Bull. Mar. Sci.* 83:53–67.

Su Y-S, Yajima M. 2015. R2jags: Using R to Run 'JAGS'. R package version 0.5-7. https://CRAN.R-project.org/package=R2jags

Svanbäck R, Bolnick DI. 2007. Intraspecific competition drives increased resource use diversity within a natural population. *Proc. R. Soc. B Biol. Sci.* 274:839–844. doi:10.1098/rspb.2006.0198.

Swanson HK, Lysy M, Power M, Stasko AD, Johnson JD, Reist JD. 2015. A new probabilistic method for quantifying n-dimensional ecological niches and niche overlap. *Ecology* 96:318–324. doi:10.1890/14-0235.1.

Syväranta J, Lensu A, Marjomäki TJ, Oksanen S, Jones RI. 2013. An empirical evaluation of the utility of convex hull and standard ellipse areas for assessing population niche widths from stable isotope data. *PLoS One* 8:e56094. doi:10.1371/journal.pone.0056094.

Thompson EN, Biknevicius AR, German RZ. 2003. Ontogeny of feeding function in the gray short-tailed opossum Monodelphis domestica: empirical support for the constrained model of jaw biomechanics. *J. Exp. Biol.* 206:923–932. doi:10.1242/jeb.00181.

Timm LL. 2013. Feeding biomechanics and craniodental morphology in otters (Lutrinae). PhD Dissertation. Texas A&M University, College Station, TX.

Verwaijen D, Van Damme R, Herrel A. 2002. Relationships between head size, bite force, prey handling efficiency and diet in two sympatric lacertid lizards. *Funct. Ecol.* 16:842–850. doi:10.1046/j.1365-2435.2002.00696.x.

Wainwright PC. 1988. Morphology and ecology: functional basis of feeding constraints in Caribbean labrid fishes. *Ecology* 69:635–645.

Warton DI, Duursma RA, Falster DS, Taskinen S. 2012. smatr 3- an R package for estimation and inference about allometric lines. *Methods Ecol. Evol.* 3:257–259. doi:10.1111/j.2041-210X.2011.00153.x.

Werner EE, Gilliam JF. 1984. The ontogenetic niche and species interactions in size-structured populations. *Annu. Rev. Ecol. Syst.* 15:393–425.

Werry J, Lee S, Otway N, Hu Y, Sumpton W. 2011. A multi-faceted approach for quantifying the estuarine-nearshore transition in the life cycle of the bull shark, Carcharhinus leucas. *Mar. Freshw. Res.* 62:1421–1431. doi:10.1071/MF11136.

Whitenack L, Motta P. 2010. Performance of shark teeth during puncture and draw: implications for the mechanics of cutting. *Biol. J. Linn. Soc.* 100:271–286.

Wilga C, Motta P. 2000. Durophagy in sharks: feeding mechanics of the hammerhead Sphyrna tiburo. *J. Exp. Biol.* 203:2781–2796.

Yurkowski DJ, Hussey NE, Ferguson SH, Fisk AT. 2018. A temporal shift in trophic diversity among a predator assemblage in a warming Arctic. *R. Soc. Open Sci.* 5:180259. doi:10.1098/rsos.180259.

Vander Zanden MJ, Cabana G, Rasmussen JB. 1997. Comparing trophic position of freshwater fish calculated using stable nitrogen isotope ratios (δ15N) and literature

dietary data. *Can. J. Fish. Aquat. Sci.* 54:1142–1158.

Vander Zanden MJ, Clayton MK, Moody EK, Solomon CT, Weidel BC. 2015. Stable isotope turnover and half-life in animal tissues: A literature synthesis. *PLoS One* 10:e0116182. doi:10.1371/journal.pone.0116182.

CHAPTER III

DO SHARKS EXHIBIT HETERODONTY BY TOOTH POSITION AND OVER ONTOGENY? A COMPARISON USING ELLIPTIC FOURIER ANALYSIS*

Introduction

Morphology of the feeding apparatus can constrain the ecological niche of an organism through its performance and behavioral application during the acquisition of food items (Lauder 1982; Arnold 1983; Wainwright 1988; Losos 1990; Ricklefs and Miles 1994). By integrating ecological signals over time, tooth morphology can serve as a useful indicator of diet (Sage and Selander 1975; Van Valkenburgh 1988; Ricklefs and Miles 1994; Freeman 2000; Erickson et al. 2012). The primary function of teeth is to transmit force from the jaw adductor muscles to dietary items, although other functions are also important (e.g. agonistic and mating behaviors; Le Boeuf and Mesnick 1991; Pratt and Carrier 2001; Herrel et al. 2010). Additionally, teeth are used during stages of prey capture, retention, and processing in predatory organisms. To facilitate these

---

different purposes, some organisms have distinct functional units of teeth whose morphology and location along the jaw margin or elsewhere within the cranium (i.e. pharyngeal jaws, vomerine/palatine teeth) are adept for certain functions (Janis and Fortelius 1988; Norton 1988; Mehta and Wainwright 2007; Galloway et al. 2016). The attribution of form to function has been particularly useful in the extrapolation of diet to fossil species, especially in those with heterodont dentition (Van Valkenburgh 1988; Underwood et al. 1999).

A set of teeth are typically characterized as having either a similar or different morphology, which are termed homodont and heterodont, respectively (Liem et al. 2001). Examples of homodont dentitions are ubiquitous in most major vertebrate groups, but heterodonty is much less prevalent (with the exception of mammals; Reif 1982; Davit-Béal et al. 2007; Bertrand 2014; D'Amore 2015). It is likely that homodonty represents a plesiomorphic character in vertebrates (Huysseune and Sire 1998; Ungar 2010; Bertrand 2014; Tucker and Fraser 2014). Although elasmobranchs represent one of the most basal vertebrate lineages, heterodonty is prevalent within many of these fishes. Traditionally, tooth function in elasmobranchs has been inferred from morphology (Cappetta 1986; Cappetta 1987; Frazzetta 1988), but recent studies that have incorporated measures of performance show that this relationship is complex (Huber et al. 2009; Whitenack and Motta 2010; Corn et al. 2016). The attribution of ecology to morphology has been straightforward in some species, such as white sharks (*Carcharodon carcharias*; Ferrara et al. 2011; French et al. 2017), sandtiger sharks (*Carcharias taurus*; Ferrara et al. 2011), horn sharks (*Heterodontus francisci*; Summers

et al. 2004; Huber et al. 2005), bonnethead sharks (*Sphyrna tiburo*; Wilga and Motta 2000; Mara et al. 2010), and cownose rays (*Rhinoptera bonasus*; Kolmann et al. 2015). However, the traditional method of attributing form to function has not been helpful for other elasmobranchs. This issue is best exemplified in batoids that possess a plate-like dentition and feed on soft-bodied stingrays (Dean et al. 2017). The cuspidate teeth of white-spotted bamboo sharks (*Chiloscyllium plagiosum*) have been difficult to characterize as well since these teeth can be reoriented to form crushing plates for hard prey (Ramsay and Wilga 2007). In some cases, tooth morphology can even be modified on a seasonal basis. The dentition of mature male batoids can change from molariform to cuspidate teeth to facilitate a better grasp of females during copulation (H. Bigelow and Schroeder 1953a; Kajiura and Tricas 1996; Gutteridge and Bennett 2014). Moreover, Whitenack and Motta (2010) found many different tooth morphologies to be functionally equivalent with respect to puncture and draw performance in extant and extinct elasmobranchs. Although the relationship between tooth morphology and feeding ecology is complex, the dignathic heterodonty exhibited in many carcharhiniform sharks (Bigelow and Schroeder 1948; Compagno 1988; Frazzetta 1994) may have functional importance depending on the stage of feeding.

In many large-bodied sharks, the differentiation in tooth morphology between the upper and lower jaws as well as along the tooth row (the mesio-distal direction parallel to the jaw margin; (Bigelow and Schroeder 1953b; Cappetta 1987) has been hypothesized to differ in function during prey capture, retention, and processing (Applegate 1965; Frazzetta 1988; Liem et al. 2001; Lucifora et al. 2001). In

carcharhiniform sharks, anterior teeth on the lower jaw are typically gracile, smooth-edged, and often make first contact with prey items during jaw closure. They have also been postulated to puncture and hold prey in place during feeding events (Springer 1961; Moss 1972; Frazzetta 1994; Motta and Wilga 2001). Once the teeth on the upper jaw have punctured the prey item, small prey are often swallowed whole, while large prey is processed into smaller-sized pieces (Frazzetta 1994). Many carcharhiniform sharks use a head-shaking behavior to remove pieces of flesh from large prey, which is effective since the labio-lingually flattened teeth have sharp, blade-like edges in the majority of these species (Moss 1972; Frazzetta and Prange 1987; Frazzetta 1988; Motta et al. 1997). If differences in tooth morphology serve a functional purpose, as has often been hypothesized, it should have consequences for the time and energy required to process or handle prey. Prey handling efficiency may increase if a tooth's shape is suited to a particular function compared to one that is not (Emerson et al. 1994; Anderson and LaBarbera 2008; Huber et al. 2009). This may be of particular importance for young conspecifics, whose prey selection can be constrained by gape, bite force, and the ability of their teeth to puncture and process prey items (Mara et al. 2010; Whitenack and Motta 2010; Habegger et al. 2012; Bergman et al. 2017).

Since ontogenetic dietary shifts in the diversity, size, and material properties of shark prey are common (Lowe et al. 1996; Bethea et al. 2004; Estrada et al. 2006; Barry et al. 2008; Habegger et al. 2012; Newman et al. 2012), it is likely that a concomitant change in tooth morphology (i.e. ontogenetic heterodonty) may occur to meet the functional demands of these dietary shifts. Ontogenetic changes in diet and dentition

have been characterized in heterodontiform (Reif 1976; Summers et al. 2004; Powter et al. 2010) and lamniform (Tricas and McCosker 1984; Powlik 1995; French et al. 2017) sharks, but have not been fully investigated in the dignathic heterodont carcharhiniforms to date (but see Raschi et al. 1982). These studies have primarily evaluated ontogenetic heterodonty using qualitative methods (Reif 1976; Raschi et al. 1982; Tricas and McCosker 1984; McCosker 1985; Powlik 1995; Summers et al. 2004), but recent studies have begun using quantitative analyses as a more robust approach (Powter et al. 2010; French et al. 2017).

In general, studies of shark tooth morphology have often been conducted using linear or geometric morphometrics (Nyberg et al. 2010; Whitenack and Gottfried 2010; Whitenack and Motta 2010; French et al. 2017; Marramà and Kriwet 2017), but these methods do not fully capture the complexity of tooth morphology in most instances (Crampton 1995). Unlike linear and geometric morphometrics, elliptic Fourier analysis (EFA) is able to create a more accurate representation of complex organismal morphologies by characterizing the whole outline of the structure of interest (Kuhl and Giardina 1982; Ferson et al. 1985). This method would be preferable to investigate ontogenetic changes in shark tooth morphologies compared to landmark-based geometric morphometrics. The accuracy of outlines produced by EFA can be selected *a priori*, allowing the detail to be controlled for features of different resolutions. Previous studies have used EFA to characterize and classify the shape of fish otoliths (Tracey et al. 2006), bivalves (Ferson et al. 1985), plants (Neto et al. 2006), pinniped whiskers (Ginter et al. 2012), and shark body shape (Fu et al. 2016). Since EFA enables a more

accurate characterization of tooth morphology than previously used methods, inter- and intraspecific comparisons are expected to be more accurate as well.

Bull sharks *Carcharhinus leucas* (Müller & Henle 1839), blacktip sharks *Carcharhinus limbatus* (Müller & Henle 1839), and bonnethead sharks *Sphyrna tiburo* (Linnaeus 1758) are carcharhiniforms that exhibit dignathic heterodonty, differ in feeding ecology, and exhibit ontogenetic dietary shifts (Cliff and Dudley 1991; Bethea et al. 2007; Barry et al. 2008). If differences in the performance of shark teeth during prey capture and handling are reflective of differences in morphology, then it is expected that tooth morphology will vary within and among species by relative crown height, base crown width, and notch angle to efficiently puncture, cut, or crush prey. Different combinations of these variables may potentially be tied to feeding behaviors such as biting and swallowing small, soft prey, cutting through large or functionally difficult prey, or crushing hard prey. It was hypothesized that ontogenetic heterodonty is exhibited in each species concomitant with an ontogenetic shift in diet. Additionally, the extent of heterodonty was hypothesized to be greatest in the generalist bull shark compared to the piscivorous blacktip and durophagous bonnethead sharks. This is because the extent of heterodonty is expected to serve as a potential measure of the number of different functional roles that the teeth perform. Since dietary breadth and material properties of prey items differ for each species, it was also hypothesized that tooth morphology differs among species (for all size classes) at each of the six selected tooth positions.

Table 3-1. Sample sizes (N), sex ratios, and mean (± SD) body length measurements (min – max) for each species

Species	N	Sex Ratio F/M	TL (cm)	FL (cm)	PCL (cm)
Bull (*C. leucas*)	21	3/18	118.4 ± 43.6 (74.4 – 215.0)	94.5 ± 36.0 (59.5 – 174.5)	85.7 ± 33.0 (53.9 – 159.0)
Blacktip (*C. limbatus*)	28	15/13	124.4 ± 29.2 (67.4 – 171.1)	99.5 ± 23.2 (52.7 – 135.6)	90.1 ± 22.1 (47.8 – 122.5)
Bonnethead (*S. tiburo*)	24	17/7	85.5 ± 18.3 (51.7 – 125.4)	67.9 ± 15.3 (40.8 – 99.8)	62.1 ± 14.4 (36.6 – 92.4)

Materials and Methods

Sample collection

Bull (N = 21), blacktip (N = 28), and bonnethead sharks (N = 24) were opportunistically sampled from fishing charters or from routine long-line surveys conducted by the Texas Parks and Wildlife Department in Galveston, Texas in March through October from 2014 to 2016. Sex was identified for each shark and measurements of total (TL, cm), fork (FL, cm) and pre-caudal length (PCL, cm) were recorded (Table 3-1). Four size classes were delineated for bull and blacktip sharks (young-of-the-year (YoY), juvenile, sub-adult, adult), but only three were used for bonnethead sharks (YoY, juvenile, adult). Size classes for each species were based upon previous studies from Texas or from a nearby location at a similar latitude, which has been shown to affect growth rates in bonnethead sharks (Branstetter 1987; Branstetter and Stiles 1987; Lombardi-Carlson et al. 2003). In all species, teeth were extracted from the functional row at six positions on the left side of the head. To account for possible

Table 3-2. Descriptions of tooth positions (from anterior to posterior) used for evaluating differences in morphology within and among species

Position	Description
Anterior-Upper Jaw (AntUp)	The tooth position immediately lateral to the symphyseal tooth on the upper jaw (palatoquadrate).
Anterior-Lower Jaw (AntLow)	The tooth position immediately lateral to the symphyseal tooth on the lower jaw (Meckel's cartilage).
Lateral-Upper Jaw (LatUp)	The tooth position 50% of the jaw length (distance between the symphyseal tooth and the jaw joint) on the upper jaw.
Lateral-Lower Jaw (LatLow)	The tooth position 50% of the jaw length on the lower jaw.
Posterior-Upper Jaw (PostUp)	The tooth position 25% of the jaw length from the joint on the upper jaw.
Posterior-Lower Jaw (PostLow)	The tooth position 25% of the jaw length from the joint on the lower jaw.

Table 3-3. Sample sizes (n) for each size class by tooth position within each species

Species	Size Class	AntUp	AntLow	LatUp	LatLow	PostUp	PostLow
Bull (*C. leucas*)	YoY	6	6	6	6	6	6
	Juvenile	11	10	10	9	11	10
	Sub-adult	2	2	2	2	2	2
	Adult	2	2	2	2	2	1
Blacktip (*C. limbatus*)	YoY	3	3	3	3	3	3
	Juvenile	5	5	4	4	5	6
	Sub-adult	11	11	9	9	11	11
	Adult	8	8	7	7	8	8
Bonnethead (*S. tiburo*)	YoY	7	7	7	7	7	7
	Juvenile	8	8	8	8	8	8
	Adult	8	8	9	9	8	9

changes in morphology at different positions along the upper and lower jaws, three positions were sampled along each jaw margin. These positions included an anterior position on the upper (AntUp) and lower jaws (AntLow), a lateral position on the upper (LatUp) and lower jaws (LatLow), and a posterior position on the upper (PostUp) and lower jaws (PostLow), illustrated in Figure 3-1 and described in detail in Table 3-2. These positions were selected to be representative of the whole tooth row in the upper and lower jaws. Teeth were only extracted if there were no visible signs of damage. If teeth were not considered to be in good condition, the contralateral side of the head was used as a suitable alternative; images of these teeth were reflected to match the orientation of the teeth from the left side of the head. Missing or damaged teeth in each species resulted in a variation of sample sizes by tooth position (Table 3-3).

Sample clean-up and processing

After extraction, all teeth were soaked in 9% hydrogen peroxide for 30 minutes to loosen soft tissue attached to the root for removal via scalpel. Digital images of teeth were collected using a SPOT Pursuit camera mounted on a Nikon SMZ 1500 stereomicroscope if they were small enough to fit within the field of view. These images were collected using SPOT Advanced (ver 5.2) software. Teeth that did not fit within the field of view of the stereomicroscope were imaged with a Canon EOS-1D Mark II camera fitted with a 50 mm Sigma EX macro lens that used a remote shutter release to ensure sharp images. All images were collected from the labial side of the tooth, which was oriented normal to the lens to reduce distortion caused by parallax. Images were

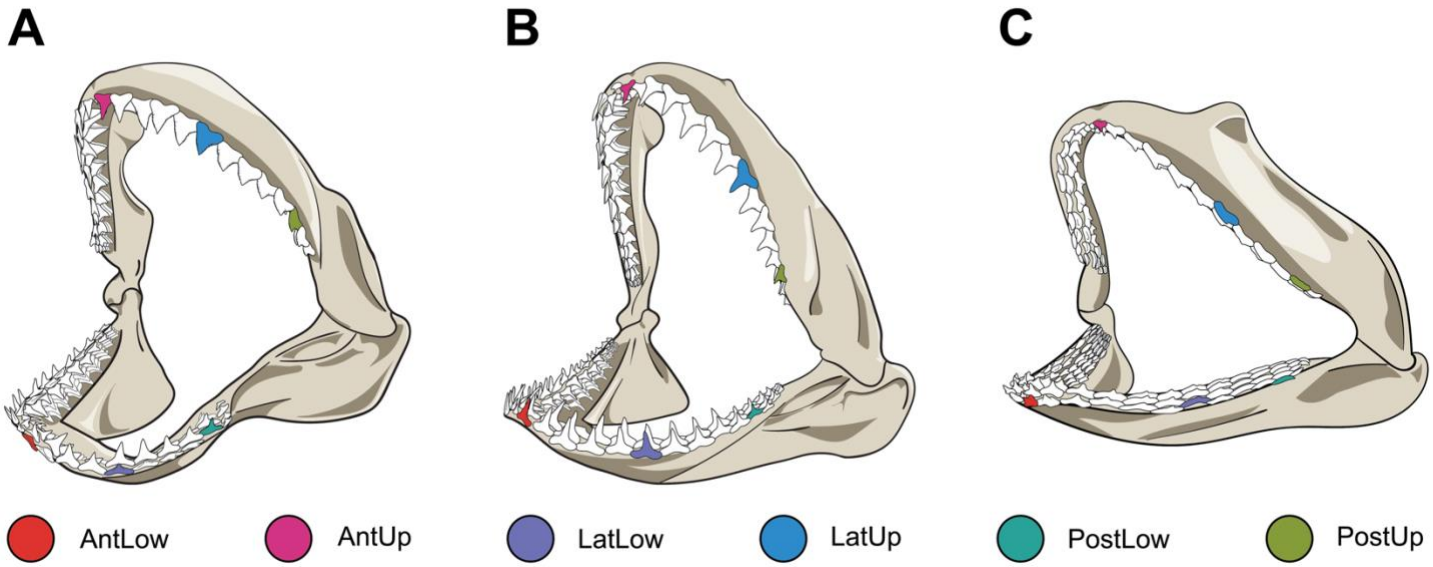

Figure 3-1. Positions of teeth sampled from the functional row of the upper and lower jaws are illustrated for bull (**A**), blacktip (**B**), and bonnethead sharks (**C**). These teeth include the anterior position on the lower (AntLow) and upper jaws (AntUp), the lateral position on the lower (LatLow) and upper jaws (LatUp), and the posterior position on the lower (PostLow) and upper jaws (PostUp). Further details regarding the exact positions can be found in Table 3-2.

prepared for EFA by creating silhouettes of all teeth in grayscale using Adobe Photoshop CC 2017 (Adobe Systems, San José, CA, USA).

Elliptic Fourier analysis (EFA) and tooth morphometrics

EFA is a preferred method for capturing the outline of an object by fitting a function to an ordered set of coordinates within a Cartesian plane (Kuhl and Giardina 1982; Ferson et al. 1985). This function consists of a sum of harmonics (trigonometric curves) produced by orthogonal Fourier decomposition that fits greater complexity of the outline with each successive harmonic. Each harmonic is also described by four coefficients (two Fourier coefficients each for the x and y components). These coefficients describe the size, shape, and orientation of each harmonic ellipse along the closed outline. Due to the method by which these harmonics are generated, the lower-ordered harmonics roughly capture most of the variance in shape while the higher-ordered harmonics capture the finer details (Kuhl and Giardina 1982; Crampton 1995; Figure 3-2). The accuracy of the function used to fit an outline can be selected for *a priori* using an average Fourier power spectrum, which allows the average cumulative power of a set of harmonics to be chosen for a given analysis (Crampton 1995; Bonhomme et al. 2014). To capture the greatest accuracy in tooth morphology, the number of harmonics chosen for each tooth comparison was selected to describe 99.9% of the total variation in shape. All EFA was conducted using the 'Momocs' package (ver 1.2.9; Bonhomme et al. 2014) in the R statistical environment (R Core Team 2018). All

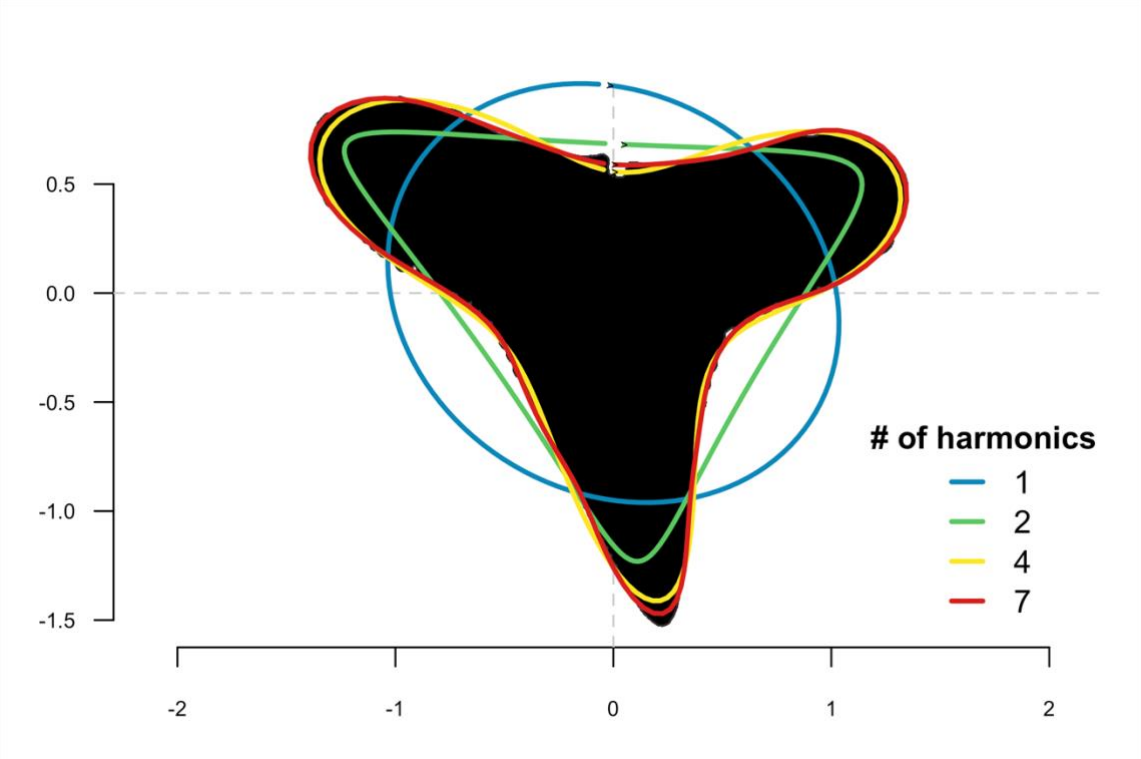

Figure 3-2. A visual representation of elliptic Fourier analysis fitting the silhouette of a centered and scaled shark tooth. This demonstration uses one, two, four, and seven harmonics, which describe 90, 98, 99, and 99.9% of the total shape of the outline, respectively.

tooth outlines were centered and scaled to centroid size prior to EFA to align all teeth and remove the effect of tooth size for a given comparison, respectively (Figure 3-3). Smoothing was conducted on the curves produced by EFA using a simple moving average (nine iterations) to reduce any noise generated during this process (Haines and Crampton 2000). Since shape analysis using EFA is conducted on outlines generated from an automated algorithm using nearest neighbor values of pixels around the entire contour of the shape of interest (Rohlf 1990; Claude 2008), user-based error is decreased

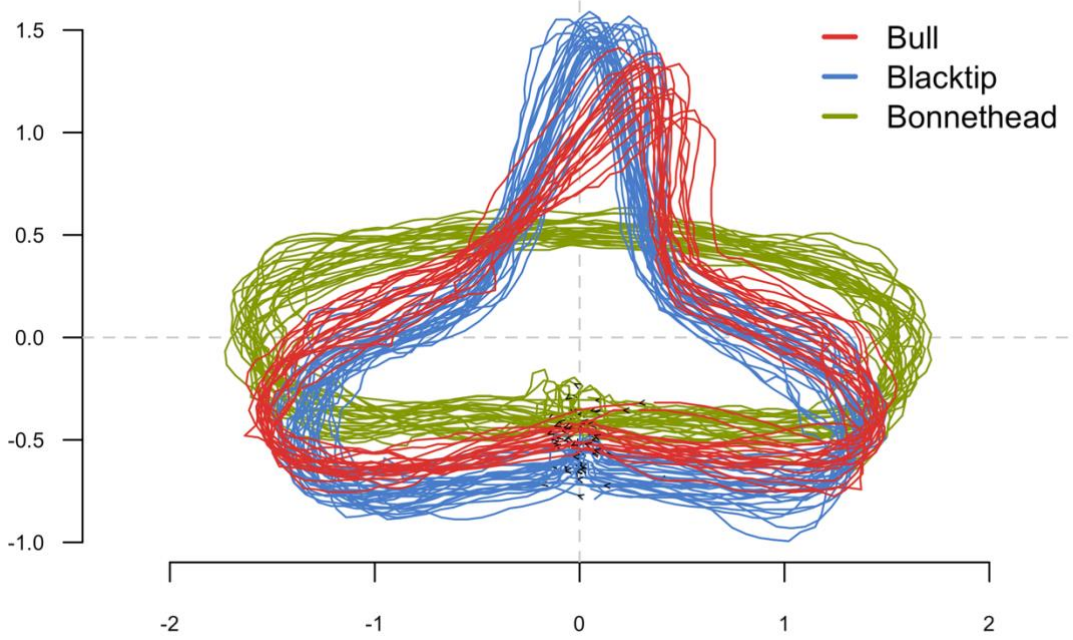

Figure 3-3. An example of raw centered and scaled tooth outlines from the posterior position along the lower jaw of each species (PostLow). These outline traces display the variation in morphology at this tooth position both within and among species.

during the digitization process. This method is generally quicker to conduct shape analysis than linear and geometric morphometrics due to the automated process, especially given a large number of selected landmarks.

Since EFA uses harmonic coefficients to describe tooth shape rather than linear measurements common in traditional morphometrics, relative characteristics of tooth morphology are used to qualitatively describe these teeth. These characteristics include base crown width, crown height (perpendicular to base crown width), and notch angle (angle between the tip of the crown and base crown width on the distal edge of the

tooth), which are expected to be functionally relevant characteristics (Figure 3-4; Anderson and LaBarbera 2008; Whitenack and Motta 2010; Crofts and Summers 2014). Although these traditional tooth morphometrics were not explicitly measured, they were used to make qualitative comparisons among tooth outlines in support of the quantitative statistical analyses.

Statistical analyses

All intra- and interspecific comparisons of tooth morphology were initially evaluated by principal component analysis (PCA) on the harmonic coefficients. The ordination of multivariate data is useful for the exploratory visualization of individual teeth within morphological space (morphospace). Although unconstrained ordination

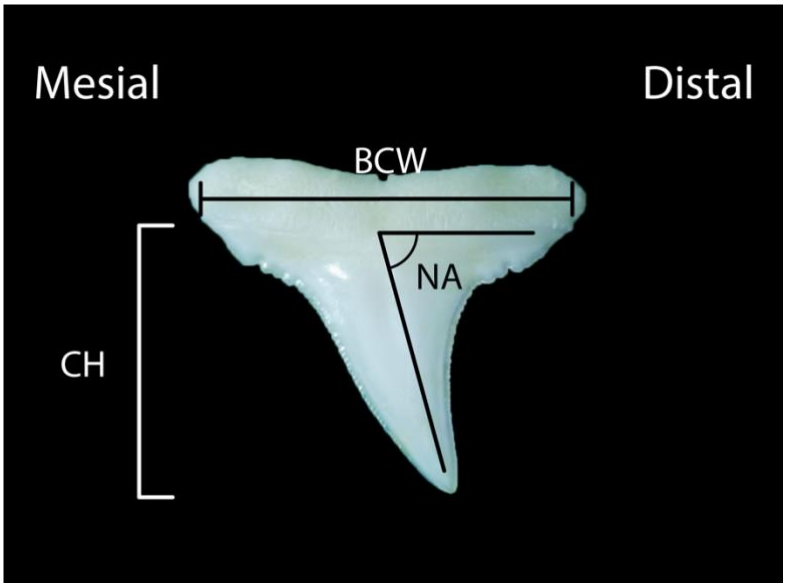

Figure 3-4. Morphometrics used to describe and make comparisons among teeth after statistical analyses. BCW, base crown width; CH, crown height; NA, notch angle.

methods (e.g. PCA) are useful for dimensional reduction, they are not able to directly test for differences among groups. Quantitative comparisons among groups (size class, tooth position, species) were conducted by permutational multivariate analysis of variance (PERMANOVA) with the 'vegan' package (ver 2.5-2; Oksanen et al. 2018) using 1000 permutations on selected PC scores (Anderson 2001a; Anderson 2001b). This method is a non-parametric analogue of MANOVA that is robust to violations of multivariate normality by using a permutation procedure (Anderson 2001a). The number of informative PC axes were determined by comparing against randomly generated eigenvalues using 1000 permutations, where eigenvalues from the original dataset were greater than the permuted dataset. Following significant results from the PERMANOVAs, pairwise comparisons (using 1000 permutations) were calculated using Bonferroni-adjusted p-values. All size classes were grouped together during intraspecific comparisons among tooth positions as well as during interspecific comparisons by tooth position since it was expected that the variation over ontogeny would be much smaller than among tooth positions or species. Significance was set at $\alpha = 0.05$ for all tests.

Results

Ontogenetic comparisons

Within bull sharks, significant ontogenetic differences in tooth morphology were detected at the LatLow (pseudo-$F_{3,15} = 2.55$, $p = 0.046$), LatUp (pseudo-$F_{3,16} = 3.62$, $p = 0.018$), PostLow (pseudo-$F_{3,15} = 6.51$, $p = 0.012$), and PostUp positions (pseudo-$F_{3,17}$ =

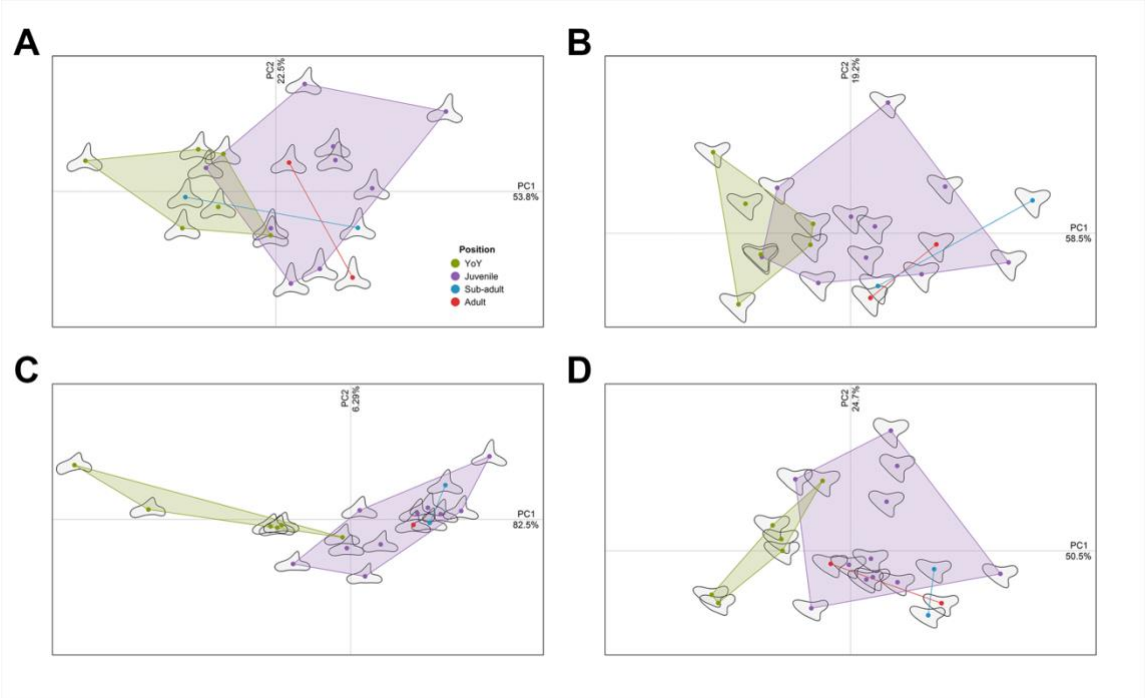

Figure 3-5. PCA ordinations of significant ontogenetic differences in tooth morphology from bull sharks plotted in morphospace. Numbers next to axis labels indicate the percentage of explained variation in morphology for that axis in a given ordination. These plots display the ontogenetic comparisons in tooth morphology at the lateral position along the lower (LatLow; **A**) and upper jaws (LatUp; **B**), as well as at the posterior position along the lower (PostLow; **C**) and upper jaws (PostUp; **D**). Gray silhouettes of teeth depict the outline generated using the harmonic coefficients produced by elliptic Fourier analysis to achieve 99.9% of total harmonic power.

4.68, $p = 0.003$), whereas AntLow and AntUp positions did not exhibit significant ontogenetic differences ($p > 0.05$; Table 3-4). Of the four tooth positions with significant ontogenetic differences, only pairwise comparisons between YoY and juvenile size classes were significant ($p < 0.05$). However, these results may have been affected by the low sample sizes for sub-adult and adult bull sharks (Table 3-3). Teeth from YoY and juvenile size classes at the LatLow position were separated along the PC1 axis (53.8%

Table 3-4. Results of PERMANOVA (1000 permutations) for ontogenetic comparisons by tooth position within each species based on the informative PCs analyzed

Species	Tooth Position	PCs Retained	df	Pseudo-F	*p*
Bull (*C. leucas*)	AntLow	3	3,16	1.60	0.176
	AntUp	3	3,17	0.81	0.550
	LatLow	2	3,15	2.55	**0.046**
	LatUp	2	3,16	3.62	**0.018**
	PostLow	2	3,15	6.51	**0.012**
	PostUp	2	3,17	4.68	**0.003**
Blacktip (*C. limbatus*)	AntLow	3	3,23	1.50	0.195
	AntUp	3	3,23	0.57	0.746
	LatLow	3	3,19	1.36	0.260
	LatUp	3	3,19	1.47	0.204
	PostLow	2	3,24	0.07	0.996
	PostUp	2	3,23	0.02	1.000
Bonnethead (*S. tiburo*)	AntLow	2	2,20	1.29	0.291
	AntUp	2	2,20	0.93	0.419
	LatLow	2	2,21	2.38	0.087
	LatUp	3	2,21	0.89	0.432
	PostLow	2	2,21	0.18	0.918
	PostUp	2	2,20	1.26	0.282

explained variation), while sub-adult and adult conspecifics overlapped more with juveniles. Relative crown height slightly increased from YoY teeth on the negative side of the PC1 axis to the positive side where juvenile, sub-adult, and adult teeth were positioned in morphospace (Figure 3-5A). The PCA of the LatUp position showed greatest differences between YoY and juveniles along the PC1 axis as well, which explained 58.5% of the variation (Figure 3-5B). Differences in morphology appeared to be driven by a slight change in the notch angle, which increased (i.e. greater notch angle) from the negative side (YoY) to the positive side (juvenile, sub-adult, adult) of the PC1

axis. At the PostLow position, morphological differences were more pronounced compared to the other tooth positions, for which YoY and juvenile bull sharks were separated along the PC1 axis (82.5% of the variation; Figure 3-5C). This pattern of changes was primarily a result of increases in relative crown height from YoY (negative PC1 axis) to juvenile conspecifics (positive PC1 axis). At the PostUp position, YoY and juvenile size classes were separated along the PC1 axis as well, which explained 50.5% of the total variation (Figure 3-5D). YoY individuals on the negative side of the PC1 axis appeared to exhibit more pointed cusps compared to juveniles on the positive side based upon a qualitative assessment. Although sub-adult and adult size classes did not exhibit significant pairwise differences in any of these analyses, tooth morphology in both of these groups frequently clustered with juvenile conspecifics. All other ontogenetic comparisons by tooth position in blacktip and bonnethead sharks were not significant ($p > 0.05$; Table 3-4).

Intraspecific comparisons among tooth positions

Significant differences in tooth morphology by position were detected in bull sharks following the PERMANOVA on four retained PCs (pseudo-$F_{5,114} = 28.50$, $p < 0.001$). All 15 pairwise comparisons found significant differences with the exception of the PostLow-PostUp comparison ($p = 0.150$). The bull shark PCA showed that PC1 accounted for morphological differences among tooth positions (53.9% of the total variation), whereas PC2 explained variation within each tooth position (24.2% of the variation; Figure 3-6A). Teeth in bull sharks change morphology from a greater relative

crown height with an approximately 90° notch angle (on the negative side of the PC1 axis; AntLow, AntUp) towards a lower relative crown height and a more acute notch angle (on the positive side of PC1 axis; PostLow, PostUp). Variation in tooth morphology was reasonably consistent within each tooth position along the PC2 axis, which represented other small differences in morphology. This is indicative of a similar level of intrinsic morphological variability at each tooth position regardless of whether ontogenetic differences had been detected or not.

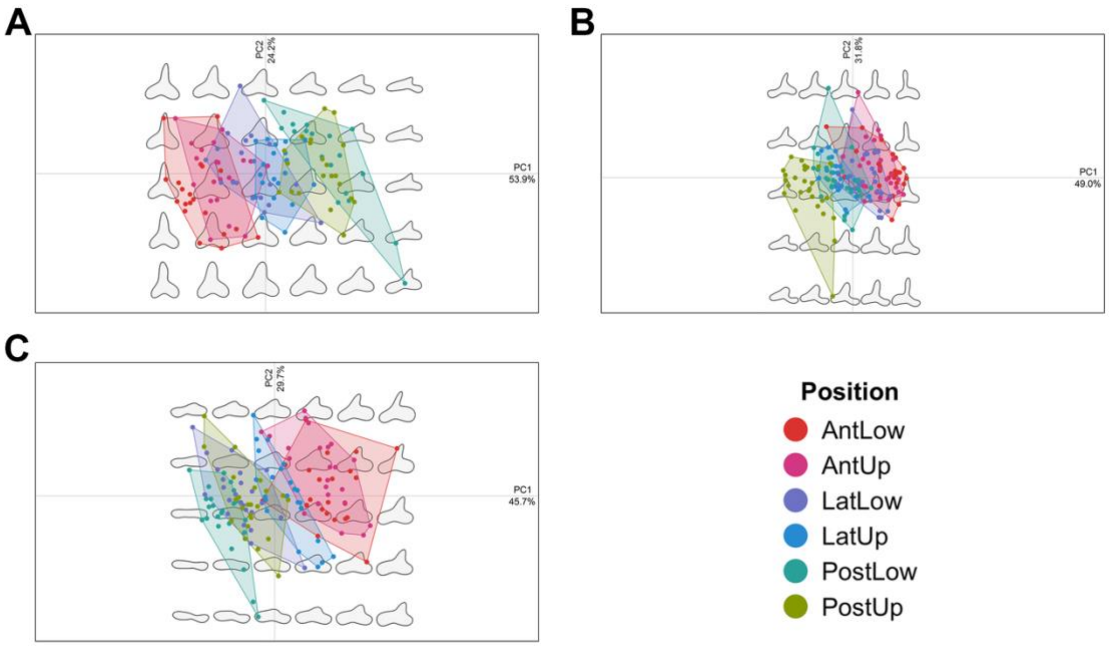

Figure 3-6. PCA ordinations of tooth morphology among tooth positions in bull (**A**), blacktip (**B**), and bonnethead sharks (**C**). Numbers next to axis labels indicate the percentage of explained variation in morphology for that axis in a given ordination. Points that fall within the minimum convex polygons represent the realized morphology of each tooth position. Gray tooth silhouettes depict the full continuum of morphospace among all tooth positions for each species as calculated using the harmonic coefficients from elliptic Fourier analysis.

Tooth morphology also significantly differed among positions in blacktip sharks (using 4 retained PCs; pseudo-$F_{5,149} = 26.08$, $p < 0.001$) with the exception of the AntLow-AntUp, AntLow-LatLow, AntUp-LatLow, and LatUp-PostLow pairwise comparisons ($p > 0.05$). The PC1 axis explained 49.0% of the total variation and represented differences in relative crown height and notch angle (Figure 3-6B). A large overlap in morphospace was observed among AntLow, AntUp, and LatLow teeth on the positive side of the PC1 axis, which were all characterized by a large relative crown height and a notch angle that approximated 90°. Relative crown height decreased and the notch angle became more acute on the negative side of the PC1 axis where the PostUp teeth were clustered. Teeth from LatUp and PostLow were located near zero along the PC1 axis, which represented an intermediate morphotype between the AntLow, AntUp, and LatLow positions and the PostUp position. Similar to the comparison in bull sharks, the PC2 axis represented smaller differences in morphology within each tooth position and explained 31.8% of the total variation. This variability along the PC2 axis was relatively consistent with the exception of a single outlier for the PostUp position.

Significant differences were detected among all tooth positions in bonnethead sharks as well (using 4 retained PCs; pseudo-$F_{5,135} = 26.10$, $p < 0.001$) with the exception of the LatLow-PostLow, LatLow-PostUp, and PostLow-PostUp pairwise comparisons ($p > 0.05$). Tooth positions were separated by an increase in relative crown height from the negative to the positive side of the PC1 axis, which explained 45.7% of the total variation (Figure 3-6C). AntLow and AntUp teeth clustered together on the positive PC1 axis (high crowns) while PostLow, PostUp, and LatLow were clustered on

Table 3-5. Results of PERMANOVA (1000 permutations) for interspecific comparisons by tooth position based on the informative PCs analyzed

Tooth Position	PCs Retained†	df	Pseudo-F	*p*
AntLow	3	2,67	71.09	**< 0.001**
AntUp	3	2,68	60.23	**< 0.001**
LatLow	3	2,63	152.16	**< 0.001**
LatUp	3	2,64	76.72	**< 0.001**
PostLow	4	2,68	93.50	**< 0.001**
PostUp	2	2,68	51.68	**< 0.001**

the negative PC1 axis (low crowns). Teeth from the LatUp position did not group together with any of the other tooth positions and was found near zero along the PC1axis. Teeth from the AntLow position also appeared to display greater variation in shape compared to other tooth positions with respect to the PC1 axis, demonstrating greater variability in relative crown height. The PC2 axis explained 29.7% of the total variation and also explained smaller differences in tooth morphology, which was consistent across all tooth positions.

Interspecific comparisons

Comparisons among species found significant differences at all six tooth positions ($p < 0.001$; Table 3-5), for which pairwise relationships varied. At the AntLow position, bull and blacktip sharks were both significantly different from bonnetheads (*p*

= 0.003), but not from each other (p = 0.147). The PC1 axis (70.2% of variation) represented relative crown height, which was greater in bull and blacktip sharks compared to bonnetheads (Figure 3-7A). At the AntUp position, however, morphology among all three species significantly differed (p = 0.003) and PC1 explained 62.5% of the total variation. AntUp teeth in bonnethead sharks exhibited a lower relative crown height than the other species in addition to a more acute notch angle (Figure 3-7B). The primary difference between bull and blacktip shark teeth at the AntUp position appeared to be the greater relative width at the base of the crown in bulls compared to blacktips. Similarly, significant differences among all species were found at the LatLow (p = 0.003), LatUp (p = 0.003), and PostLow positions (p = 0.003). Differences in tooth morphology at the LatLow position were characterized by relative crown height and separated along the PC1 axis (81.1% of variation; Figure 3-7C). Although tooth morphology at this position was most noticeably different in bonnetheads, bull sharks primarily differed from blacktips by possessing a greater relative base crown width. Teeth at the LatUp position decreased in relative crown height and notch angle from the negative to the positive side of the PC1 axis, which explained 68.0% of the variation (Figure 3-7D). At this position, blacktip sharks had slightly greater relative crown heights and notch angles than bull sharks, both of which were greater than in bonnethead teeth. PostLow tooth morphology varied greatly among all species and also separated along the PC1 axis, which explained 72.2% of the variation (Figure 3-7E). Bonnethead sharks possessed molariform teeth (low relative crown height) at this position, whereas

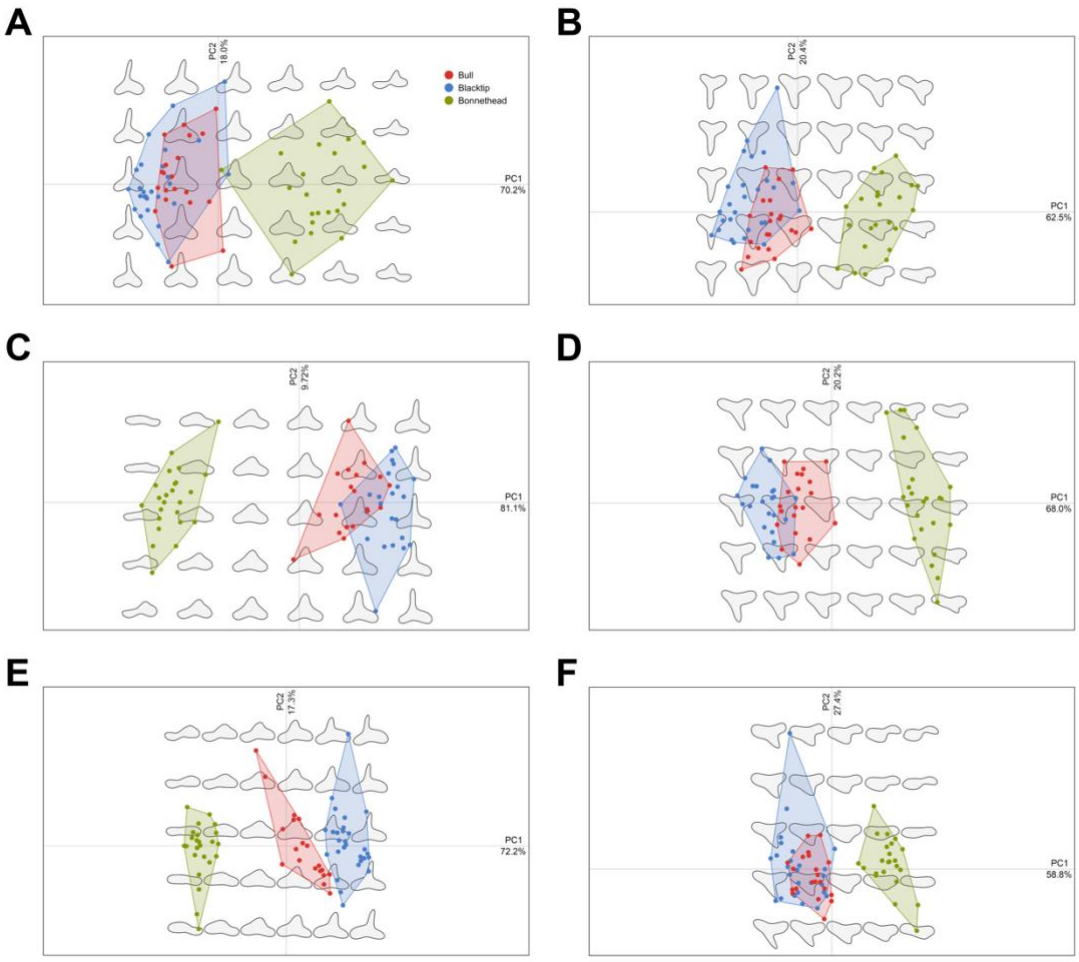

Figure 3-7. PCA ordinations of interspecific comparisons by tooth position, including the anterior position on the lower (AntLow; **A**) and upper jaws (AntUp; **B**), the lateral position on the lower (LatLow; **C**) and upper jaws (LatUp; **D**), and the posterior position on the lower (PostLow; **E**) and upper jaws (PostUp; **F**). Numbers next to axis labels indicate the percentage of explained variation in morphology for that axis in a given ordination. Points that fall within the minimum convex polygons represent the realized morphology of each species. Gray tooth silhouettes depict the full range of morphospace among all species for a given tooth position as calculated using the harmonic coefficients from elliptic Fourier analysis**.**

the teeth of bull and blacktip teeth were cusped. However, blacktip teeth were more gracile and exhibited a greater relative crown height than bull sharks. At the PostUp position, significant differences were only detected in the bull – bonnethead and blacktip – bonnethead pairwise comparisons ($p = 0.003$), but not between bull and blacktip sharks ($p = 0.348$). The PC1 axis (58.8% of variation) separated bonnethead teeth that were molariform from bull and blacktip sharks that both exhibited greater relative crown heights and acute notch angles (Figure 3-7F).

Discussion

Ontogenetic dietary shifts have been reported for each of the three species in the present study, but these did not appear to be associated with a change in tooth morphology. Although bull sharks were the only species to exhibit statistically significant differences in morphology over ontogeny, most of these changes do not appear to be functionally significant. Of the four tooth positions in bull sharks with significant ontogenetic differences, only the PostLow position appeared to exhibit a functional shift in tooth shape. Although there may be implications with regard to cutting performance at this single position (e.g. an increase in relative crown height may more securely hold prey in place to be cut by teeth on the upper jaw), it is unclear why only one of the six evaluated tooth positions would exhibit these differences. This could possibly be the result of greater selection pressure at this tooth position since functionally difficult prey may need to be secured by teeth with higher crowns in the posterior region of the lower jaw during forceful head-shaking behavior. However,

further functional testing would be required to support this hypothesis. Over ontogeny, the diet of bull sharks shifts from primarily small-bodied teleost prey as YoY and juveniles to including greater proportions of birds, marine mammals, and other elasmobranchs as sub-adults and adults (Snelson and Williams 1981; Snelson et al. 1984; Cliff and Dudley 1991). It is possible that a functional change in tooth morphology could be useful for this dietary shift. The prey consumed by these larger size-classes are more difficult to process than that of younger conspecifics (Habegger et al. 2012) and a change in tooth morphology may assist in cutting through tough tissue (e.g. skin, scales, tendons/ligaments, bones, connective tissue) as opposed to the puncture of soft tissues by younger bull sharks. More specifically, an increase in relative crown height at the PostLow position over ontogeny may assist larger conspecifics to securely hold the prey in place during lateral head-shaking behavior. This may be difficult for some prey due to an integument that is compliant, thick, and/or covered in puncture-resistant scales. These interpretations of ontogenetic changes in tooth morphology (or lack thereof) are potentially limited as a result of the small sample size of sub-adult and adult conspecifics. In blacktip and bonnethead sharks, no significant differences in tooth morphology were found over ontogeny. However, these patterns likely reflect the consumption of prey items with comparable material properties. This is exemplified by sustained piscivory in blacktip sharks and an increase in the proportion of hard-shelled crustaceans consumed by bonnetheads (Bethea et al. 2007; Barry et al. 2008).

When making intraspecific comparisons in morphology among tooth positions, few of the teeth displayed similarities within each species. In bull sharks, only teeth at the posterior positions along the tooth row (PostLow and PostUp) were morphologically equivalent while all other pairwise comparisons significantly differed. Teeth from the upper jaw typically have crowns with a broader labial face and serrated edges whereas teeth from the lower jaw are often gracile with smooth edges. These morphological differences may result in the partitioning of functions between the upper and lower jaws. With less surface area to make contact with the prey item and therefore less friction during puncture, gracile teeth from the lower jaw can penetrate tissue more easily than teeth from the upper jaw of this species (Frazzetta 1988). In blacktip sharks, however, gracile teeth at the AntLow, AntUp, and LatLow positions were morphologically equivalent. Patterns of morphological equivalency in bonnetheads were similar to blacktip sharks, in which molariform teeth at PostLow, PostUp, and LatLow positions did not significantly differ from one another. The blacktip pattern results in more teeth used to capture and retain elusive fish prey, but expands the dental battery of molariform teeth used to process hard-shelled prey in bonnethead sharks. Therefore, these results suggest that there are functional units of teeth along the jaws, which also exhibit species-specific patterns. Given the intraspecific patterns of dissimilarity among tooth positions, bull sharks exhibited a slightly greater level of heterodonty than the other two species. These patterns of heterodonty among species may have implications for the duration and efficiency of prey handling, such that the dentition of a given species may confer an advantage to only certain types of prey. The dentition of blacktip and bonnethead sharks

appear specialized for piscivory and durophagy, respectively, which is supported by the unit of morphologically equivalent gracile teeth in blacktips and molariform teeth in bonnetheads. By possessing a greater number of teeth with these respective morphologies, blacktip sharks may be able to capture and consume fishes more efficiently, whereas bonnethead sharks may be able to efficiently crush and consume crustaceans. The high level of heterodonty in bull sharks appears to fit with their status as a generalist consumer, which would require a diversity of tooth shapes that are appropriate for puncturing and cutting tissue of teleosts, elasmobranchs, and marine mammals. If these species attempted to capture and process atypical prey items (e.g. the consumption of hard-shelled prey by blacktips), however, it is expected that prey-processing would require longer durations and be more energetically expensive due to an unsuitable tooth morphology. To support these hypotheses, further functional testing must be conducted.

Prey handling efficiency is influenced by morphology of the feeding apparatus, which can dictate the type or size of prey that are selected (Werner 1977; Hoyle and Keast 1988; Emerson et al. 1994; Hampton 2018). In sharks that use lateral head-shaking to process prey, the shape of teeth at the lateral and posterior regions along the jaws may substantially impact the cutting efficiency of functionally difficult tissue. Notched blades can greatly increase the cutting efficiency (up to 50%) through compliant material by concentrating the stress on the tissue at the base of that notch, which causes it to fracture (Abler 1992; Anderson and LaBarbera 2008). This results in less wasted energy and therefore decreases the level of stress needed for material fracture. Additionally, the

cutting efficiency of a notched blade increases as the angle becomes more acute (Anderson and LaBarbera 2008). A common pattern in many carcharhiniform sharks is a decrease in the notch angle from anterior to posterior along the tooth row (i.e. the angle becomes more acute), which would confer increased efficiency during draw at the lateral and posterior positions compared to the anterior positions. Therefore, anterior teeth are more suitable for initial prey capture whereas lateral and posterior teeth are advantageous for processing large prey.

Constraints related to prey handling efficiency may be strongest at smaller size classes. This is because smaller sharks are restricted by both gape and bite force, which limits their ability to puncture or fracture the prey item (Wainwright 1988; Hernandez and Motta 1997; Verwaijen et al. 2002; Mara et al. 2010). Although teeth from the upper jaw of young bull sharks would require more force to puncture the integument of a teleost fish compared to young blacktips (Whitenack and Motta 2010), bite force in bull sharks is greater on average for all overlapping body lengths (Huber et al. 2006; Habegger et al. 2012). Therefore, the increased force required by bull sharks to puncture the same prey item as blacktips is not expected to constrain their ability to capture and process prey. Additionally, young bull and blacktip sharks may be limited in their ability to puncture the integument of some teleost fishes (e.g. ladyfish *Elops saurus*) due to deformation of these compliant prey (Whitenack and Motta 2010). This occurs when the deformation of prey tissue exceeds crown height of these small shark size classes, thereby preventing puncture of the integument (Whitenack and Motta 2010). Since bonnethead sharks have a smaller gape and lower bite force compared to the other two

species, they are likely constrained by the size of their hard-shelled prey. This may particularly limit young conspecifics to smaller prey since the force required to fracture the shell of its primary prey item (blue crab *Callinectes sapidus*) increases with crab carapace length (Mara et al. 2010).

Interspecific comparisons by tooth position found species-specific patterns in morphology, which often differed by relative crown height and notch angle. This was most apparent in four of the six positions (AntUp, LatLow, LatUp, PostLow), in which all species significantly differed from one another. However, teeth from the AntLow and PostUp positions in bull and blacktip sharks were morphologically equivalent. If morphology does confer a particular function (or a difference in prey handling efficiency), the teeth in each of these species may reflect the functional properties of their prey and the mode of prey processing necessary for consumption. However, testing this hypothesis was beyond the scope of this study.

Based upon observations of feeding behavior and diet in these species, inferences can be made regarding tooth function. The diet of adult bonnethead sharks consists almost entirely of portunid crabs (Cortés et al. 1996; Bethea et al. 2007; Plumlee and Wells 2016), whose exoskeleton requires greater force to fracture than the integument of teleost fishes (Mara et al. 2010; Whitenack and Motta 2010). Bonnethead teeth at the anterior region of the jaws have short relative crown heights compared to bull and blacktip sharks, in addition to molariform teeth along the posterior margin of the jaws. Teeth from the AntLow position appear to match the ideal morphology to fracture hard-shelled prey, which was suggested by functional testing on snail shells (Crofts and

Summers 2014). This implies that the cusped AntLow teeth of bonnetheads are also suitable to crush crabs in addition to the posterior molariform teeth, although lower bite force at the anterior teeth may impose a constraint (Mara et al. 2010). However, large crabs are not always crushed before consumption. Bonnetheads often use lateral head-shaking to remove the legs of their prey before swallowing them whole (Myrberg and Gruber 1974; Wilga and Motta 2000). Large blacktip size classes prey upon small to medium-sized teleost fishes and a lower proportion of small elasmobranchs (Castro 1996). Following the initial capture of small or medium-sized prey, blacktip sharks typically readjust their grasp on the prey or may swallow it immediately (Frazzetta and Prange 1987). The size and material properties of these soft-bodied prey items appears to only necessitate a secure grasp before consumption. Therefore, the gracile teeth located towards the anterior region of the jaws (AntLow, AntUp, LatLow) are suitable to capture elusive fishes. For the occasional large prey item, such as elasmobranchs, a slight decrease in notch angle from anterior to posterior along the tooth row may facilitate greater cutting efficiency prior to consumption. Compared to blacktips, common prey items of large bull sharks are difficult to process and may exceed maximum gape (Werry et al. 2011; Habegger et al. 2012). Large base crown widths of teeth from the upper jaw likely resist high lateral forces (Williams 2001), which typically occur during head-shaking behavior. The presence of serrations and acute notch angles at the lateral and posterior positions are thought to increase cutting efficiency of compliant material (Abler 1992; Anderson and LaBarbera 2008). This is important for large bull sharks since they consume greater proportions of elasmobranchs, marine mammals, birds, and

large teleost fishes compared to smaller conspecifics (Cliff and Dudley 1991; Heithaus 2001; Werry et al. 2011). Although the material properties of large bull shark prey have not yet been tested, it is expected that they are more difficult to process than small-bodied teleosts due to the presence of larger skeletal elements and an integument that requires greater force to puncture (Currey 1987; Horton and Summers 2009; Whitenack and Motta 2010; Habegger et al. 2012). As characterized in each of these species, it appears that the interaction of prey processing behavior and material properties of the prey item is reflected by the collective morphology at all tooth positions.

While the present study focuses on the tooth morphology of extant sharks, these methods and findings can be used to guide paleoichthyological studies and to test functional hypotheses in extant and extinct fishes. We recommend the use of EFA to evaluate the morphology of elasmobranch teeth, which may benefit from the fusion of traditional morphometrics (linear measurements) to quantitatively describe any significant differences among tooth outlines (*sensu* Ginter et al. 2012). Additionally, we suggest a cautious approach to the identification of isolated fossil elasmobranch teeth due to the intrinsic variables (sex, age, position in jaws) that may contribute to morphological differences within a single species. We suggest that future functional testing of shark teeth include the measurement of performance of a given morphology *in situ* using the upper and lower jaws to perform dynamic movements as used by the species of interest. This approach is likely to address any possible discrepancies in proposed function while maintaining the natural arrangement of teeth, which could be obscured by the analysis of an individual tooth (tooth vs teeth). Prey handling efficiency

could also be evaluated for a variety of prey types by measuring the duration required to process a prey item, as well as to measure the concomitant energy expenditure. Furthermore, the present study proposes that there may be different levels of heterodonty within elasmobranchs. Future studies should evaluate other species with varying levels of heterodonty to discern whether there is a relationship between the extent of heterodonty and the properties of the primary prey that are consumed.

References

Abler WL. 1992. The serrated teeth of Tyrannosaurid dinosaurs, and biting structures in other animals. *Paleobiology* 18:161–183.

Anderson M J. 2001a. A new method for non-parametric multivariate analysis of variance. *Austral Ecol.* 26:32–46.

Anderson M J. 2001b. Permutation tests for univariate or multivariate analysis of variance and regression. *Can. J. Fish. Aquat. Sci.* 58:626–639. doi:10.1139/f01-004.

Anderson P, LaBarbera M. 2008. Functional consequences of tooth design: effects of blade shape on energetics of cutting. *J. Exp. Biol.* 211:3619–3626. doi:10.1242/jeb.020586.

Applegate SP. 1965. Tooth terminology and variation in sharks with special reference to the sand shark Carcharias taurus Rafinesque. *Los Angeles Cty. Museum Contrib. Sci.* 86:1–18.

Arnold SJ. 1983. Morphology, performance and fitness. *Am. Zool.* 23:347–361.

Barry K, Condrey R, Driggers W, Jones C. 2008. Feeding ecology and growth of neonate and juvenile blacktip sharks Carcharhinus limbatus in the Timbalier-Terrebone Bay complex, LA, U.S.A. *J. Fish Biol.* 73:650–662. doi:10.1111/j.1095-8649.2008.01963.x.

Bergman J, Lajeunesse M, Motta P. 2017. Teeth penetration force of the tiger shark Galeocerdo cuvier and sandbar shark Carcharhinus plumbeus. *J. Fish Biol.* 91:460–472. doi:10.1111/jfb.13351.

Bertrand NG. 2014. Distribution and evolution of heterdonty in the ray-finned fishes

(Actinopterygii). MS Thesis, Texas A&M University, College Station, TX.

Bethea D, Buckel J, Carlson J. 2004. Foraging ecology of the early life stages of four sympatric shark species. *Mar. Ecol. Prog. Ser.* 268:245–264. doi:10.3354/meps268245.

Bethea DM, Hale L, Carlson JK, Cortés E, Manire CA, Gelsleichter J. 2007. Geographic and ontogenetic variation in the diet and daily ration of the bonnethead shark, Sphyrna tiburo, from the eastern Gulf of Mexico. *Mar. Biol.* 152:1009–1020. doi:10.1007/s00227-007-0728-7.

Bigelow HB, Schroeder WC. 1948. Lancelets, cyclostomes, sharks. In: Fishes of the Western North Atlantic. Part 1. New Haven, CT, USA: Sears Foundation for Marine Research. p. 59–546.

Bigelow HB, Schroeder WC. 1953a. Sawfishes, guitarfishes, skates, rays and chimaeroides. In: Fishes of the Western North Atlantic. Part 2. New Haven, CT, USA: Sears Foundation for Marine Research. p. 1–514.

Bigelow HB, Schroeder WC. 1953b. Fishes of the Gulf of Maine. *Fish. Bull. Fish Wildl. Serv.* 53:1–577.

Le Boeuf BJ, Mesnick S. 1991. Sexual behavior of male northern elephant seals : I. Lethal injuries to adult females. *Behaviour* 116:143–162.

Bonhomme V, Picq S, Gaucherel C, Claude J. 2014. Momocs: Outline analysis using R. *J. Stat. Softw.* 56:1–24. doi:10.18637/jss.v056.i13.

Branstetter S. 1987. Age and growth estimates for blacktip, Carcharhinus limbatus, and spinner, C. brevipinna, sharks from the northwestern Gulf of Mexico. *Copeia*

1987:964–974.

Branstetter S, Stiles R. 1987. Age and growth estimates of the bull shark, Carcharhinus leucas, from the northern Gulf of Mexico. *Environ. Biol. Fishes* 20:169–181.

Cappetta H. 1986. Types dentaires adaptatifs chez les sélaciens actuels et post-paléozoiques. *Paleovertebrata* 16:57–76.

Cappetta H. 1987. Handbook of Paleoichthyology, Vol. 3B, Chondrichthyes II.

Castro JI. 1996. Biology of the blacktip shark, Carcharhinus limbatus, off the southeastern United States. *Bull. Mar. Sci.* 59:508–522.

Claude, J. (2008). *Morphometrics with R*. New York: Springer-Verlag.

Cliff G, Dudley SF. 1991. Sharks caught in the protective gill nets off Natal, South Africa. 4. The bull shark Carcharhinus leucas Valenciennes. *South African J. Mar. Sci.* 10:253–270. doi:10.2989/02577619109504636.

Compagno LJ. 1988. Sharks of the order Carcharhiniformes. Princeton: Princeton University Press.

Corn KA, Farina SC, Brash J, Summers AP. 2016. Modelling tooth – prey interactions in sharks: the importance of dynamic testing. *R. Soc. Open Sci.* 3:160141. doi:http://dx.doi.org/10.1098/rsos.160141.

Cortés E, Manire CA, Hueter RE. 1996. Diet, feeding habits, and diel feeding chronology of the bonnethead shark, Sphyrna tiburo, in southwest Florida. *Bull. Mar. Sci.* 58:353–367. doi:10.1007/s00227-006-0325-1.

Crampton JS. 1995. Elliptic Fourier shape analysis of fossil bivalves: some practical considerations. *Lethaia* 28:179–186. doi:10.1111/j.1502-3931.1995.tb01611.x.

Crofts S, Summers A. 2014. How to best smash a snail: the effect of tooth shape on crushing load. *J. R. Soc. Interface* 11:20131053. doi:10.1098/rsif.2013.1053.

Currey J. 1987. The evolution of the mechanical properties of amniote bone. *J. Biomech.* 20:1035–1044.

D'Amore DC. 2015. Illustrating ontogenetic change in the dentition of the Nile monitor lizard, Varanus niloticus: A case study in the application of geometric morphometric methods for the quantification of shape-size heterodonty. *J. Anat.* 226:403–419. doi:10.1111/joa.12293.

Davit-Béal T, Chisaka H, Delgado S, Sire JY. 2007. Amphibian teeth: Current knowledge, unanswered questions, and some directions for future research. *Biol. Rev.* 82:49–81. doi:10.1111/j.1469-185X.2006.00003.x.

Dean MN, Bizzarro JJ, Clark B, Underwood CJ, Johanson Z. 2017. Large batoid fishes frequently consume stingrays despite skeletal damage. *R. Soc. Open Sci.* 4:170674. doi:10.1098/rsos.170674.

Emerson SB, Greene HW, Charnov EL. 1994. Allometric aspects of predator-prey interactions. In: Ecological Morphology: Integrative Organismal Biology. Chicago: University of Chicago Press. p. 123–139.

Erickson GM, Gignac PM, Steppan SJ, Lappin AK, Vliet KA, Brueggen JD, Inouye BD, Kledzik D, Webb GJW. 2012. Insights into the ecology and evolutionary success of crocodilians revealed through bite-force and tooth-pressure experimentation. *PLoS One* 7:e31781. doi:10.1371/journal.pone.0031781.

Estrada JA, Rice AN, Natanson LJ, Skomal GB. 2006. Use of isotopic analysis of

vertebrae in reconstructiong ontogenetic feeding ecology in white sharks. *Ecology* 87:829–834. doi:10.1890/0012-9658(2006)87[829:UOIAOV]2.0.CO;2.

Ferrara T, Clausen P, Huber D, McHenry C, Peddemors V, Wroe S. 2011. Mechanics of biting in great white and sandtiger sharks. *J. Biomech.* 44:430–435. doi:10.1016/j.jbiomech.2010.09.028.

Ferson S, Rohlf FJ, Koehn RK. 1985. Measuring shape variation of two-dimensional outlines. *Syst. Biol.* 34:59–68.

Frazzetta T. 1988. The mechanics of cutting and the form of shark teeth (Chondrichthyes, Elasmobranchii). *Zoomophology* 108:93–107.

Frazzetta T. 1994. Feeding mechanisms in sharks and other elasmobranchs. In: Biomechanics of Feeding in Vertebrates. Berlin, Heidelberg: Springer. p. 31–57.

Frazzetta T, Prange C. 1987. Movements of cephalic components during feeding in some requiem sharks (Carcharhiniformes: Carcharhinidae). *Copeia* 1987:979–993.

Freeman PW. 2000. Macroevolution in Microchiroptera: Recoupling morphology and ecology with phylogeny. *Evol. Ecol. Res.* 2:317–335.

French G, Stürup M, Rizzuto S, van Wyk J, Edwards D, Dolan R, Wintner S, Towner A, Hughes W. 2017. The tooth, the whole tooth and nothing but the tooth: tooth shape and ontogenetic shift dynamics in the white shark Carcharodon carcharias. *J. Fish Biol.* 91:1032–1047. doi:10.1111/jfb.13396.

Fu AL, Hammerschlag N, Lauder G V, Wilga CD, Kuo C-Y, Irschick DJ. 2016. Ontogeny of head and caudal fin shape of an apex marine predator: the tiger shark (Galeocerdo cuvier). *J. Morphol.* 277:556–564. doi:10.1002/jmor.20515.

Galloway KA, Anderson PS, Wilga CD, Summers AP. 2016. Performance of teeth of lingcod, Ophiodon elongatus, over ontogeny. *J. Exp. Zool. Part A Ecol. Genet. Physiol.* 325A:99–105. doi:10.1002/jez.1967.

Ginter CC, DeWitt TJ, Fish FE, Marshall CD. 2012. Fused traditional and geometric morphometrics demonstrate pinniped whisker diversity. *PLoS One* 7:e34481. doi:10.1371/journal.pone.0034481.

Gutteridge AN, Bennett MB. 2014. Functional implications of ontogenetically and sexually dimorphic dentition in the eastern shovelnose ray, Aptychotrema rostrata. *J. Exp. Biol.* 217:192–200. doi:10.1242/jeb.089326.

Habegger ML, Motta PJ, Huber DR, Dean MN. 2012. Feeding biomechanics and theoretical calculations of bite force in bull sharks (Carcharhinus leucas) during ontogeny. *Zoology* 115:354–364. doi:10.1016/j.zool.2012.04.007.

Haines AJ, Crampton JS. 2000. Improvements to the method of Fourier shape analysis as applied in morphometric studies. *Palaeontology* 43:765–783. doi:10.1111/1475-4983.00148.

Hampton PM. 2018. Ontogenetic prey size selection in snakes: predator size and functional limitations to handling minimum prey sizes. *Zoology* 126:103–109. doi:10.1016/j.zool.2017.11.006.

Heithaus M. 2001. Predator-prey and competitive interactions between sharks (order Selachii) and dolphins (suborder Odontoceti): a review. *J. Zool.* 253:53–68. doi:10.1017/S0952836901000061.

Hernandez LP, Motta PJ. 1997. Trophic consequences of differential performance:

ontogeny of oral jaw-crushing performance in the sheepshead, Archosargus probatocephalus (Teleostei, Sparidae). *J. Zool.* 243:737–756. doi:10.1111/j.1469-7998.1997.tb01973.x.

Herrel A, Moore J, Bredeweg E, Nelson N. 2010. Sexual dimorphism, body size, bite force and male mating success in tuatara. *Biol. J. Linn. Soc.* 100:287–292. doi:10.1111/j.1095-8312.2010.01433.x.

Horton J, Summers A. 2009. The material properties of acellular bone in a teleost fish. *J. Exp. Biol.* 212:1413–1420. doi:10.1242/jeb.020636.

Hoyle JA, Keast A. 1988. Prey handling time in two piscivores, Esox americanus vermiculatus and Micropterus salmoides, with contrasting mouth morphologies. *Can. J. Zool.* 66:540–542.

Huber DR, Claes JM, Mallefet J, Herrel A. 2009. Is extreme bite performance associated with extreme morphologies in sharks? *Physiol. Biochem. Zool.* 82:20–28. doi:10.1086/588177.

Huber DR, Eason TG, Hueter RE, Motta PJ. 2005. Analysis of the bite force and mechanical design of the feeding mechanism of the durophagous horn shark Heterodontus francisci. *J. Exp. Biol.* 208:3553–3571. doi:10.1242/jeb.01816.

Huber DR, Weggelaar CL, Motta PJ. 2006. Scaling of bite force in the blacktip shark Carcharhinus limbatus. *Zoology* 109:109–119. doi:10.1016/j.zool.2005.12.002.

Huysseune A, Sire J-Y. 1998. Evolution of patterns and processes in teeth and tooth-related tissues in non-mammalian vertebrates. *Eur. J. Oral Sci.* 106:437–481. doi:10.1111/j.1600-0722.1998.tb02211.x.

Janis CM, Fortelius M. 1988. On the means whereby mammals achieve increased functional durability of their dentitions, with special reference to limiting factors. *Biol. Rev.* 63:197–230.

Kajiura S, Tricas T. 1996. Seasonal dynamics of dental sexual dimorphism in the Atlantic stingray Dasyatis sabina. *J. Exp. Biol.* 199:2297–2306.

Kolmann MA, Huber DR, Motta PJ, Grubbs RD. 2015. Feeding biomechanics of the cownose ray, Rhinoptera bonasus, over ontogeny. *J. Anat.* 227:341–351. doi:10.1111/joa.12342.

Kuhl FP, Giardina CR. 1982. Elliptic Fourier features of a closed contour. *Comput. Graph. Image Process.* 18:236–258. doi:10.1016/0146-664X(82)90034-X.

Lauder G V. 1982. Patterns of evolution in the feeding mechanism of Actinopterygian fishes. *Am. Soc. Zool.* 285:275–285. doi:10.1093/icb/22.2.275.

Liem KF, Bemis WE, Walker WF, Grande L. 2001. Functional Anatomy of the Vertebrates: An Evolutionary Perspective. 3rd ed. New York: Harcourt College Publishers.

Lombardi-Carlson L, Cortés E, Parsons G, Manire C. 2003. Latitudinal variation in life-history traits of bonnethead sharks, Sphyrna tiburo, (Carcharhiniformes : Sphyrnidae) from the eastern Gulf of Mexico. *Mar. Freshw. Res.* 54:875–883.

Losos JB. 1990. Ecomorphology, performance capability, and scaling of West Indian anolis lizards: An evolutionary analysis. *Ecol. Monogr.* 60:369–388.

Lowe C, Wetherbee B, Crow G, Tester A. 1996. Ontogenetic dietary shifts and feeding behavior of the tiger shark, Galeocerdo cuvier, in Hawaiian waters. *Environ. Biol.*

Fishes 47:203–211.

Lucifora LO, Menni RC, Escalante AH. 2001. Analysis of dental insertion angles in the sand tiger shark, *Carcharias taurus* (Chondrichthyes: Lamniformes). *Cybium* 25:23–31.

Mara KR, Motta PJ, Huber DR. 2010. Bite force and performance in the durophagous bonnethead shark, Sphyrna tiburo. *J. Exp. Zool. Part A Ecol. Genet. Physiol.* 313:95–105. doi:10.1002/jez.576.

Marramà G, Kriwet J. 2017. Principal component and discriminant analyses as powerful tools to support taxonomic identification and their use for functional and phylogenetic signal detection of isolated fossil shark teeth. *PLoS One* 12:e0188806. doi:10.1371/journal.pone.0188806.

McCosker JE. 1985. White shark attack behavior: observations of and speculations about predator and prey strategies. *Mem. South. Calif. Acad. Sci.* 9:123–135.

Mehta RS, Wainwright PC. 2007. Raptorial jaws in the throat help moray eels swallow large prey. *Nature* 449:79–82. doi:10.1038/nature06062.

Moss SA. 1972. The feeding mechanism of sharks of the family Carcharhinidae. *J. Zool.* 167:423–436. doi:10.1111/j.1469-7998.1972.tb01734.x.

Motta P, Wilga C. 2001. Advances in the study of feeding behaviors, mechanisms, and mechanics of sharks. *Environ. Biol. Fishes* 60:131–156. doi:10.1023/A:1007649900712.

Motta PJ, Tricas TC, Hueter RE, Summers AP. 1997. Feeding mechanism and functional morphology of the jaws of the lemon shark Negaprion brevirostris (Chondrichthyes,

Carcharhinidae). *J. Exp. Biol.* 200:2765–2780.

Myrberg AA, Gruber SH. 1974. The behavior of the bonnethead shark, Sphyrna tiburo. *Copeia* 1974:358–374.

Neto JC, Meyer GE, Jones DD, Samal AK. 2006. Plant species identification using Elliptic Fourier leaf shape analysis. *Comput. Electron. Agric.* 50:121–134. doi:10.1016/j.compag.2005.09.004.

Newman SP, Handy RD, Gruber SH. 2012. Ontogenetic diet shifts and prey selection in nursery bound lemon sharks, Negaprion brevirostris, indicate a flexible foraging tactic. *Environ. Biol. Fishes* 95:115–126. doi:10.1007/s10641-011-9828-9.

Norton SF. 1988. Role of the gastropod shell and operculum in inhibiting predation by fishes. *Science* 241:92–94. doi:10.1126/science.241.4861.92.

Nyberg K, Ciampaglio C, Wray G. 2010. Tracing the ancestry of the great white shark, Carcharodon carcharias, using morphometric analyses of fossil teeth. *J. Vertebr. Paleontol.* 26:806–814. doi:10.1671/0272-4634(2006)26.

Oksanen, J., Guillaume Blanchet, F., Friendly, M., Kindt, R., Legendre, P., McGlinn, D., Minchin, P. R., O'Hara, R. B., Simpson, G. L., Solymos, P. (2018). vegan: Community Ecology Package. R package version 2.5-2. https://CRAN.R-project.org/package=vegan.

Plumlee JD, Wells RD. 2016. Feeding ecology of three coastal shark species in the northwest Gulf of Mexico. *Mar. Ecol. Prog. Ser.* 550:163–174. doi:10.3354/meps11723.

Powlik JJ. 1995. On the geometry and mechanics of tooth position in the white shark,

Carcharodon carcharias. *J. Morphol.* 226:277–288. doi:10.1002/jmor.1052260304.

Powter DM, Gladstone W, Platell M. 2010. The influence of sex and maturity on the diet, mouth morphology and dentition of the Port Jackson shark, Heterodontus portusjacksoni. *Mar. Freshw. Res.* 61:74–85. doi:10.1071/MF09021.

Pratt HL, Carrier JC. 2001. A review of elasmobranch reproductive behavior with a case study on the nurse shark, Ginglymostoma cirratum. *Environ. Biol. Fishes* 60:157–188. doi:10.1023/A:1007656126281.

R Core Team. 2018. R: A Language and Environment for Statistical Computing.

Ramsay JB, Wilga CD. 2007. Morphology and mechanics of the teeth and jaws of white-spotted bamboo sharks (Chiloscyllium plagiosum). *J. Morphol.* 268:664–682. doi:10.1002/jmor.

Raschi W, Musick JA, Compagno LJ. 1982. Hypoprion bigelowi, a synonym of Carcharhinus signatus (Pisces: Carcharhinidae), with a description of ontogenetic heterodonty in this species and notes on its natural history. *Copeia* 1982:102-109.

Reif WE. 1976. Morphogenesis, pattern formation and function of the dentition of Heterodontus (Selachii). *Zoomorphologie* 83:1–47. doi:10.1007/BF00995429.

Reif WE. 1982. Evolution of dermal skeleton and dentition in vertebrates. In: Evolutionary Biology. Boston, MA: Springer. p. 287–368.

Ricklefs RE, Miles DB. 1994. Ecological and evolutionary inferences from morphology: An ecological perspective. In: Ecological Morphology: Integrative Organismal Biology. Chicago: University of Chicago Press. p. 13–41.

Rohlf, F. J. (1990). An Overview of Image Processing and Analysis Techniques for

Morpho metrics. In *Proceedings of the Michigan Morphometrics Workshop, Special Publication Number 2* (pp. 47–60). University of Michigan Museum of Zoology, Ann Arbor.

Sage RD, Selander RK. 1975. Trophic radiation through polymorphism in cichlid fishes. *Proc. Natl. Acad. Sci. U. S. A.* 72:4669–4673.

Snelson F, Williams S. 1981. Notes on the occurrence, distribution, and biology of elasmobranch fishes in the Indian River lagoon system, Florida. *Estuaries* 4:110–120.

Snelson FF, Mulligan TJ, Williams SE. 1984. Food habits, occurrence, and population structure of the bull shark, Carcharhinus leucas, in Florida coastal lagoons. *Bull. Mar. Sci.* 34:71–80.

Springer S. 1961. Dynamics of the feeding mechanism of large galeoid sharks. *Am. Zool.* 1:183–185.

Summers AP, Ketcham RA, Rowe T. 2004. Structure and function of the horn shark (Heterodontus francisci) cranium through ontogeny: Development of a hard prey specialist. *J. Morphol.* 260:1–12. doi:10.1002/jmor.10141.

Tracey SR, Lyle JM, Duhamel G. 2006. Application of elliptical Fourier analysis of otolith form as a tool for stock identification. *Fish. Res.* 77:138–147. doi:10.1016/j.fishres.2005.10.013.

Tricas TC, McCosker JE. 1984. Predatory behavior of the white shark (Carcharodon carcharias), with notes on its biology. *Proc. Calif. Acad. Sci.* 43:221–238.

Tucker AS, Fraser GJ. 2014. Evolution and developmental diversity of tooth

regeneration. *Semin. Cell Dev. Biol.* 25–26:71–80. doi:10.1016/j.semcdb.2013.12.013.

Underwood CJ, Mitchell SF, Veltkamp KJ. 1999. Shark and ray teeth from the Hauterivian (Lower Cretaceous) of North-East England. *Palaeontology* 42:287–302.

Ungar PS. 2010. Mammal teeth: origin, evolution, and diversity. Johns Hopkins University Press.

Van Valkenburgh B. 1988. Trophic diversity within past and present guilds of large predatory mammals. *Paleobiology* 14:155–173.

Verwaijen D, Van Damme R, Herrel A. 2002. Relationships between head size, bite force, prey handling efficiency and diet in two sympatric lacertid lizards. *Funct. Ecol.* 16:842–850. doi:10.1046/j.1365-2435.2002.00696.x.

Wainwright PC. 1988. Morphology and ecology: functional basis of feeding constraints in Caribbean labrid fishes. *Ecology* 69:635–645.

Werner EE. 1977. Species packing and niche complementarity in three sunfishes. *Am. Nat.* 111:553–578. doi:10.1086/283184.

Werry J, Lee S, Otway N, Hu Y, Sumpton W. 2011. A multi-faceted approach for quantifying the estuarine-nearshore transition in the life cycle of the bull shark, Carcharhinus leucas. *Mar. Freshw. Res.* 62:1421–1431. doi:10.1071/MF11136.

Whitenack L, Motta P. 2010. Performance of shark teeth during puncture and draw: implications for the mechanics of cutting. *Biol. J. Linn. Soc.* 100:271–286.

Whitenack LB, Gottfried MD. 2010. A morphometric approach for addressing tooth-

based species delimitation in fossil mako sharks, Isurus (Elasmobranchii: Lamniformes). *J. Vertebr. Paleontol.* 30:17–25. doi:10.1080/02724630903409055.

Wilga C, Motta P. 2000. Durophagy in sharks: feeding mechanics of the hammerhead Sphyrna tiburo. *J. Exp. Biol.* 203:2781–2796.

Williams ME. 2001. Tooth retention in Cladodont sharks: with a comparison between primitive grasping and swallowing, and modern cutting and gouging feeding mechanisms. *J. Vertebr. Paleontol.* 21:214–226. doi:10.1671/0272-4634(2001)021.

CHAPTER IV

INTEGRATION OF MULTI-TISSUE PAH AND PCB BURDENS WITH BIOMARKER ACTIVITY IN THREE COASTAL SHARK SPECIES FROM THE NORTHWESTERN GULF OF MEXICO*

Introduction

Polycyclic aromatic hydrocarbons (PAHs) and polychlorinated biphenyls (PCBs) are among the most ubiquitous environmental contaminants in estuarine and coastal ecosystems that are commonly introduced through anthropogenic activities (Islam and Tanaka 2004; Hylland 2006). Some of these pollutants can accumulate in exposed organisms due to long half-lives and high lipophilicity (Fisk et al. 2001; Van der Oost et al. 2003; Borgå et al. 2004). Consequently, these persistent contaminants can be transferred from the base of the food web to higher trophic levels, resulting in biomagnification of potentially toxic burdens of contaminants (Fisk et al. 2001; Borgå et al. 2004). Although the production of PCBs was banned in many countries by the late 1970s, this legacy contaminant still persists in aquatic systems worldwide. In contrast, PAHs are currently continually released into coastal ecosystems from a combination of pyrogenic (combustion-derived) and petrogenic (petroleum-derived) sources (Hylland 2006).

---

* Reprinted with permission from "Integration of multi-tissue PAH and PCB burdens with biomarker activity in three coastal shark species from the northwestern Gulf of Mexico" by Cullen JA, Marshall CD, and Hala D, 2019. *Science of the Total Environment*, 650, 1158-1172.

There are marked differences in the accumulation potential of PAHs and PCBs by many marine organisms. While PCBs undergo bioaccumulation (over ontogeny) and biomagnification (across trophic levels), PAHs may exhibit trophic dilution (Wan et al. 2007; Gilbert et al. 2015; Romero-Romero et al. 2017; Sun et al. 2018). These differences are proposed to be a result of intrinsic variability in organismal metabolic capabilities (Baumard et al. 1998; Livingstone 1998). PAHs (and PCBs to a lesser extent) are metabolized by phase I cytochrome P450 enzymes (e.g. CYP1A) subsequent to activation of the aryl hydrocarbon receptor (AhR) in exposed vertebrate organisms (Meador et al. 1995; Nilsen et al. 1998; Billiard et al. 2002). Phase I metabolites can be further biotransformed by phase II conjugation reactions (with glucuronic acid, sulfate, or glutathione groups), increasing their polarity prior to final elimination in urine or feces. Both phase I and II enzymes can be induced by some of these contaminants and often show elevated activities in exposed organisms (Livingstone 1998; Van der Oost et al. 2003; Hylland 2006).

Since sharks often occupy high trophic positions, they are especially vulnerable to the bioaccumulation and biomagnification potential of PAHs and PCBs. Their large, lipid-rich livers provide a significant compartment (up to 20% of body mass) for the accumulation of these lipophilic pollutants (Hussey et al. 2010; Corsolini et al. 2014). Many large-bodied sharks are long-lived, slow to mature, and have low fecundity (Cortés 2000) and these traits contribute to increased individual- and population-level exposure risks relative to other sympatric fish species (Gelsleichter and Walker 2010). Although only a limited number of studies have evaluated the effects of PAHs and PCBs

on the health of sharks and their relatives (Gelsleichter et al. 2006; Marsili et al. 2016; Alves et al. 2016; Sawyna et al. 2017), PCB bioaccumulation in marine mammals (e.g. pinnipeds and cetaceans) is associated with poor health outcomes such as immunosuppression, endocrine disruption, and reproductive impairment (Nomiyama et al. 2014; Desforges et al. 2016; Jepson et al. 2016). Additionally, the uptake of PAHs in fishes and mammals can cause genotoxicity (and associated carcinogenesis), as well as endocrine and metabolic disruption (Hawkins et al. 2002; Lemiere et al. 2005; Schwacke et al. 2014).

While considerable attention has focused on the quantification of tissue-based PCB burdens in sharks (Serrano et al. 2000; Storelli et al. 2005; Corsolini et al. 2014; Olin et al. 2014; Beaudry et al. 2015; Gilbert et al. 2015), to our knowledge only Al-Hassan et al. (2000) and Marsili et al. (2016) have measured PAH burdens in elasmobranchs. The northern Gulf of Mexico (GoM) region is highly impacted by offshore-drilling for fossil fuels, which also includes a high-intensity shipping and transportation corridor (Steichen et al. 2012). In particular, Galveston Bay, Texas, USA is one of the most impacted bodies of water in this region due to its proximity to the numerous industrial facilities in Houston (Santschi et al. 2001; Wade et al. 2014) and whose associated waterways host the largest petrochemical complex in the country (and second largest in the world; Port of Houston Authority 2018). The frequent dredging of the Houston Ship Channel likely contributes to the resuspension and increased availability of PAHs and PCBs that have been bound to sediment particles and buried (Bocchetti et al. 2008). Additionally, there are nine US Environmental Protection

Agency (USEPA) Superfund sites that border Galveston Bay (USEPA 2017), demonstrating legacy pollution. Therefore, there is a need to assess the extent of PAH and PCB exposure in resident organisms, especially those occupying high trophic positions.

Exposure to PAHs and PCBs was evaluated in three species of sharks common in the GoM, bull (*Carcharhinus leucas*), blacktip (*Carcharhinus limbatus*), and bonnethead sharks (*Sphyrna tiburo*). These species were selected due to their differences in life history characteristics (Cortés 2000) and ecological niche (Snelson et al. 1984; Cortés 1999; Plumlee and Wells 2016), which likely influence their exposure to these pollutants. With respect to trophic ecology, bull and blacktip sharks are tertiary consumers while bonnethead sharks are secondary consumers (Cortés 1999). Additionally, these sharks are likely prone to the exposure of high levels of PAHs and PCBs since these contaminants can enter estuarine and coastal habitats from point and non-point sources (Kennish 2002; Gelsleichter et al. 2008; Gelsleichter and Walker 2010). This is of great concern since many coastal sharks use these habitats as nursery grounds (Castro 1993; Heupel et al. 2010). Furthermore, chronic exposure to these pollutants in sensitive juvenile fishes can result in sublethal effects that affect physiology, growth and development, fitness, and survival (Varanasi et al. 1987; Meador et al. 2002; Incardona et al. 2004; Meador et al. 2006). Therefore, PAH/PCB burdens, possible sources of ecological exposure, and biomarker activity were investigated over multiple size classes of sharks from Galveston Bay, TX.

The present study measures and characterizes patterns of tissue-based burdens of PAHs and PCBs in each of the three species of sharks. Biochemical responses to PAH/PCB burdens were assessed by quantifying phase I (ethoxyresorufin-*O*-deethlyase; EROD) and phase II (glutathione *S*-transferase; GST) enzyme activity assays in hepatic tissue. Last, toxic equivalents (TEQs) were used to assess the likelihood of toxicity due to both PAHs and PCBs. The direct integration of tissue-based burdens with enzymatic biomarker activities provides a comprehensive approach to evaluating pollution-induced stress.

Materials and Methods

Sample collection

Bull (N = 9), blacktip (N = 24), and bonnethead sharks (N = 21) were opportunistically sampled from fishing charters or from routine long-line surveys conducted by the Texas Parks and Wildlife Department in Galveston, Texas, USA from April to October in 2015 and 2016. Of the 54 sharks sampled, 48 were used for quantifying EROD activity (bull: n = 3; blacktip: n = 24; bonnethead: n = 21) and 41 of these for quantifying GST activity (bull: n = 3; blacktip: n = 20; bonnethead: n = 18). PAH/PCB tissue-based burdens were quantified in 29 sharks (bull: n = 9; blacktip: n = 10; bonnethead: n = 10), of which only 3 bull, 10 blacktip, and 10 bonnethead sharks also had biomarkers measured. Sample sizes for each of these measurements varied since some samples were not immediately stored at -80°C or tissue mass was limited (Table 4-1). Sex was determined for each shark and total (TL, cm), fork (FL, cm) and

Table 4-1. Sample sizes (N), sex ratios of females (F)/males (M)/not identified (NI), and mean (± SD) body length measurements (min – max) for three species of sharks

Species	N	Sex Ratio F/M/NI	TL (cm)	FL (cm)	PCL (cm)
Bull (*C. leucas*)	9	1/8/0	137.1 ± 56.4 (69.9 – 215.0)	110.8 ± 47.0 (54.9 – 174.5)	100.6 ± 42.9 (49.8 – 159.0)
Blacktip (*C. limbatus*)	24	11/13/0	130.1 ± 19.9 (72.5 – 167.9)	102.9 ± 15.9 (56.2 – 134.8)	93.2 ± 14.7 (50.8 – 122.5)
Bonnethead (*S. tiburo*)	21	14/5/2	92.5 ± 14.0 (67.7 – 124.5)	73.4 ± 12.7 (51.8 – 106)	67.5 ± 11.5 (48.2 – 93.2)

pre-caudal length (PCL) morphometrics were collected (Table 4-1). Size classes for each species were distinguished based upon previous studies from Texas or from a nearby location at a similar latitude, which has been shown to affect growth rates in bonnethead sharks (Branstetter 1987; Branstetter and Stiles 1987; Lombardi-Carlson et al. 2003). Four size classes were delineated in bull sharks, which included young-of-the-year (YoY; TL < 90.0 cm), juvenile (90.0 < TL < 160.0 cm), sub-adult (160.0 < TL < 210.0 cm), and adult (TL > 210.0 cm) groups (Branstetter and Stiles 1987); YoY individuals are sharks within the first year of life. Additionally, four size classes were delineated in blacktip sharks, which included YoY (TL < 83.0 cm), juvenile (83.0 < TL < 111.5 cm), sub-adult (111.5 < TL < 140.0 cm), and adult (TL > 140.0 cm) classes (Branstetter 1987). Only three size classes were delineated for bonnetheads (YoY, juvenile, adult) since this species reaches maturity much faster (3-4 years) than bull (14-18 years) and blacktip sharks (4-8 years) (Branstetter 1987; Branstetter and Stiles 1987; Lombardi-Carlson et al. 2003). Due to a latitudinal gradient in growth rate, age-growth curves of bonnethead sharks from northwest Florida were used to develop size classes for individuals sampled from Galveston, TX since these locations share a similar latitude

(Lombardi-Carlson et al. 2003). These size classes were delineated as YoY (TL < 70.0 cm), juvenile (70.0 < TL < 88.5 cm), and adult (TL > 88.5 cm). Liver samples (~ 5 g) were collected from the lower left lobe and muscle samples (~ 5 g) were taken from the epaxial region near the anterior dorsal fin. Samples were transported on ice for up to 30 minutes before storage at -80°C for further analysis.

Sample extraction and clean-up

A ~1 gram sub-sample was excised in duplicate from each tissue (i.e. muscle or liver). Each sub-sample was homogenized in a 7-mL polypropylene tube containing ceramic beads (Fisher Scientific) and filled with 3 mL of 1:1 (v/v) hexane:ethyl acetate. Tubes were placed in a Fisherbrand™ Bead Mill 4 Homogenizer (Fisher Scientific) and homogenized at a processing power of 150 *g* for 2 minutes. Homogenate was transferred to an acid-washed 50-mL glass tube. A 5 µL aliquot of 100 ppm benzo[a]pyrene-d_{12} (Sigma-Aldrich) and 100 ppm PCB 65-d_5 (CDN Isotopes) was spiked to each sample as internal standards (2.5 ppm at final volume). Recovery efficiency for spiked PAH/PCB analytes (as standard addition) was also assessed (Pethybridge et al. 2010a; Corsolini and Sara 2017). The mixture used for standard addition comprised two PAHs (Acenaphthene, Benzo[a]pyrene) and two PCBs (PCBs 101, 138) at a 2.5 ppm final concentration (along with internal standards benzo[a]pyrene-d_{12} and PCB 65-d_5). The standard addition samples were compared with matching 'control' samples (spiked only with internal standards). After spiking tissue homogenates, glass tubes were placed in a Branson Ultrasonics™ M2800 Ultrasonic Bath (Fisher Scientific) for 30 minutes to

further extract PAHs and PCBs into 1:1 (v/v) hexane:ethyl acetate solvent. Phase separation of the solvent from the tissue matrix was assisted by centrifugation at 2000 *g* for 10 minutes. The supernatant was pipetted into pre-weighed 20-mL glass vial and dried under N_2 gas for 30 minutes. Following extraction, lipid content of each sample was determined gravimetrically. The remaining residue was rinsed with 1 mL of acetonitrile (ACN) and pipetted into a 2-mL amber vial. All samples were then dried in a Savant™ SPD121P SpeedVac™ Concentrator (Thermo Scientific) and reconstituted into 200 µL ACN before transferring to a glass insert. Following Hong et al. (2004), sample freezing was conducted at -20°C for one hour to precipitate lipids out of solution. Afterwards, a clean 50 µL sub-aliquot was removed, dried (SpeedVac™) and reconstituted into 50 µL dichloromethane (DCM) prior to gas chromatography and mass spectrometry (GC-MS) analysis.

Sample analysis

Concentrations of the USEPA's 16 priority PAHs and 29 individual PCB congeners were quantified in shark liver and muscle tissues. All PAHs with two or three rings (naphthalene, acenaphthene, acenaphthylene, fluorene, anthracene, phenanthrene) were classified as low molecular weight (LMW) PAHs, while congeners with four to six rings (fluoranthene, chrysene, pyrene, benzo[a]anthracene, benzo[b]fluoranthene, benzo[k]fluoranthene, benzo[a]pyrene, dibenz[a,h]anthracene, benzo[g,h,i]perylene, indeno[1,2,3-cd]pyrene) were classified as high molecular weight (HMW) PAHs. Of the 29 PCB congeners, 12 were dioxin-like (DL-PCBs): PCBs 77, 81, 105, 114, 118, 123,

126, 156, 157, 167, 169, and 189. Analytical grade standards were obtained from the following sources: acenaphthene (ACE), acenaphthylene (ACY), benzo[a]pyrene (BaP), benzo[b]fluoranthene (BbF), benzo[g,h,i]perylene (BghiP), fluoranthene (FLT), pyrene (PYR), and PCBs 1, 18, 52, 101, 138, and 180 from Sigma-Aldrich; anthracene (ANT), chrysene (CHR), benzo[a]anthracene (BaA), benzo[k]fluoranthene (BkF), dibenz[a,h]anthracene (DahA), fluorene (FLU), indeno[1,2,3-cd]pyrene (IcdP), phenanthrene (PHE), and naphthalene (NAP) from Supelco; PCBs 28, 33, 77, 81, 95, 105, 114, 118, 123, 126, 128, 149, 153, 156, 157, 167, 169, 170, 171, 177, 183, 187, and 189 from Ultra Scientific. All PCBs are identified according to the IUPAC numbering system.

Samples were analyzed for the 45 individual PAH/PCB congeners by GC-MS. This analysis was conducted on a Hewlett Packard HP-6890 gas chromatograph coupled to an Agilent 5973 mass spectrometer. Samples were injected in splitless mode (2 μL) equipped with a DB-5MS (J&W Scientific) capillary column (30 m x 0.25 mm i.d.; 0.25 μm film thickness). Helium was the carrier gas at a flow rate of 1.0 mL/min. Temperatures at the front inlet and the MS interface were set at 250 and 280°C, respectively. Following injection of the sample, the GC oven was programmed at 40°C and held for 1 min, then ramped up to 180°C at 20°C/min, and finally ramped up to 300°C at 5°C/min and then held for 10 min. The MS was operated in electron impact (EI) mode at an electron energy of 70 eV while the MS source temperature was maintained at 230°C. Selected ion monitoring (SIM) mode was used for identification and quantification of all 45 analytes. Quantification of all PAH and PCB congeners were

performed against a linear 13-point calibration curve ($R^2 > 0.97$) using serially diluted standards that were prepared in DCM (2.5 to 10000 ng/mL).

Sample quality assurance and quality control measures were conducted by running a solvent blank and a mixed standard after every eight samples analyzed. The limit of detection (LOD) was quantified by the signal-to-noise ratio of 5:1 for the lowest detectable calibration point. Blanks showed no signs of external contamination above the LOD and accuracy of the mixed standards fell within ± 30% for all 45 analytes, with the exception of benzo[b]fluoranthene (67.1 ± 5.85%). Mean (± SD) intra-day variability (via coefficient of variation) of mixed standards was 7.85 ± 1.99%, while inter-day variability was 9.36 ± 5.73%. Recovery rates for the four analytes used in the standard addition spike were as follows: acenaphthene = 95.0 ± 22.6%, benzo(a)pyrene = 100 ± 2.61%, PCB 101 = 70.7 ± 11.7%, PCB 138 = 91.9 ± 22.0%. All samples were analyzed in duplicate, for which mean (± SD) variability between these samples was 4.06 ± 2.10% for all analytes. Sample concentrations were not corrected for recovery.

EROD and GST quantification

For quantification of enzyme activity, 200 mg liver samples were homogenized in a 1:5 (w/v) of 0.1 M monobasic sodium phosphate buffer (pH 7.4), containing 0.15 M potassium chloride, 1 mM ethylenediaminetetraacetic acid (EDTA), 1 mM dithiothreitol (DTT), and 10% (v/v) glycerol (Nilsen et al. 1998). Homogenates were centrifuged for 20 min at 12,000 *g* and 4°C, after which the supernatant (post-mitochondrial fraction) was obtained for subsequent enzyme assays. Protein content was quantified by Bradford

method (Bradford 1976) using bovine serum albumin (BSA) as a standard. Absorbance was measured at 595 nm on a Cytation™ 5 Multi-Mode microplate reader (BioTek Instruments).

EROD activity was quantified by a modification of the fluorimetric method conducted by Burke and Mayer (1974). Hepatic S9 fractions were incubated for 20 min at 25°C, in a 200 μL final volume containing 180 μL of S9 (1 mg/mL final concentration), 10 μL NADPH as cofactor (2 mM final concentration), and 10 μL 7-ethoxyresorufin as substrate (2 μM final concentration). Reactions were stopped by adding 200 μL of ice-cold methanol. Samples were centrifuged at 2000 *g* for 5 min and fluorescence was quantified in a 100 μL aliquot of supernatant at 535 nm/590 nm excitation/emission wavelengths. All reactions were run in duplicate and in parallel with controls, including no NADPH control (i.e. reaction mix comprising all components except NADPH) and negative control (7-ethoxyresorufin and buffer only). EROD activity was expressed as pmol/min/mg protein.

GST activity was determined by modification of the procedure described by Habig et al. (1974). Reactions took place in a 200 μL final volume containing 170 μL of S9 (1 mg/mL final concentration), 20 μL reduced glutathione as cofactor (2 mM final concentration), and 10 μL 1-chloro-2,4-dinitrobenzene as substrate (CDNB; 1 mM final concentration). Change in absorbance was quantified once per minute for 10 minutes at an absorbance of 340 nm at 25°C. All reactions were run in duplicate and in parallel with controls. GST activity was quantified using a molar extinction coefficient of 9.6 mM^{-1} cm^{-1} (Habig et al. 1974) and expressed as nmol/min/mg protein.

TEQs – potential toxicity of PAH and PCB burdens

To evaluate the potential toxicity of PAH and PCB burdens, toxic equivalents (TEQs) were calculated in both liver and muscle samples. The TEQ concept assumes a common toxic mechanism of action, in which the congeners included in the calculation activate the aryl hydrocarbon receptor (AhR) in a similar fashion to 2,3,7,8-tetrachlorodibenzo-*p*-dioxin (TCDD) (Giesy and Kannan 1998). It is also assumed that the effects among dioxin-like congeners are additive within a mixture of contaminants and are the critical effects on an organism (Giesy and Kannan 1998). TEQs were calculated for both the non-*ortho* and mono-*ortho* substituted DL-PCBs (TEQ_{PCBs}) based upon toxic equivalent factors (TEFs) for fish as proposed by Van den Berg et al. (1998). Additionally, TEQs were calculated for PAHs (TEQ_{PAHs}) using relative potency factors for fishes (fish potency factors; FPFs) based upon AhR binding and CYP1A induction relative to 2,3,7,8-TCDD (Barron et al. 2004). These FPFs were available primarily for four-, five-, and six-ring PAHs that would activate a transduction pathway similar to that of TCDD. Fish-specific TEFs and relative potencies are used due to the toxicokinetic differences in these congeners among taxonomic groups (Hahn and Stegeman 1992; Van den Berg et al. 1998; Zhou et al. 2010). Since six of the ten PAHs with FPFs are considered to be probable human carcinogens (benzo[a]anthracene, benzo[b]fluoranthene, benzo[k]fluoranthene, benzo[a]pyrene, dibenz[a,h]anthracene, and indeno[1,2,3-cd]pyrene), negative health outcomes to the local population may result if these compounds are found in high concentrations (NTP, 2016).

Statistical analyses

Sex, size, and species comparisons were conducted for variables such as lipid content, concentrations of ∑PAHs and ∑PCBs, biomarker activity, and TEQ values in liver and muscle tissues. Since lipid content has previously been reported to differ between sexes, by reproductive status, and among species, it was necessary to determine whether this variable could confound comparisons of tissue-based burdens (Rossouw 1987; Lucifora et al. 2002; Pethybridge et al. 2010b, 2011; Lyons and Lowe 2013). Within the subset of individuals analyzed for tissue-based burdens, only two bull sharks were mature, while one blacktip and five bonnethead sharks were mature. Of these adults, one individual of each species was captured during its mating season. Intraspecific analyses were conducted to evaluate sex differences and bioaccumulation of PAH/PCB burdens over ontogeny, in addition to interspecific comparisons of burdens among species; comparisons by sex were not conducted on bull sharks due to the presence of only a single female. All PAHs and PCBs were analyzed on a ng/g wet weight (ww) basis unless otherwise noted. If data exhibited normality and homoscedasticity, Welch's *t*-test was conducted for pairwise comparisons and an ANOVA on a weighted generalized least squares (GLS) model was performed for more than two groups to explicitly account for unequal sample sizes. Non-parametric data were analyzed using Mann-Whitney *U* for pairwise comparisons or were $\log_{10}$-transformed to meet parametric assumptions before conducting an ANOVA on a weighted GLS for more than two groups. Significant results for ANOVAs were followed by post-hoc general linear hypothesis tests using Tukey contrasts and Westfall-adjusted

p-values. Bioaccumulation of PAHs and PCBs over ontogeny were analyzed by linear or quadratic regression depending on the fit with the data. Since these contaminants are expected to accumulate with increasing body size, ANCOVAs were conducted to account for size (FL) when testing for differences in tissue-based burdens between sexes of each species. Data that did not meet assumptions of normality and homoscedasticity were $\log_{10}$-transformed and analyzed via a weighted GLS model for the ANCOVA. If the interaction of FL and sex was not significant in the ANCOVA, the model was reduced to only the main effects. This approach was also applied to interspecific comparisons of tissue-based burdens and biomarker activity, where FL was also treated as the covariate. Pearson correlations were implemented for parametric data while Spearman correlations were conducted for non-parametric data when assessing the relationship between contaminant classes and biomarker activity, as well as burdens between tissues. Sex and FL were accounted for in species comparisons of TEQ_{PCBs} and TEQ_{PAHs} by conducting ANCOVAs following $\log_{10}$-transformation of the response variable. If interaction terms were significant, no post-hoc testing was conducted. All statistical analyses were conducted within the R statistical program (ver. 3.3.3; R Core Team 2017) and significance was set at $\alpha = 0.05$ for all tests.

Comparisons of liver and muscle congener profiles among the three species were conducted using one-way PERMANOVAs on Bray-Curtis dissimilarity matrices with the vegan package (ver. 2.4-4; Oksanen et al. 2017) in R. If significant differences were detected, pairwise comparisons with Bonferroni-adjusted p-values were calculated. Additionally, a SIMPER analysis was conducted using a Bray-Curtis dissimilarity matrix

to determine the congeners contributing to the greatest differences between species. All concentrations that were below the LOD (< LOD) were treated as zero and included in subsequent multivariate analyses. If concentrations of a particular congener were zero in all samples of a given tissue (liver or muscle), these congeners were removed from all further multivariate analyses in that tissue. This included the removal of BbF from the analysis of individual congeners in liver tissue, in addition to the removal of BaA, BbF, BghiP, PCB 28, PCB 33, PCB 53, PCB 77, PCB 81, PCB 95, PCB 101, PCB 114, PCB 171, PCB 177, and PCB 189 from analysis of muscle tissue.

Multivariate ordination methods were performed to explore relationships among species via congener profiles, and to explicitly test for correlations with biomarker activity using the vegan package in R. Principal component analysis (PCA) was conducted to visually evaluate relationships of individual sharks using congener profiles, which helped to reduce the effect of contaminants with disproportionately high concentrations. This was followed by a partial redundancy analysis (pRDA) to determine which congeners were correlated with EROD and GST activity while the effect of species differences was held constant. An adjusted R^2 (bimultivariate redundancy statistic; R^2_{adj}) and a permutation test (using 999 permutations) of marginal effects (Type III sum of squares) were calculated for the pRDAs to determine if there were significant relationships of congener profiles with biomarker activity. Angles between the positions of individual congeners and enzymatic biomarkers (with respect to the origin) were reflective of correlations between these variables.

Results

Comparisons of lipid content and PAH/PCB burdens

Lipid content did not exhibit a significant relationship with body size (FL) in liver or muscle tissue for any species ($p > 0.05$). Of the two species that could be evaluated for sex differences (blacktips and bonnetheads), only the lipid content of the liver in bonnethead sharks exhibited a significant difference in which males were greater than females ($df = 6.809$, $t = 2.855$, $p = 0.025$). No significant interspecific differences were found for lipid content in the liver ($F_{2,26} = 1.309$, $p = 0.287$) or muscle ($F_{2,26} = 1.217$, $p = 0.312$; Table 4-2). Since lipid content was essentially equivalent within and among species for each tissue, all tissue concentrations were reported and analyzed on a ng/g ww basis.

PAH burdens did not significantly differ by sex in blacktip liver ($F_{1,7} = 0.211$, $p = 0.660$) or muscle tissue ($F_{1,7} = 5.486$, $p = 0.052$). Additionally, no sex differences were found for PCB burdens in either liver ($F_{1,7} = 0.417$, $p = 0.539$) or muscle ($F_{1,7} = 0.494$, $p = 0.505$) in blacktips. Likewise, no significant differences between sexes were detected for ∑PAHs in the liver ($F_{1,6} = 0.001$, $p = 0.975$) and muscle ($F_{1,6} = 0.087$, $p = 0.778$) of bonnetheads, as well as ∑PCBs in the muscle ($F_{1,6} = 0.146$, $p = 0.716$). Although ∑PCBs did significantly differ between sexes in the liver of bonnetheads ($F_{1,6} = 13.372$, $p = 0.011$), only two males were evaluated. Therefore, both sexes were treated equivalently since PCB burdens in the males (273 and 347 ng/g ww) were close to that of a female at a similar size (385 ng/g ww). The interaction term was not significant in any of the ANCOVAs ($p > 0.05$) and was removed prior to final analysis of the results.

Table 4-2. Percent lipid content and individual congener concentrations of PAHs and PCBs (mean ± SE; ng/g ww)

	Bull (*C. leucas*)		Blacktip (*C. limbatus*)		Bonnethead (*S. tiburo*)	
	Liver	Muscle	Liver	Muscle	Liver	Muscle
% Lipid	63.0 ± 8.16	0.911 ± 0.178	62.8 ± 3.21	1.02 ± 0.227	50.6 ± 6.95	1.11 ± 0.0924
PAHs						
NAP	61.8 ± 5.90	38.3 ± 0.765	73.9 ± 5.70	37.4 ± 0.176	77.0 ± 7.87	37.7 ± 0.153
ACY	52.4 ± 2.78	8.36 ± 5.53	47.8 ± 1.97	38.9 ± 0.398	85.0 ± 25.0	36.6 ± 4.35
ACE	85.6 ± 11.2	61.6 ± 3.79	83.0 ± 4.17	58.8 ± 0.413	82.8 ± 3.21	59.2 ± 0.364
FLU	57.4 ± 4.62	40.3 ± 0.950	44.7 ± 1.50	38.8 ± 0.149	39.5 ± 4.54	39.1 ± 0.119
PHE	83.5 ± 7.22	41.6 ± 1.02	68.3 ± 9.99	39.9 ± 0.151	58.9 ± 3.59	40.2 ± 0.168
ANT	48.9 ± 2.81	23.5 ± 5.93	47.0 ± 1.80	10.3 ± 5.23	42.9 ± 1.35	10.3 ± 5.23
FLT	60.7 ± 3.89	43.4 ± 1.44	46.6 ± 1.04	41.2 ± 0.151	46.8 ± 1.46	41.6 ± 0.139
PYR	48.9 ± 10.4	38.1 ± 1.11	7.80 ± 5.20	36.4 ± 0.131	30.7 ± 5.13	36.7 ± 0.120
BaA	23.6 ± 9.31	< LOD	5.73 ± 5.73	< LOD	< LOD	< LOD
CHR	8.65 ± 5.73	4.42 ± 4.42	< LOD	< LOD	< LOD	< LOD
BbF	< LOD	< LOD	< LOD	< LOD	< LOD	< LOD
BkF	39.7 ± 7.74	41.3 ± 1.66	46.1 ± 1.96	38.5 ± 0.164	41.8 ± 5.13	39.0 ± 0.217
BaP	5.16 ± 5.16	45.6 ± 1.63	< LOD	43.1 ± 0.151	< LOD	43.3 ± 0.134
DahA	361 ± 81.4	548 ± 99.5	514 ± 84.5	393 ± 53.6	488 ± 80.0	357 ± 40.7
BghiP	5.06 ± 5.06	< LOD	< LOD	< LOD	< LOD	< LOD
IcdP	618 ± 181	392 ± 57.8	1140 ± 104	370 ± 23.1	1210 ± 181	343 ± 29.3
PCBs						
non-*ortho*						
77	37.4 ± 7.76	< LOD	3.71 ± 3.71	< LOD	3.71 ± 3.71	< LOD
81	8.06 ± 5.33	< LOD	< LOD	< LOD	< LOD	< LOD
126	80.2 ± 13.3	4.77 ± 4.77	48.5 ± 6.31	< LOD	27.7 ± 7.59	< LOD
169	38.1 ± 7.87	29.6 ± 5.64	< LOD	11.1 ± 5.65	< LOD	7.19 ± 4.80

Table 4-2. Continued

	Bull (*C. leucas*)		Blacktip (*C. limbatus*)		Bonnethead (*S. tiburo*)	
	Liver	Muscle	Liver	Muscle	Liver	Muscle
mono-*ortho*						
105	78.5 ± 7.59	4.41 ± 4.41	51.5 ± 1.94	< LOD	30.0 ± 6.60	< LOD
114	36.2 ± 4.64	< LOD	< LOD	< LOD	< LOD	< LOD
118	205 ± 31.1	36.7 ± 0.777	82.4 ± 8.75	36.1 ± 0.375	46.1 ± 3.01	33.5 ± 3.73
123	52.2 ± 2.32	17.1 ± 6.80	8.31 ± 5.54	25.9 ± 5.66	3.85 ± 3.85	26.3 ± 5.75
156	59.6 ± 4.31	4.20 ± 4.20	31.4 ± 6.95	< LOD	8.42 ± 5.67	< LOD
157	40.6 ± 1.37	32.2 ± 4.12	7.50 ± 5.00	35.1 ± 0.175	3.80 ± 3.80	35.3 ± 0.169
167	55.5 ± 5.00	13.6 ± 6.88	31.5 ± 9.66	3.59 ± 3.59	12.9 ± 6.65	< LOD
189	22.2 ± 7.06	< LOD	< LOD	< LOD	3.41 ± 3.41	< LOD
NDL						
1	18.5 ± 5.86	3.58 ± 3.58	3.04 ± 3.04	< LOD	2.89 ± 2.89	2.88 ± 2.88
18	12.4 ± 6.23	< LOD	< LOD	3.65 ± 3.65	< LOD	< LOD
28	45.5 ± 2.22	< LOD	34.7 ± 3.90	< LOD	22.6 ± 6.17	< LOD
33	20.4 ± 6.48	< LOD	< LOD	< LOD	3.22 ± 3.22	< LOD
52	56.1 ± 9.11	< LOD	< LOD	< LOD	< LOD	< LOD
95	52.2 ± 9.81	< LOD	< LOD	< LOD	< LOD	< LOD
101	81.7 ± 10.9	< LOD	< LOD	< LOD	< LOD	< LOD
128	102 ± 23.8	21.7 ± 8.72	73.2 ± 22.4	3.96 ± 3.96	31.0 ± 6.84	3.95 ± 3.95
138	471 ± 104	25.8 ± 6.50	136 ± 26.3	24.8 ± 5.42	55.5 ± 5.08	3.49 ± 3.49
149	92.5 ± 18.2	< LOD	< LOD	6.95 ± 4.64	11.6 ± 5.89	< LOD
153	950 ± 226	38.0 ± 5.09	268 ± 65.6	35.3 ± 3.95	93.2 ± 15.8	7.66 ± 5.11
170	161 ± 31.6	12.7 ± 6.34	64.8 ± 12.3	7.07 ± 4.71	17.3 ± 7.25	< LOD
171	55.4 ± 8.37	< LOD	9.40 ± 6.31	< LOD	3.63 ± 3.63	< LOD
177	82.3 ± 11.2	< LOD	13.3 ± 6.81	< LOD	7.64 ± 5.09	< LOD
180	282 ± 63.0	17.8 ± 5.66	103 ± 25.4	17.7 ± 4.83	45.2 ± 6.87	< LOD
183	119 ± 22.0	4.14 ± 4.14	44.6 ± 5.74	< LOD	11.7 ± 5.96	< LOD
187	286 ± 61.0	17.5 ± 6.93	92.0 ± 15.4	7.40 ± 4.94	52.8 ± 4.17	< LOD
∑PAHs	1560 ± 197	1330 ±164	2120 ± 106	1150 ± 75.7	2200 ± 219	1080 ± 44.2
∑PCBs	3600 ± 594	284 ± 52.7	1110 ± 203	219 ± 24.1	498 ± 80.1	120 ± 11.6

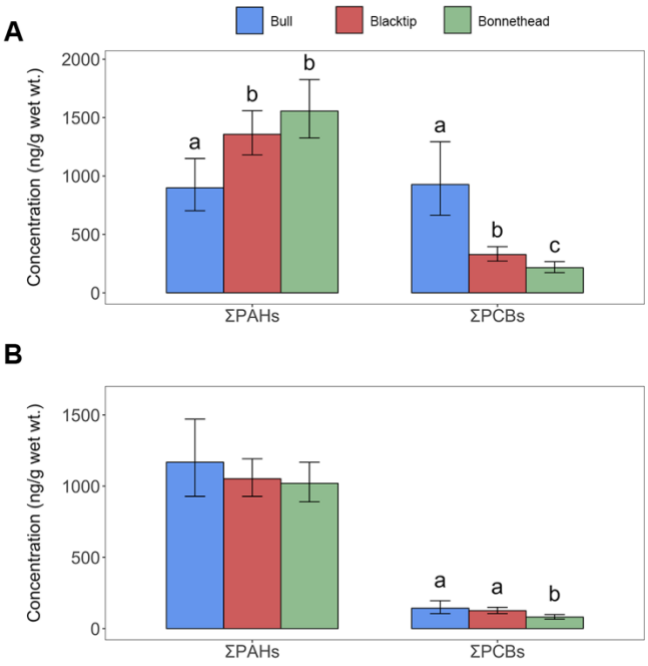

Figure 4-1. Log_{10}-transformed PAH/PCB burdens were compared among species for each tissue within an ANCOVA framework that included FL as a covariate. Back-transformed adjusted means (± SE) from the ANCOVA are presented for both liver (**A**) and muscle (**B**). Significant differences in PAH and PCB burdens were found in the liver (**A**), but only for PCBs in the muscle (**B**). Lowercase letters denote significant differences ($p < 0.05$).

Comparisons between sex were not analyzed for bull sharks since only a single female had PAH/PCB burdens quantified.

Interspecific comparisons of PAH and PCB burdens found that relationships among species differed by tissue. Significant differences in hepatic ∑PAHs ($F_{2,24} = 6.793$, $p = 0.005$) were detected among species, for which bull sharks had significantly lower concentrations of ∑PAHs relative to blacktips ($p = 0.007$) and bonnetheads ($p = 0.006$; Figure 4-1A). Significant differences in hepatic ∑PCBs ($F_{2,24} = 25.423$, $p <$

0.0001) were also detected among species, but all species significantly differed in concentrations of ∑PCBs from each other ($p < 0.05$). PCB burdens were greatest in bull sharks, followed by blacktip and bonnethead sharks (Figure 4-1A). While no interspecific differences were found for ∑PAHs in the muscle ($F_{2,24} = 0.508$, $p = 0.608$), significant differences were detected for ∑PCBs ($F_{2,24} = 4.432$, $p = 0.023$; Figure 4-1B). A post-hoc test determined that bonnetheads had significantly lower burdens of PCBs than bull ($p = 0.023$) or blacktip sharks ($p = 0.025$) in muscle tissue. The interaction of FL and species was not significant in any of the ANCOVAs ($p > 0.05$). Correlations conducted separately on PAH and PCB burdens between liver and muscle tissues were only found to be significant in the case of ∑PCBs for bull ($r = 0.721$, $p = 0.028$) and blacktip sharks ($r = 0.770$, $p = 0.014$). Only weak and non-significant correlations were found for all other relationships (ranges: $r = -0.115 – 0.343$, $p = 0.332 – 0.810$).

Bioaccumulation of PAHs and PCBs

The linear regressions of PAH and PCB burdens with FL showed significant bioaccumulation of PCBs in the liver of bull sharks ($F_{1,7} = 6.205$, $p = 0.042$), but no significant relationship in muscle nor for either PAH regression ($p > 0.05$; Figure 4-2A,B). Unlike bull sharks, blacktips accumulated PCBs in both liver ($F_{2,7} = 30.840$, $p = 0.0003$) and muscle ($F_{1,8} = 9.333$, $p = 0.016$), but similarly did not accumulate PAHs ($p > 0.05$) with increasing length (Figure 4-2C,D**)**. However, the regression of hepatic PCB burdens over increasing FL in blacktip sharks was best explained by a second-order polynomial that increased the R^2 from 0.49 to 0.87 compared to a simple linear

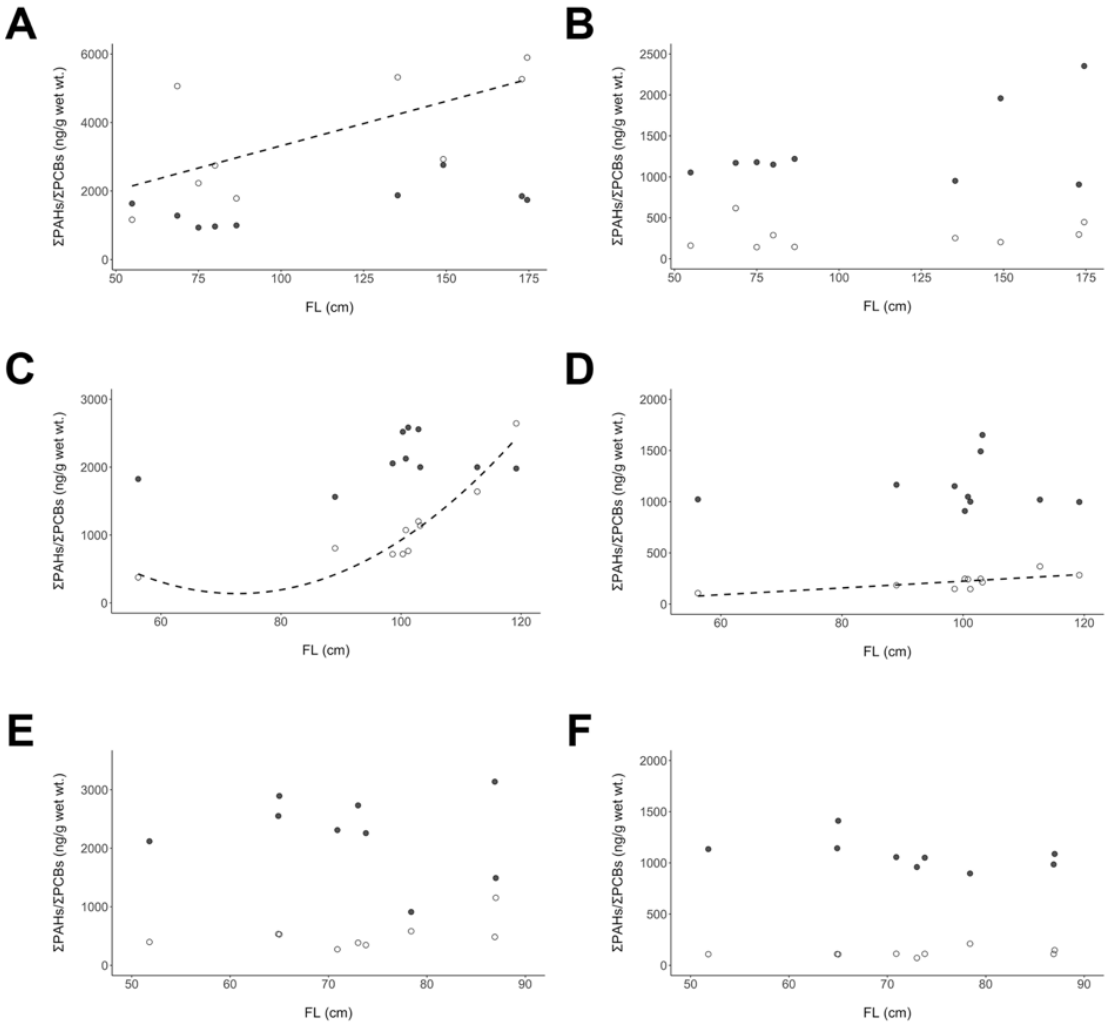

Figure 4-2. Relationships were discerned between burdens of ΣPAHs(●)/PCBs(○) and FL for liver (**A,C,E**) and muscle (**B,D,F**) tissues for bull (**A,B**), blacktip (**C,D**), and bonnethead sharks (**E,F**). Although none of the PAH regressions were significant, significant relationships of PCB burdens over FL are shown as dashed regression lines.

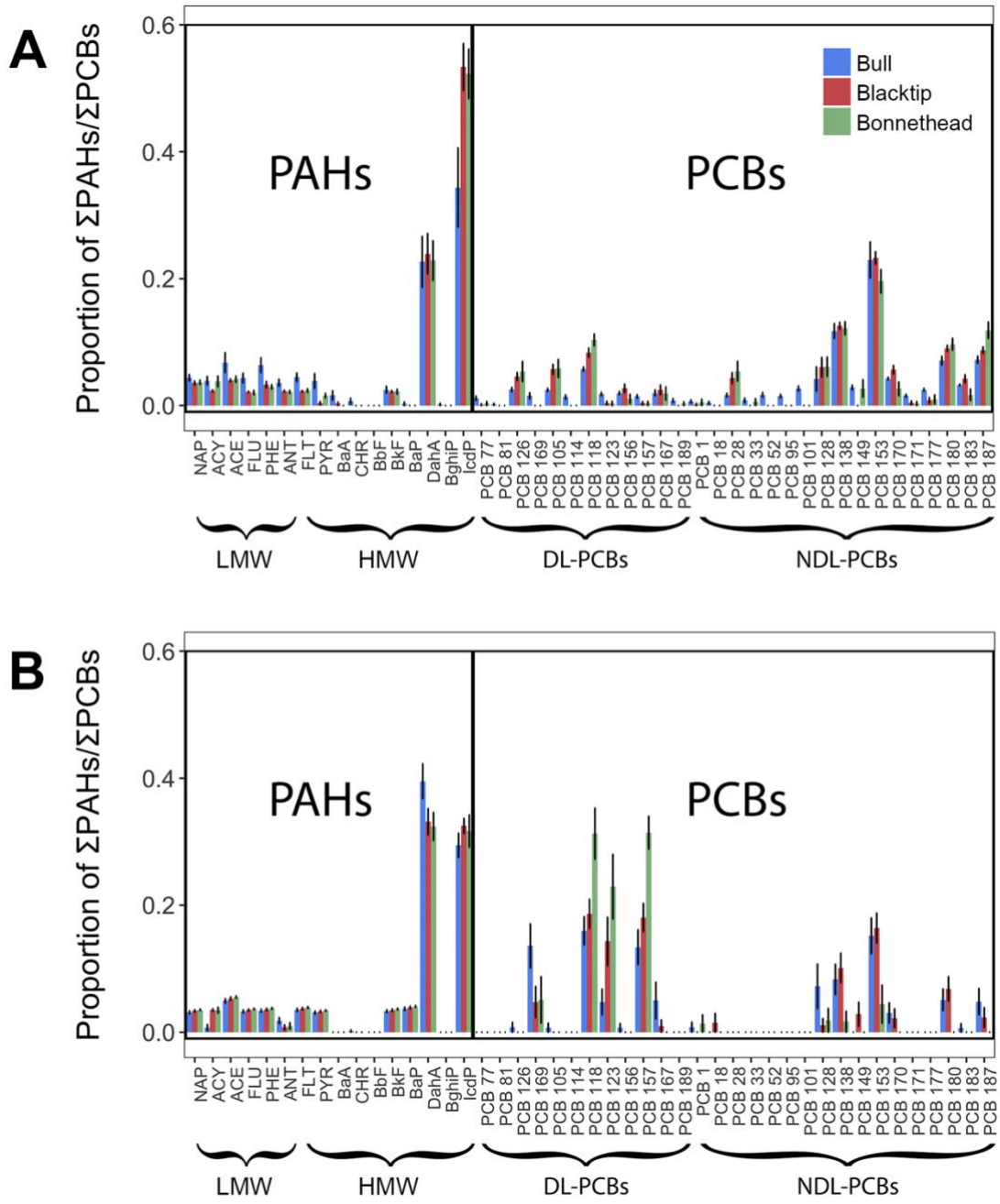

Figure 4-3. Individual congener profiles were compared among species in liver (**A**) and muscle (**B**), normalized to ΣPAHs and ΣPCBs (mean ± SE). PAHs are denoted as either low (LMW) and high molecular weight (HMW) congeners while PCBs are grouped as either dioxin-like (DL-PCBs) or non-dioxin-like PCBs (NDL-PCBs).

regression. No significant bioaccumulation of PAHs or PCBs was found in the liver or muscle for bonnethead sharks ($p > 0.05$; Figure 4-2E,F).

Of the PAHs quantified, species means of indeno[1,2,3-cd]pyrene and dibenz[a,h]anthracene accounted for 57 to 77% of ∑PAHs in liver tissue (Figure 4-3A), which was similar to proportions of these congeners in muscle (64 – 69% of ∑PAHs; Figure 4-3B). Furthermore, species means of PCB 153 and PCB 138 comprised 32 to 36% of ∑PCBs in liver (Figure 4-3A), whereas PCB 118 and PCB 157 were in greatest proportions (29 – 63% of ∑PCBs) in muscle (Figure 4-3B). Overall congener profiles significantly differed among species in both liver (pseudo-$F_{2,26} = 5.532$, $p = 0.001$) and muscle (pseudo-$F_{2,26} = 4.277$, $p = 0.001$) samples. In the liver, the congener profile of bull sharks differed from both blacktips ($p = 0.003$) and bonnetheads ($p = 0.003$) following a Bonferroni-adjusted pairwise test. In muscle, however, only bull and bonnethead sharks had significantly different congener profiles ($p = 0.009$). Indeno[1,2,3-cd]pyrene, dibenz[a,h]anthracene, PCB 153, and PCB 128 were consistently responsible for the greatest separation among species (mean ± SE: 37.4 ± 1.43%) in the liver of the total 45 PAH and PCB congeners. The SIMPER analysis of hepatic congener profiles determined that blacktip and bonnethead sharks exhibited the least dissimilarity (~23%) on an individual congener basis, while the pairwise comparisons of bull – blacktip (~31%) and bull – bonnethead (~36%) displayed greater differences in their congener profiles. PCB 123 was responsible for the greatest separation among all comparisons in the muscle (mean ± SE: 12.8 ± 1.18%), but

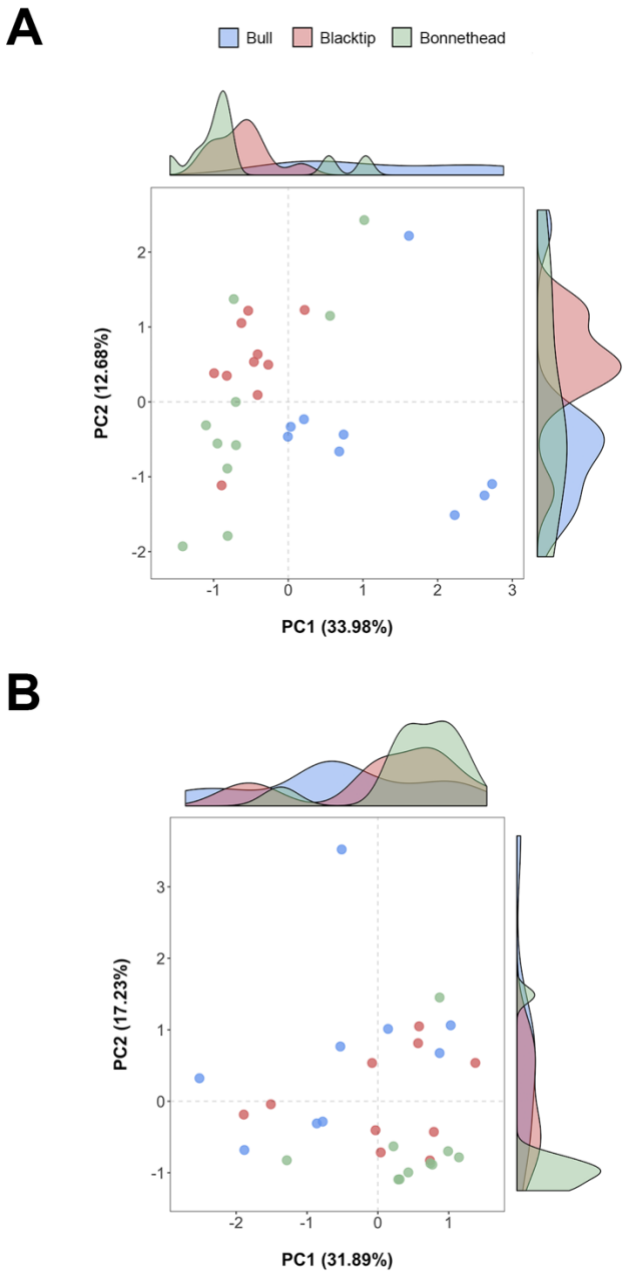

Figure 4-4. Congener profiles were used to determine relationships among species by PCA in liver (**A**) and muscle (**B**). Marginal density plots are included on the PC1 and PC2 axes to visualize the distribution of individuals within each species.

subsequent influential congeners varied with each pairwise comparison; many were DL-PCBs, however. Comparisons of overall dissimilarity in the muscle were lower for bull – blacktip and blacktip – bonnethead (~30%) than the comparison of bull – bonnethead (~38%). These relationships among species appear consistent with those established using ∑PAHs/∑PCBs in associated tissues.

To visualize species relationships in multivariate space, PCA ordinations were plotted for each species using congener profiles that were also scaled to unit variance. Ordinations of the liver congener profiles displayed a separation among species along the PC1 axis, where bull sharks occupied space along the positive PC1 axis and the other two species were found on the negative side of this axis (Figure 4-4A). Blacktip and bonnethead sharks were primarily separated along the PC2 axis. While no size patterns were apparent in bonnetheads, relationships were present for the other species. The single YoY blacktip shark was on the opposite side of the PC2 axis from the larger conspecifics. In bull sharks, the largest conspecifics and a single YoY individual were found near the origin, another YoY individual was found on the opposite side of the PC2 axis, and the remaining three juveniles were clustered to the far side of the positive PC1 axis. Clustering of bull sharks was primarily driven by greater proportions of LMW PAHs compared to the other species, while most blacktips were influenced by HMW PAHs and bonnetheads were associated with greater proportions of recalcitrant PCB congeners. Although the sample size of bull sharks (n = 3) precluded the analysis of a relationship between biomarker activity and LMW/HMW PAHs, relationships were examined in bonnetheads. Proportions of LMW and HMW PAHs did not exhibit a

significant relationship with $\log_{10}$-transformed EROD activity ($F_{1,8} = 4.853$, $p = 0.059$). High overlap was found within the multivariate ordination of muscle congener profiles, where blacktip sharks were located between bull and bonnethead sharks (Figure 4-4B). Despite the level of overlap, conspecifics were relatively dispersed compared to interspecific overlap. However, bonnetheads were primarily concentrated on the positive side of the PC1 axis and negative side of the PC2 axis. Clustering of bonnethead sharks in the muscle PCA was primarily affected by greater proportions of a few mono-*ortho* DL-PCBs and indeno[1,2,3-cd]pyrene. While there was no clear pattern for the congeners driving the distribution of bull and blacktip sharks, these species were broadly impacted by HMW PAHs and the remaining PCB congeners. Additionally, there did not appear to be any patterns due to size within or among species.

Biomarker activity

EROD and GST activities did not significantly differ by sex or with FL in blacktip or bonnethead sharks (ANCOVA: $p > 0.05$) and could not be evaluated in bull sharks. Differences in $\log_{10}$-transformed EROD activity were found among species ($F_{2,45} = 5.027$, $p = 0.011$); mean activity was greater in bonnethead sharks (4.11 pmol/min/mg protein) than blacktip (2.19 pmol/min/mg protein; $p = 0.005$) and bull sharks (2.02 pmol/min/mg protein; $p = 0.034$) (Figure 4-5A). Significant differences in $\log_{10}$-transformed GST activity were also detected among species ($F_{2,38} = 14.394$, $p < 0.0001$); mean activity in bull sharks (121 nmol/min/mg protein) was significantly lower than blacktip (200 nmol/min/mg protein; $p < 0.0001$) and bonnethead sharks (197

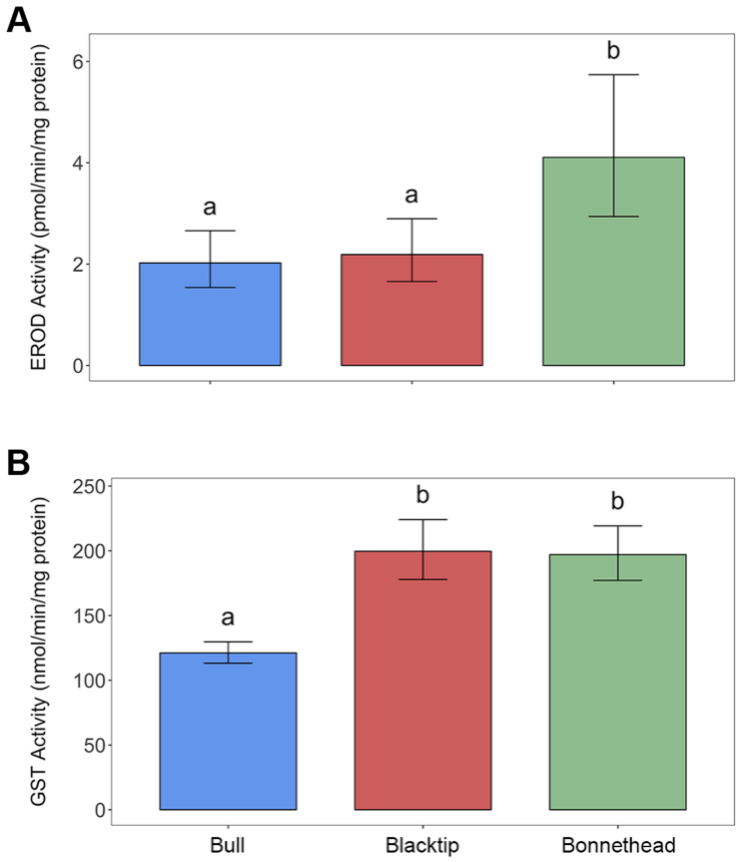

Figure 4-5. Log_{10}-transformed EROD (**A**) and GST (**B**) data were analyzed by a weighted GLS ANOVA to determine relationships among species with unequal sample sizes. Although transformed data were analyzed for omnibus and pairwise comparisons, back-transformed mean ± SE are displayed for interpretability. Lowercase letters denote significant differences ($p < 0.05$).

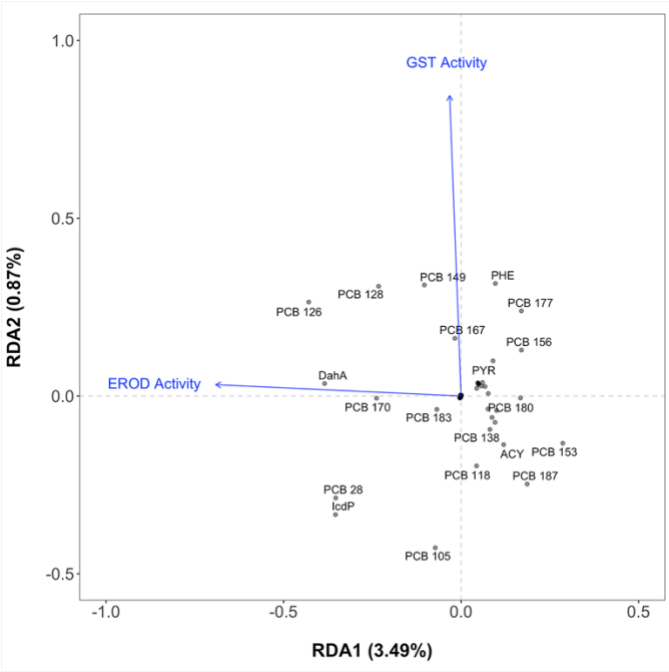

Figure 4-6. The pRDA did not appear to be strongly informed by biomarker activity in the liver, but some correlations with individual congeners were present. Congeners that were tightly clustered, particularly around the origin, were not labeled to improve interpretation of the ordination. Additionally, these unlabeled congeners are not well-explained by either biomarker due to their presence close to the origin.

nmol/min/mg protein; $p < 0.0001$) (Figure 4-5B). No significant correlations of EROD or GST activity with hepatic burdens of ∑PAHs, ∑PCBs, DL-PCBs, or non-dioxin-like PCBs (NDL-PCBs) were found for bull or bonnethead sharks ($p > 0.05$). Significant correlations were detected in the liver of blacktips for concentrations of ∑PCBs ($\rho = 0.69$, $p = 0.035$) and DL-PCBs ($\rho = 0.79$, $p = 0.0098$) with GST activity. However, correlations between GST activity and other classes of contaminants (∑PAHs and NDL-PCBs) were not significant ($p > 0.05$). No significant correlations were measured with respect to EROD in blacktip sharks ($p > 0.05$).

Integration of tissue burdens and biomarker activity

The pRDA explained little variance (R^2_{adj} = - 0.064) of the congener profiles with EROD (p = 0.551) and GST (p = 0.983) following permutation tests, but tentatively displayed some relationships of individual congeners with specific biomarkers (Figure 4-6). An assessment of the angles between explanatory and response variables of the pRDA ordination in the liver showed a positive correlation between EROD activity and proportions of congeners dibenz[a,h]anthracene and PCB 170, as well as between GST activity and PCB 167. Additionally, PCBs 126, 128, and 149 were found between the two constraints (EROD and GST activity), which suggests positive correlations with both biomarkers. Alternatively, PCB 105 was found to be strongly opposite of the GST activity vector and therefore displayed a negative correlation with this biomarker. A similar relationship was observed between PCB 153 and EROD activity, which suggests a negative relationship as well.

Potential toxicity of tissue burdens (TEQs)

Comparisons of TEQ_{PCBs} in the liver among species was confounded by interactions of species with sex (p = 0.0003) as well as FL (p = 0.0037), which prevented direct comparisons. Liver TEQ_{PCBs} in bull sharks appeared greater than in the other species with no discernible differences over FL, while the two male bonnetheads had lower TEQ_{PCBs} than most females. Although there did not appear to be any sex differences in blacktip sharks, liver TEQ_{PCBs} appeared to increase with increasing FL.

Similarly, interspecific comparisons of TEQ_{PCBs} in muscle tissue were confounded by an interaction between species and sex ($p < 0.0001$). The only apparent sex difference occurred within blacktip sharks, for which most males had greater muscle TEQ_{PCBs} than females. When comparing between tissues, the range of mean TEQ_{PCBs} by species in the liver (140 – 414 pg/g ww) was much higher than in the muscle (0.840 – 25.9 pg/g ww) across all species (Table 4-3). Of all the DL-PCBs, PCB 126 represented the greatest contributor to TEQ_{PCBs} calculations (median 98.6%) across all species in the liver. In the muscle, more mono-*ortho* and other non-*ortho* DL-PCBs contributed to the TEQ_{PCBs} calculation besides PCB 126. For comparison with established threshold levels of physiological effects from the literature, hepatic TEQ_{PCBs} were also calculated on a pg/g lipid weight (lw) basis. Although these interspecific comparisons were also confounded by interactions with sex ($p = 0.0005$) and FL ($p = 0.0066$), the mean for each species (range: 445 – 1550 pg/g lw TEQ_{PCBs}) was well above the lower threshold for physiological effects in multiple taxonomic groups. Kannan et al. (2000) suggested that the lower threshold for physiological effects induced by PCB burdens in pinnipeds (*Phoca vitulina*), cetaceans (*Tursiops truncatus*, *Delphinapterus leucas*), and mustelids (*Lutra lutra*, *Mustela vison*) is 160 pg/g lw TEQ_{PCBs}. Furthermore, the 99% tissue-residue benchmark (TRB) for early life stage fish is suggested to be 57 pg/g lw TEQ_{PCBs} (Steevens et al. 2005) (Figure 4-7). Outliers from individual bull (3810 pg/g lw) and bonnethead sharks (1760 pg/g lw) were much higher than the upper limits set by both Kannan et al. (2000) and Steevens et al. (2005).

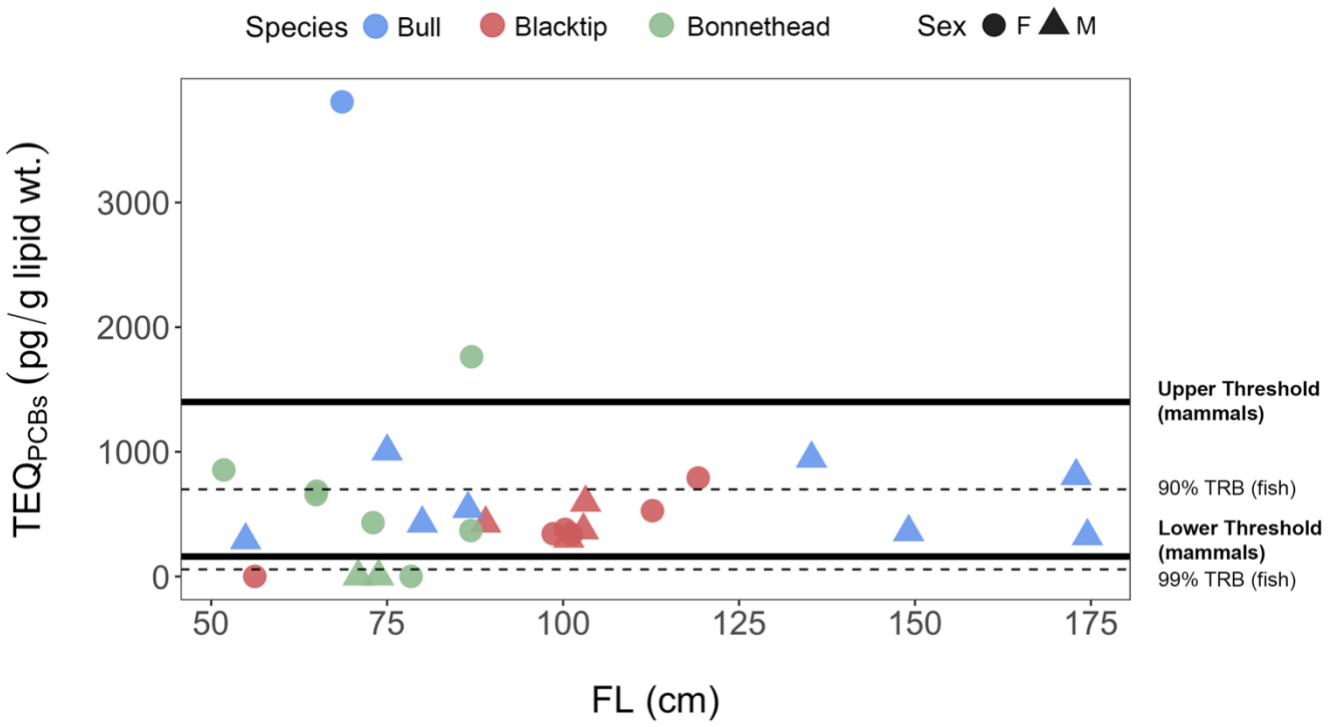

Figure 4-7. A comparison with established thresholds in aquatic mammals (pinnipeds, cetaceans, mustelids; Kannan et al. 2000) and tissue residue-based toxicity benchmarks (TRBs) for early life stage fishes (Steevens et al. 2005) shows that the TEQ_{PCBs} in the liver of these sharks may result in possible physiological impacts. Since significant interactions of species with sex and body size (FL) were detected, direct species comparisons could not be made. Two high outliers (bull: 3807.24 pg/g lw; bonnethead 1762.80 pg/g lw) had measurements above the upper threshold established for aquatic mammals.

Table 4-3. Mean concentrations of DL-PCBs (non-*ortho* and mono-*ortho*) and PAHs (ng/g ww) and associated TEQs (pg/g ww) in the liver and muscle based on fish TEFs and FPFs

		Bull (*C. leucas*)				Blacktip (*C. limbatus*)				Bonnethead (*S. tiburo*)			
		Liver		Muscle		Liver		Muscle		Liver		Muscle	
Non-ortho	TEF[a]	Conc.	TEQ	Conc.	TEQ	Conc.	TEQ	Conc.	TEQ	Conc.	TEQ	Conc.	TEQ
77	0.0001	37.4	3.74	<LOD	0.00	3.71	0.370	<LOD	0.00	3.71	0.370	<LOD	0.00
81	0.0005	8.06	4.03	<LOD	0.00	<LOD	0.00	<LOD	0.00	<LOD	0.00	<LOD	0.00
126	0.005	80.2	401	4.77	23.9	48.6	243	<LOD	0.00	27.7	139	<LOD	0.00
169	0.00005	38.1	1.91	29.6	1.48	<LOD	0.00	11.1	0.555	<LOD	0.00	7.19	0.360
Total		**164**	**411**	**34.4**	**25.4**	**52.3**	**243**	**11.1**	**0.555**	**31.4**	**139**	**7.19**	**0.360**
Mono-ortho													
105	0.000005	78.5	0.393	4.41	0.0221	51.5	0.258	<LOD	0.00	30.0	0.150	<LOD	0.00
114	0.000005	36.2	0.181	<LOD	0.00	<LOD	0.00	<LOD	0.00	<LOD	0.00	<LOD	0.00
118	0.000005	205	1.03	36.7	0.184	82.4	0.412	36.1	0.181	46.1	0.231	33.5	0.168
123	0.000005	52.2	0.261	17.2	0.0860	8.31	0.0416	25.9	0.130	3.85	0.0193	26.3	0.132
156	0.000005	60.0	0.300	4.20	0.0210	31.4	0.157	<LOD	0.00	8.42	0.0421	<LOD	0.00
157	0.000005	40.6	0.203	32.2	0.161	7.50	0.0375	35.1	0.176	3.80	0.0190	35.3	0.177
167	0.000005	55.5	0.278	13.6	0.0680	31.5	0.158	3.59	0.0180	12.9	0.0645	<LOD	0.00
189	0.000005	22.2	0.111	<LOD	0.00	<LOD	0.00	<LOD	0.00	3.41	0.0171	<LOD	0.00
Total		**550**	**2.76**	**108**	**0.542**	**213**	**1.06**	**101**	**0.505**	**108**	**0.543**	**95.1**	**0.477**
Total PCBs		**714**	**414**	**142**	**25.9**	**265**	**244**	**112**	**1.06**	**139**	**140**	**102**	**0.837**
PAHs	FPF[b]												
FLT	0.000000002	60.7	1.21×10^{-4}	43.4	8.68×10^{-5}	46.6	9.32×10^{-5}	41.2	8.24×10^{-5}	46.8	9.36×10^{-5}	41.6	8.32×10^{-5}
PYR	0.000000385	48.9	0.0188	38.1	0.0147	7.80	3.00×10^{-3}	36.4	0.0140	30.7	0.0118	36.7	0.0141
BaA	0.0002	23.6	4.72	<LOD	0.00	5.73	1.15	<LOD	0.00	<LOD	0.00	<LOD	0.00
CHR	0.0000659	8.65	0.570	4.42	0.291	<LOD	0.00	<LOD	0.00	<LOD	0.00	<LOD	0.00
BbF	0.000166	<LOD	0.00	<LOD	0.00	<LOD	0.00	<LOD	0.00	<LOD	0.00	<LOD	0.00
BkF	0.00128	39.7	50.8	41.4	53.0	46.1	59.0	38.5	49.3	41.8	53.5	39.0	49.9
BaP	0.00024375	5.16	1.26	45.6	11.1	<LOD	0.00	43.1	10.5	<LOD	0.00	43.4	10.6
DahA	0.000272	361	98.2	548	149	514	140	393	107	488	133	357	97.1
BghiP	0.0000102	5.06	0.0516	<LOD	0.00	<LOD	0.00	<LOD	0.00	<LOD	0.00	<LOD	0.00
IcdP	0.00188	618	1160	392	737	1140	2140	370	696	1210	2270	343	645
Total PAHs		**1170**	**1320**	**1110**	**950**	**1760**	**2340**	**922**	**863**	**1820**	**2460**	**861**	**803**

By comparison, TEQ_{PAHs} were much greater than TEQ_{PCBs} despite having fewer compounds contributing to its calculation. In the liver, mean TEQPAHs for the three species ranged from 1320 to 2460 pg/g ww (Table 4-3) and significant differences were detected among species ($F_{2,24} = 11.464$, $p = 0.0003$). Similar to the analyses using ∑PAHs and congener profiles, TEQ_{PAHs} were lower in bull sharks than blacktips ($p < 0.001$) and bonnetheads ($p < 0.001$). Proportions of indeno[1,2,3-cd]pyrene in the liver accounted for nearly the entire amount of TEQ_{PAHs} for each species (range of means: 85 – 91%). Although no differences were found among species for muscle TEQ_{PAHs} ($F_{2,25} = 0.623$, $p = 0.5446$), mean values for each species (803 – 950 pg/g ww) were still higher than in either tissue for TEQ_{PCBs}. The greatest contributor to TEQ_{PAHs} in the muscle was also indeno[1,2,3-cd]pyrene for all species (range of means: 77 – 81%), followed by dibenz[a,h]anthracene (range of means: 12 – 16%). The only significant correlation found between TEQs and biomarker activity was a negative relationship ($\rho = - 0.68$, $p = 0.035$) between hepatic TEQ_{PCBs} and EROD activity in blacktip sharks.

Discussion

Comparisons of PAH and PCB burdens in Galveston Bay sharks

Interspecific relationships defined by ∑PAHs and ∑PCBs varied by tissue, for which blacktip and bonnethead sharks were most similar in their hepatic burdens of both contaminants (Figure 4-1A), but blacktips and bulls were more similar in their muscle PCB burdens (Figure 4-1B). Since diet and life history characteristics are known to

affect differences in the accumulation of PAHs and PCBs (Baumard et al. 1998; Fisk et al. 2001; Van der Oost et al. 2003; Borgå et al. 2004; Gelsleichter and Walker 2010), the similarity of blacktip sharks with bonnetheads is unexpected given how closely related the former is to bull sharks phylogenetically, as well as by trophic position and life history. Crustaceans comprise the majority of the diet in bonnetheads (Bethea et al. 2007; Plumlee and Wells 2016), while blacktips primarily consume teleost fishes (Barry et al. 2008; Plumlee and Wells 2016) and bull sharks consume crustaceans, teleosts, marine mammals, and other elasmobranchs at varying ontogenetic stages (Snelson et al. 1984; Cliff and Dudley 1991). Niche partitioning may provide an explanation for the apparent similarity of blacktip and bonnethead sharks in and around Galveston Bay, in which blacktips and bonnetheads overlap by geographic location and bull sharks occupy different sections of this coastal system. Furthermore, ontogenetic shifts in diet and habitat can impact exposure to PAHs and PCBs by changes in prey size, composition, and contamination status of foraging locale (Cliff and Dudley 1991; Bethea et al. 2007; Barry et al. 2008; Plumlee and Wells 2016). It is important to note that not all shark size classes were evenly sampled from each species, which might obscure some relationships.

Since sharks rely upon hepatic lipid stores for energy, burdens of organic contaminants can become concentrated during periods of stress-induced lipid mobilization (Kelly et al. 2011; Belicka et al. 2012; Daley et al. 2014; Olin et al. 2014). Liver burdens are considered to be indicative of acute exposure because of the highly

dynamic nature of this tissue compared to muscle (Albaigés et al. 1987). However, muscle burdens are useful to assess chronic exposure because of the slower turnover rate of this tissue and lower likelihood of concentrating these contaminants due to lipid mobilization (Albaigés et al. 1987; Daley et al. 2014; Beaudry et al. 2015). Since muscle concentrations of ∑PAHs did not differ among species and ∑PCBs were more similar between bull and blacktip sharks than with bonnetheads, these results indicate that all species are exposed to similar chronic concentrations of PAHs, but PCBs accumulate at greater concentrations in the higher trophic position carcharhinids (bulls and blacktips). However, it appears that blacktip and bonnethead sharks are more similar in terms of recent exposure to PAHs and PCBs than bull sharks based on hepatic burdens. Additionally, significant positive correlations of ∑PCBs between tissues in bull and blacktip sharks suggest that PCB burdens in muscle can serve as a non-lethal measure of liver burdens in these species. Future studies should determine whether this relationship is only reliable in high trophic level organisms.

Bioaccumulation of PAHs and PCBs

PAHs did not significantly bioaccumulate over increasing FL in any species, but mean concentrations were consistently higher than expected in both liver (1560 – 2200 ng/g ww) and muscle (1080 – 1330 ng/g ww). To date, only two other studies have quantified PAH burdens in shark tissue (Al-Hassan et al. 2000; Marsili et al. 2016). Mean concentrations of ∑PAHs measured by Al-Hassan et al. (2000) varied from 130 to 33460 ng/g ww in the liver and < LOD to 34840 ng/g ww in muscle of sharks sampled

from the Arabian Gulf after the first Gulf war. Additionally, concentrations of ∑PAHs measured in white sharks (*Carcharodon carcharias*) by Marsili et al. (2016) ranged from 2769.20 – 7278.40 ng/g dry weight (426.46 – 1120.87 ng/g ww; mean of 84.6% water content) in muscle tissue. Samples in the present study fall within the middle of these ranges quantified by previous studies. High concentrations of PAHs in muscle and liver demonstrate chronic exposure to these contaminants and an inability to effectively metabolize and eliminate them faster than they are absorbed. This can be partially attributed to low CYP1A activity (as measured by EROD) of elasmobranchs compared to teleosts (min – max: ~ 0.5 – 5 and 1.1 – 205.9 pmol/min/mg protein, respectively; Gorbi et al. 2004; Solé et al. 2009, 2010) and marine mammals (min – max: 199 - 2167; Van den Berg et al. 1998; Tanabe 2002; Letcher et al. 2014). However, it is likely that this does not fully account for the concentrations found in both tissues in sharks from the present study. These findings suggest that trophic dilution of PAHs may not occur with respect to elasmobranchs since concentrations measured in oysters from 2010 (range of means: 134 – 333 ng/g dry wt.; Apeti et al. 2013) in Galveston Bay (not including the Houston ship channel) are lower than the sharks from the present study.

PCBs bioaccumulated in the liver of bull sharks as well as the liver and muscle of blacktips, which was similar to data reported by Gilbert et al. (2015). Previous studies of bull sharks (Olin et al. 2014) and blacktips (Gelsleichter et al. 2007) may not have detected PCB bioaccumulation with increasing body size since their datasets had a limited ontogenetic range of samples. Mean hepatic ∑PCB concentrations in these prior studies were lower for bulls (2654 ng/g ww), but higher for blacktips (2930 ng/g ww).

Compared to the muscle ∑PCB concentrations in bull sharks collected from two different time periods (1993-1994: 6440 ng/g lw; 2002-2004: 71200 ng/g lw; Johnson-Restrepo et al. 2005) in Florida, the mean ∑PCBs in the present study (35400 ng/g lw) was similar. Although bonnethead sharks did not bioaccumulate PCBs, mean hepatic ∑PCBs were very similar to burdens measured in conspecifics from a historically polluted site in Georgia (520 ng/g ww; Gelsleichter et al. 2008). Since many invertebrates lack comprehensive PAH/PCB biotransformation capabilities (Livingstone 1998; Hylland 2006), the consumption of crabs and other benthic invertebrates may explain the exposure of bonnetheads to such high concentrations of these contaminants. Thus, it appears that the low trophic position of this species does not buffer it from the accumulation of high concentrations of PCBs in contaminated habitats.

Congener profiles of PAH/PCB burdens

Results analyzed on an individual congener basis corroborated the relationships found by comparing ∑PAHs and ∑PCBs, with the exception that the congener profile of blacktip sharks did not significantly differ from bull or bonnethead sharks in muscle tissue. PCB 123 was the primary driver of separation for this different pattern in muscle tissue, for which blacktips had greater proportions of this congener than bulls, but less than what was measured in bonnetheads. It is currently unclear why these species have accumulated different proportions of this particular PCB congener. Additionally, bull and bonnethead sharks were consistently found to be the most different based on congener profiles from both tissues. Differences between these species were primarily

influenced by greater proportions of indeno[1,2,3-cd]pyrene in bonnetheads for liver, but by greater proportions of PCB 123 in bonnetheads for muscle. Congener profiles in the muscle, reflective of chronic exposure, may indicate that blacktip sharks share sources of PAHs with the other two species, but sources of PCB exposure primarily with bull sharks.

With respect to contributions of all congeners, PAHs were dominated by indeno[1,2,3-cd]pyrene and dibenz[a,h]anthracene among all species for both tissues. LMW PAHs are often indicative of petrogenic sources, whereas a greater proportion of HMW PAHs reflect pyrogenic sources. It is difficult to assess the history of PAH exposure from tissue concentrations since this organic contaminant is readily metabolized by most vertebrates and ratios can be altered during trophic transfer (Varanasi et al. 1987; Meador et al. 1995; Baumard et al. 1998). Galveston Bay is primarily impacted by pyrogenic sources as a result of incomplete combustion (Brooks et al. 1992), which would explain the large proportions of HMW PAHs indeno[1,2,3-cd]pyrene and dibenz[a,h]anthracene. Dominant PCB congeners differed by tissue for all species: two highly recalcitrant congeners (PCB 153 and PCB 138) were measured in the greatest proportions for all species in the liver, but mono-*ortho* substituted DL-PCBs 118 and 157 were the primary contributors in the muscle (with the exception of PCB 153 instead of PCB 157 in bull sharks). The differences between tissues may result from the redistribution of congeners among these compartments, especially during lipid mobilization (Van den Berg et al. 1998; Daley et al. 2014). Additionally, DL-PCBs may be accumulating in greater proportions in muscle since this tissue has negligible

CYP1A1 activity when compared to the liver (Wilson et al. 2010; Nielsen et al. 2017). Comparing PCB congener profiles between tissues, there is a greater proportion of DL-PCBs in the muscle of all species compared to the liver (Figure 4-3). This is particularly true of bonnethead sharks, whose muscle burden of DL-PCBs (91% of ∑PCBs) was nearly twice that of its hepatic burden (46% of ∑PCBs). So while the muscle may serve as a compartment reflective of chronic exposure to ∑PCBs, the congener profiles are likely distorted as a result of multiple physiological processes.

Patterns of species distributions in the PCA biplot of hepatic congener profiles appear to be reflective of differences in biotransformation capability and exposure. Clustering of bonnethead sharks was positively associated with greater proportions of recalcitrant PCB congeners, which differed from the positive correlations of HMW PAHs with blacktips and LMW PAHs in bull sharks. Although bonnetheads had greater EROD activity than the other two species, which would presumably indicate greater metabolism of PAHs by CYP1A, the relationship between EROD and proportions of LMW/HMW PAHs was not significant. Further characterization of PAH and PCB biotransformation capability in these species is needed to determine the possible factors driving these differences. Additionally, blacktip sharks had greater proportions of HMW PAHs than the other species, which is reflective of its high exposure and lesser ability to biotransform these burdens (lower EROD activity than bonnetheads). The association of bull sharks with LMW PAHs is likely an effect of having lower proportions of HMW PAHs than the other species, as well as lower proportions of the recalcitrant PCBs due to more PCB congeners being detectable in this species. The outlier YoY bull shark had

much lower hepatic lipid content (16.6%) compared to older conspecifics (mean of 68.8% for others). This is likely a result of lipid mobilization as the YoY shark depletes its intrinsic energy store in the liver, which may cause redistribution and concentration of the quantified PAH and PCB congeners. Therefore, the relationships of bull and bonnethead sharks regarding the loadings of the liver PCA values appear to be a product of differences in biotransformation capability and exposure to these pollutants. Patterns of species clusters and PC loading values were less discernible in the PCA of muscle congener profiles. Due to similar proportions of many congeners, bull and blacktip sharks exhibited high overlap. Most bonnetheads were clustered due to high proportions of the mono-*ortho* substituted DL-PCBs 118, 123, and 157. Since concentrations of PCBs 118, 123, and 157 in the muscle were comparable across all species (Table 4-2), these species clusters reflect the accumulation of a greater number of PCB congeners in bull and blacktip sharks compared to bonnetheads (Figure 4-3B).

Biomarker activity and integration with tissue-based burdens

Although comparisons of exposure can be drawn from the quantification of tissue-based burdens, additional measurements are necessary to determine if any physiological effects are elicited since these are often species-specific. EROD is a commonly measured phase I biomarker that is reflective of CYP1A1 induction, often by dioxin-like compounds and other planar aromatic hydrocarbons. The comparison of EROD activity among the sharks from the present study indicates higher and more variable activity in bonnethead sharks than in bulls or blacktips. Since this biomarker

can also be affected by extrinsic and intrinsic factors, variance may be partially attributable to variables besides known AhR ligands (Whyte et al. 2000). Additionally, none of the contaminant classes (∑PAHs, ∑PCBs, DL-PCBs, NDL-PCBs) were found to significantly correlate with EROD in any species. Therefore, further investigation that includes the measurement of fluorescent aromatic hydrocarbons (FACs) and hydroxylated PCBs in the bile may be necessary to detect a significant relationship with exposure.

GST is another commonly measured biomarker (phase II) that conjugates electrophilic compounds for elimination from the body, often after CYP1A oxidation of a xenobiotic (Van der Oost et al. 2003). Greater GST activity was measured in the two species with higher hepatic burdens of ∑PAHs (blacktip and bonnethead sharks), although no significant correlations were measured between these variables. Significant positive correlations of GST activity with hepatic ∑PCBs and DL-PCBs were found for blacktips, but no other significant correlations were detected. Without knowing the baseline activity rates of EROD and GST for each species, it is difficult to assess whether these values represent significant induction of biotransformation pathways. Therefore, future studies should quantify activity rates for these enzymes in both sexes of each species over multiple seasons to determine a robust baseline to compare against.

Despite the increased attention sharks and other elasmobranchs have recently received in the field of environmental toxicology, the integration of tissue-based burdens with biomarkers and toxic-endpoints has been very limited (Lyons et al. 2014; Alves et al. 2016). The direct approach of integrating burdens of individual congeners with

biomarker activity provides a better understanding of metabolic differences regarding bioaccumulation as opposed to the approach of summing all analyzed congeners. This sum total approach is also limited in explaining the actions of complex mixtures, especially with regard to toxic effects. In the present study, relationships between congeners and biomarker activity in the pRDA were not very clear, as indicated by the permutation test and R^2_{adj}. Congeners known to induce CYP1A (dibenz[a,h]anthracene, indeno[1,2,3-cd]pyrene, PCB 126) and those that are not typically associated with the activation of this transduction pathway (PCBs 28, 128, 170) both showed positive relationships with EROD activity. These unexpected relationships may be a result of using proportions rather than raw or transformed concentrations for each PAH/PCB congener. Conversely, PCB 153 appears to display a negative relationship with EROD activity. When at high concentrations, this recalcitrant congener has demonstrated a negative effect on EROD activity in previous studies as a result of competitive inhibition (Suh et al. 2003; Chen and Bunce 2004). If this congener were to inhibit the AhR complex, agonists of this receptor (e.g. PAHs, DL-PCBs, PCDDs, PCDFs) may accumulate at greater than expected concentrations (Suh et al. 2003). Since bull sharks accumulate particularly high concentrations of PCB 153, likely as a result of its high trophic position, this species may experience further accumulation of PAHs and DL-PCBs if CYP1A activity is substantially impacted. Only two congeners showed noticeable positive (PCB 167) and negative (PCB 105) correlations with GST activity. Since relationships of individual PAH and PCB congeners with GST have not been

explored as thoroughly as its CYP450 counterparts, it is currently unclear what mechanisms may be driving these patterns.

Potential toxicity of PAH and PCB burdens

Although many studies have quantified tissue-based burdens of organic contaminants in sharks, few have assessed the potential toxicity of these accumulated contaminants (Serrano et al. 2000; Storelli et al. 2005; Corsolini et al. 2014). Mean TEQ_{PCBs} values were greatest in bull sharks and lowest in bonnetheads, while blacktips were intermediate. An unexpected negative correlation of hepatic TEQ_{PCBs} with EROD activity was detected in blacktip sharks, for which possible causes remain unclear. Since few data are available that compare toxic endpoints with TEQ_{PCBs} in elasmobranchs, comparisons were made against thresholds set for a sensitive group of fish (early life stage) and aquatic mammals. It is not currently known whether sharks and other elasmobranchs elicit physiological responses at similar levels as these other groups, but if they do, then these species could be prone to negative health outcomes such as decreased vitamin A concentrations, thyroid hormone deficiency, and immunosuppression (Kannan et al. 2000). As a caveat, however, TEFs for DL-PCBs in fish were derived from studies that used early life stage mortality as the toxic endpoint (Van den Berg et al. 1998). Therefore, these TEFs may not be directly applicable to older age classes. Additionally, TEQs cannot explain the toxic effects resulting from high concentrations of NDL-PCBs. Although di-*ortho* through tetra-*ortho* substituted PCBs do not induce CYP1A1 activity via AhR signal transduction, these congeners may

still cause toxic effects such as carcinogenicity, neurotoxicity, and endocrine disruption (Safe 1994; Giesy and Kannan 1998). Therefore, further work is warranted for characterizing the toxic endpoints of NDL-PCBs that accumulate at high concentrations in elasmobranchs, such as PCB 153.

The toxicity of PAH burdens is often overlooked in place of quantifying their metabolites since they are considered to be readily biotransformed in vertebrates (Van den Berg et al. 1998). However, it appears that PAHs are not readily metabolized by sharks measured in the present study. Due to the lack of studies that correlate TEQ_{PAHs} (relative to TCDD) with toxic effects in fish, it is not currently feasible to assess the potential toxicity of these measurements. Additionally, the FPFs used to calculate TEQ_{PAHs} were based upon studies measuring CYP1A induction and AhR affinity as endpoints rather than toxicity, for which FPFs would be expected to be lower. It is also important to mention that the FPF for the dominating PAH congener indeno[1,2,3-cd]pyrene was derived from eight studies, of which only one was conducted on fish (Barron et al. 2004). Therefore, it is difficult to assess the potential toxicity of these PAH burdens without the inclusion of biomarkers of effect and other toxic endpoints. For comparative purposes, the TEQ_{PAHs} were greater in blacktip and bonnethead sharks than in bulls, but only for measurements in the liver. However, mean values of TEQ_{PAHs} could not be directly compared against TEQ_{PCBs} since the former are based upon biomarkers of exposure, which would result in higher TEQ_{PAHs} than if based upon toxic endpoints. Although it is currently difficult to discern the toxic effects of the TEQ_{PAHs}

measured in the present study, the use of TEQ_{PCBs} alone may underestimate the potential toxicity exhibited by the accumulated PAH/PCB burdens in these sharks.

While most of the TEQs measured in the present study did not significantly correlate with EROD activity, it is possible that these levels represent a sequestered depot of pollutants stored in lipid-rich tissues (e.g. liver; McElroy et al. 2011). Although CYP1A is an inducible enzyme system that is sensitive to certain classes of organic contaminants, such as PAHs and DL-PCBs (Bucheli and Fent 1995), it is possible that the tissue-based burdens of these contaminants are not readily available to this system. We cannot definitively comment on this as we are unable to contrast EROD activities with a reference dataset. It is possible that the EROD activities measured in the present study are not entirely reflective of the burdens measured for PAHs and DL-PCBs. However, the TEQ levels reported in the present study are within range of those shown to induce physiological effects in other animal systems. Therefore, we hypothesize that there are likely to be physiological effects in these sharks from the northwestern GoM. The use of a broader suite of biomarkers and long-term sampling efforts are likely to delineate these effects.

Tissue-based burdens of PAHs were found at higher than expected concentrations in all species, suggesting chronic exposure to this contaminant within the Galveston Bay region. By comparison, there appeared to be a general increase in tissue-based PCB burden with estimated trophic level (bull > blacktip ≥ bonnethead) and FL. Species-specific differences in EROD and GST activity were also detected, for which the major proponents of these relationships remain unclear. The integration of biomarker

activity with congener profiles suggested that only a small subset of individual PAH and PCB congeners displayed noticeable positive or negative correlations with EROD and GST. This result underlines the importance of measuring individual congener burdens during risk assessment since only certain PAHs and PCBs are key drivers of biochemical responses (CYP1A, GST) to exposure. Furthermore, effects of dioxin-like compounds (used for calculating TEQs) are assumed to be the critical effects on an organism. The TEQs of accumulated DL-PCB burdens indicate risk of physiological effects in these sharks when compared to established thresholds in mammals and fish. While TEQ_{PAHs} were much greater than TEQ_{PCBs} for all species, it is difficult to determine the extent of toxicity from this measurement since the relative potency factors for PAHs were based upon CYP1A induction and AhR affinity rather than toxic endpoints. Future work should integrate feeding ecology, additional biomarkers, and toxic endpoints to discern sources of exposure and determine which congeners may be responsible for negative health effects.

References

Al-Hassan JM, Afzal M, Rao CVN, Fayad S. 2000. Petroleum hydrocarbon pollution in sharks in the Arabian Gulf. *Bull. Environ. Contam. Toxicol.* 65:391–398. doi:10.1007/s001280000140.

Albaigés J, Farrán A, Soler M, Gallifa A, Martin P. 1987. Accumulation and distribution of biogenic and pollutant hydrocarbons, PCBs and DDT in tissues of western Mediterranean fishes. *Mar. Environ. Res.* 22:1–18. doi:10.1016/0141-1136(87)90078-X.

Alves LMF, Nunes M, Marchand P, Le Bizec B, Mendes S, Correia JPS, Lemos MFL, Novais SC. 2016. Blue sharks (Prionace glauca) as bioindicators of pollution and health in the Atlantic Ocean: Contamination levels and biochemical stress responses. *Sci. Total Environ.* 563–564:282–292. doi:10.1016/j.scitotenv.2016.04.085.

Apeti D, Whitall D, Lauenstein G, McTigue T, Kimbrough K, Jacob A, Mason A. 2013. Assessing the impacts of the Deepwater Horizon Spill: The National Status and Trends Program Response. A summary report of coastal contamination. NOAA Technical Memorandum NOS NCCOS 167. National Centers for Coastal Ocean Science (NCCOS), Center for Coastal Monitoring and Assessment (CCMA), Silver Spring, MD, USA.

Barron MG, Heintz R, Rice SD. 2004. Relative potency of PAHs and heterocycles as aryl hydrocarbon receptor agonists in fish. *Mar. Environ. Res.* 58:95–100. doi:10.1016/j.marenvres.2004.03.001.

Barry KP, Condrey RE, Driggers WB, Jones CM. 2008. Feeding ecology and growth of neonate and juvenile blacktip sharks Carcharhinus limbatus in the Timbalier-Terrebone Bay complex, LA, U.S.A. *J. Fish Biol.* 73:650–662. doi:10.1111/j.1095-8649.2008.01963.x.

Baumard P, Budzinski H, Garrigues P, Sorbe J, Burgeot T, Bellocq J. 1998. Concentrations of PAHs (Polycyclic Aromatic Hydrocarbons) in various marine organisms in relation to those in sediments and to trophic level. *Mar. Pollut. Bull.* 36:951–960. doi:10.1016/S0025-326X(98)00088-5.

Beaudry MC, Hussey NE, McMeans BC, McLeod AM, Wintner SP, Cliff G, Dudley SFJ, Fisk AT. 2015. Comparative organochlorine accumulation in two ecologically similar shark species (Carcharodon carcharias and Carcharhinus obscurus) with divergent uptake based on different life history. *Environ. Toxicol. Chem.* 34:2051–2060. doi:10.1002/etc.3029.

Belicka L, Matich P, Jaffé R, Heithaus M. 2012. Fatty acids and stable isotopes as indicators of early-life feeding and potential maternal resource dependency in the bull shark Carcharhinus leucas. *Mar. Ecol. Prog. Ser.* 455:245–256. doi:10.3354/meps09674.

Van den Berg M, Birnbaum L, Bosveld ATC, Brunström B, Cook P, Feeley M, Giesy JP, Hanberg A, Hasegawa R, Kennedy SW, Kubiak T, Larsen JC, van Leeuwen FXR, Liem AKD, Nolt C, Peterson RE, Poellinger L, Safe S, Schrenk D, Tillitt D, Tysklind M, Younes M, Wærn F, Zacharewski T. 1998. Toxic equivalency factors (TEFs) for PCBs, PCDDs, PCDFs for humans and wildlife. *Environ. Health*

Perspect. 106:775–792. doi:10.1289/ehp.98106775.

Bethea DM, Hale L, Carlson JK, Cortés E, Manire CA, Gelsleichter J. 2007. Geographic and ontogenetic variation in the diet and daily ration of the bonnethead shark, Sphyrna tiburo, from the eastern Gulf of Mexico. *Mar. Biol.* 152:1009–1020. doi:10.1007/s00227-007-0728-7.

Billiard SM, Hahn ME, Franks DG, Peterson RE, Bols NC, Hodson P V. 2002. Binding of polycyclic aromatic hydrocarbons (PAHs) to teleost aryl hydrocarbon receptors (AHRs). *Comp. Biochem. Physiol. - B Biochem. Mol. Biol.* 133:55–68. doi:10.1016/S1096-4959(02)00105-7.

Bocchetti R, Fattorini D, Pisanelli B, Macchia S, Oliviero L, Pilato F, Pellegrini D, Regoli F. 2008. Contaminant accumulation and biomarker responses in caged mussels, Mytilus galloprovincialis, to evaluate bioavailability and toxicological effects of remobilized chemicals during dredging and disposal operations in harbour areas. *Aquat. Toxicol.* 89:257–266. doi:10.1016/j.aquatox.2008.07.011.

Borgå K, Fisk AT, Hoekstra PE, Muir DCG. 2004. Biological and chemical factors of importance in the bioaccumulation and trophic transfer of persistent organochlorine contaminants in Arctic marine food webs. *Environ. Toxicol. Chem.* 23:2367–2385. doi:10.1897/03-518.

Bradford MM. 1976. A rapid and sensitive method for the quantitation of microgram quantities of protein utilizing the principle of protein-dye binding. *Anal. Biochem.* 72:248–254. doi:10.1016/0003-2697(76)90527-3.

Branstetter S. 1987. Age and Growth Estimates for Blacktip, Carcharhinus limbatus, and

Spinner, C . brevipinna, Sharks from the Northwestern Gulf of Mexico. *Copeia* 1987:964–974.

Branstetter S, Stiles R. 1987. Age and growth estimates of the bull shark, Carcharhinus leucas, from the northern Gulf of Mexico. *Environ. Biol. Fishes* 20:169–181.

Brooks JM, Wade TL, Kennicut MC, Wiesenburg DA, Wilkinson D, McDonald TJ, McDonald SJ. 1992. Toxic contaminant characterization of aquatic organisms in Galveston Bay: A pilot study. GBNEP-20. Galveston Bay National Estuary Program, Webster, TX, USA.

Bucheli TD, Fent K. 1995. Induction of cytochrome P450 as a biomarker for environmental contamination in aquatic ecosystems. *Crit. Rev. Environ. Sci. Technol.* 25:201–268. doi:10.1080/10643389509388479.

Burke MD, Mayer RT. 1974. Ethoxyresorufin: Direct fluorometric assay of a microsomal O-dealkylation which is preferentially inducible by 3-methylcholanthrene. *Drug Metab. Dispos.* 2:583–588.

Castro JI. 1993. The shark nursery of Bulls Bay, South Carolina, with a review of the shark nurseries of the southeastern coast of the United States. *Environ. Biol. Fishes* 38:37–48. doi:10.1007/BF00842902.

Chen G, Bunce NJ. 2004. Interaction between halogenated aromatic compounds in the Ah receptor signal transduction pathway. *Environ. Toxicol.* 19:480–489. doi:10.1002/tox.20053.

Cliff G, Dudley SF. 1991. Sharks caught in the protective gill nets off Natal, South Africa. 4. the bull shark Carcharhinus leucas Valenciennes. *South African J. Mar.*

Sci. 10:253–270. doi:10.2989/02577619109504636.

Corsolini S, Sara G. 2017. The trophic transfer of persistent pollutants (HCB, DDTs, PCBs) within polar marine food webs. *Chemosphere* 177:189–199. doi:10.1016/j.chemosphere.2017.02.116.

Cortés E. 1999. Standardized diet compositions and trophic levels of sharks. *ICES J. Mar. Sci.* 56:707–717. doi:10.1006/jmsc.1999.0489.

Cortés E. 2000. Life history patterns and correlations in sharks. *Rev. Fish. Sci.* 8:299–344. doi:10.1080/10408340308951115.

Daley JM, Paterson G, Drouillard KG. 2014. Bioamplification as a bioaccumulation mechanism for persistent organic pollutants (POPs) in wildlife. In: Reviews of Environmental Contamination and Toxicology, Volume 227. Springer. p. 107–155.

Desforges JPW, Sonne C, Levin M, Siebert U, De Guise S, Dietz R. 2016. Immunotoxic effects of environmental pollutants in marine mammals. *Environ. Int.* 86:126–139. doi:10.1016/j.envint.2015.10.007.

Fisk AT, Hobson KA, Norstrom RJ. 2001. Influence of chemical and biological factors on trophic transfer of persistent organic pollutants in the Northwater Polynya marine food web. *Environ. Sci. Technol.* 35:732–738. doi:10.1021/es001459w.

Gelsleichter J, Szabo NJ, Belcher CN, Ulrich GF. 2008. Organochlorine contaminants in bonnethead sharks (Sphyrna tiburo) from Atlantic and Gulf estuaries on the US east coast. *Mar. Pollut. Bull.* 56:359–363. doi:10.1016/j.marpolbul.2007.10.028.

Gelsleichter J, Szabo NJ, Morris JJ. 2007. Organochlorine contaminants in juvenile sandbar and blacktip sharks from major nursery areas on the east coast of the United

States. In: American Fisheries Society Symposium. Vol. 50. American Fisheries Society. p. 153.

Gelsleichter J, Walker CJ. 2010. Pollutant Exposure and Effects in Sharks and Their Relatives. In: Sharks And Their Relatives II: Biodiversity, Adaptive Physiology, And Conservation. p. 491–537.

Gelsleichter J, Walsh CJ, Szabo NJ, Rasmussen LEL. 2006. Organochlorine concentrations, reproductive physiology, and immune function in unique populations of freshwater Atlantic stingrays (Dasyatis sabina) from Florida's St. Johns River. *Chemosphere* 63:1506–1522. doi:10.1016/j.chemosphere.2005.09.011.

Giesy JP, Kannan K. 1998. Dioxin-Like and Non-Dioxin-Like Toxic Effects of Polychlorinated Biphenyls (PCBs): Implications For Risk Assessment. *Crit. Rev. Toxicol.* 28:511–569. doi:10.1080/10408449891344263.

Gilbert JM, Baduel C, Li Y, Reichelt-Brushett AJ, Butcher PA, McGrath SP, Peddemors VM, Hearn L, Mueller J, Christidis L. 2015. Bioaccumulation of PCBs in liver tissue of dusky Carcharhinus obscurus, sandbar C. plumbeus and white Carcharodon carcharias sharks from south-eastern Australian waters. *Mar. Pollut. Bull.* 101:908–913. doi:10.1016/j.marpolbul.2015.10.071.

Gorbi S, Pellegrini D, Tedesco S, Regoli F. 2004. Antioxidant efficiency and detoxification enzymes in spotted dogfish Scyliorhinus canicula. *Mar. Environ. Res.* 58:293–297. doi:10.1016/j.marenvres.2004.03.074.

Habig WH, Pabst MJ, Jakoby WB. 1974. Glutathione S-transferases. *J. Biol. Chem.* 249:7130–7139.

Hahn ME, Stegeman JJ. 1992. Phylogenetic ditribution of the Ah receptor in non-mammalian species: Implications for dioxin toxicity and Ah receptor evolution. *Chemosphere* 25:931–937.

Hawkins SA, Billiard SM, Tabash SP, Stephen Brown R, Hodson P V. 2002. Altering cytochrome P4501A activity affects polycyclic aromatic hydrocarbon metabolism and toxicity in rainbow trout (Oncorhynchus Mykiss). *Environ. Toxicol. Chem.* 21:1845–1853. doi:10.1002/etc.5620210912.

Heupel MR, Yeiser BG, Collins AB, Ortega L, Simpfendorfer CA. 2010. Long-term presence and movement patterns of juvenile bull sharks, Carcharhinus leucas, in an estuarine river system. *Mar. Freshw. Res.* 61:1–10. doi:10.1071/MF09019.

Hong J, Kim H-Y, Kim D-G, Seo J, Kim K-J. 2004. Rapid determination of chlorinated pesticides in fish by freezing-lipid filtration, solid-phase extraction and gas chromatography–mass spectrometry. *J. Chromatogr. A* 1038:27–35. doi:10.1016/j.chroma.2004.03.003.

Hussey NE, Wintner SP, Dudley S, Cliff G, Cocks DT, Aaron MacNeil M. 2010. Maternal investment and size-specific reproductive output in carcharhinid sharks. *J. Anim. Ecol.* 79:184–193. doi:10.1111/j.1365-2656.2009.01623.x.

Hylland K. 2006. Polycyclic aromatic hydrocarbon (PAH) ecotoxicology in marine ecosystems. *J. Toxicol. Environ. Heal. Part A* 69:109–123. doi:10.1080/15287390500259327.

Incardona JP, Collier TK, Scholz NL. 2004. Defects in cardiac function precede morphological abnormalities in fish embryos exposed to polycyclic aromatic

hydrocarbons. *Toxicol. Appl. Pharmacol.* 196:191–205. doi:10.1016/j.taap.2003.11.026.

Islam MS, Tanaka M. 2004. Impacts of pollution on coastal and marine ecosystems including coastal and marine fisheries and approach for management: A review and synthesis. *Mar. Pollut. Bull.* 48:624–649. doi:10.1016/j.marpolbul.2003.12.004.

Jepson PD, Deaville R, Barber JL, Aguilar À, Borrell A, Murphy S, Barry J, Brownlow A, Barnett J, Berrow S, et al. 2016. PCB pollution continues to impact populations of orcas and other dolphins in European waters. *Sci. Rep.* 6:1–17. doi:10.1038/srep18573.

Johnson-Restrepo B, Kannan K, Addink R, Adams DH. 2005. Polybrominated diphenyl ethers and polychlorinated biphenyls in a marine foodweb of coastal Florida. *Environ. Sci. Technol.* 39:8243–8250.

Kannan K, Blankenship AL, Jones PD, Giesy JP. 2000. Toxicity reference values for the toxic effects of polychlorinated biphenyls to aquatic mammals. *Hum. Ecol. Risk Assess.* 6:181–201. doi:10.1080/10807030091124491.

Kelly BC, Ikonomou MG, MacPherson N, Sampson T, Patterson DA, Dubetz C. 2011. Tissue residue concentrations of organohalogens and trace elements in adult Pacific salmon returning to the Fraser River, British Columbia, Canada. *Environ. Toxicol. Chem.* 30:367–376. doi:10.1002/etc.410.

Kennish MJ. 2002. Environmental threats and environmental future of estuaries. *Environ. Conserv.* 29:78–107. doi:10.1017/S0376892902000061.

Lemiere S, Cossu-Leguille C, Bispo A, Jourdain MJ, Lanhers MC, Burnel D, Vasseur P.

2005. DNA damage measured by the single-cell gel electrophoresis (Comet) assay in mammals fed with mussels contaminated by the “Erika” oil-spill. *Mutat. Res. - Genet. Toxicol. Environ. Mutagen.* 581:11–21. doi:10.1016/j.mrgentox.2004.10.015.

Letcher RJ, Chu S, McKinney MA, Tomy GT, Sonne C, Dietz R. 2014. Comparative hepatic in vitro depletion and metabolite formation of major perfluorooctane sulfonate precursors in arctic polar bear, beluga whale, and ringed seal. *Chemosphere* 112:225–231. doi:10.1016/j.chemosphere.2014.04.022.

Livingstone DR. 1998. The fate of organic xenobiotics in aquatic ecosystems: quantitative and qualitative differences in biotransformation by invertebrates and fish. *Comp. Biochem. Physiol. - A Mol. Integr. Physiol.* 120:43–49. doi:10.1016/S1095-6433(98)10008-9.

Lombardi-Carlson L, Cortés E, Parsons G, Manire C. 2003. Latitudinal variation in life-history traits of bonnethead sharks, Sphyrna tiburo, (Carcharhiniformes : Sphyrnidae) from the eastern Gulf of Mexico. *Mar. Freshw. Res.* 54:875–883.

Lucifora LO, Menni RC, Escalante AH. 2002. Reproductive ecology and abundance of the sand tiger shark, Carcharias taurus, from the southwestern Atlantic. *ICES J. Mar. Sci.* 59:553–561. doi:10.1006/jmsc.2002.1183.

Lyons K, Lavado R, Schlenk D, Lowe CG. 2014. Bioaccumulation of organochlorine contaminants and ethoxyresorufin-o-deethylase activity in southern California round stingrays (Urobatis halleri) exposed to planar aromatic compounds. *Environ. Toxicol. Chem.* 33:1380–1390. doi:10.1002/etc.2564.

Lyons K, Lowe CG. 2013. Mechanisms of maternal transfer of organochlorine contaminants and mercury in the common thresher shark (Alopias vulpinus). *Can. J. Fish. Aquat. Sci.* 70:1667–1672.

Marsili L, Coppola D, Giannetti M, Casini S, Fossi M, van Wyk J, Sperone E, Tripepi S, Micarelli P, Rizzuto S. 2016. Skin biopsies as a sensitive non-lethal technique for the ecotoxicological studies of great white shark (Carcharodon carcharias) sampled in South Africa. *Expert Opin. Environ. Biol.* 04:1–8. doi:10.4172/2325-9655.1000126.

McElroy AE, Barron MG, Beckvar N, Driscoll SBK, Meador JP, Parkerton TF, Preuss TG, Steevens JA. 2011. A review of the tissue residue approach for organic and organometallic compounds in aquatic organisms. *Integr. Environ. Assess. Manag.* 7:50–74. doi:10.1002/ieam.132.

Meador JP, Collier TK, Stein JE. 2002. Use of tissue and sediment-based threshold concentrations of polychlorinated biphenyls (PCBs) to protect juvenile salmonids listed under the US Endangered Species Act. *Aquat. Conserv. Mar. Freshw. Ecosyst.* 12:493–516. doi:10.1002/aqc.523.

Meador J, Sommers F, Ylitalo G, Sloan C. 2006. Altered growth and related physiological responses in juvenile Chinook salmon (Oncorhynchus tshawytscha) from dietary exposure to polycyclic aromatic hydrocarbons (PAHs). *Can. J. Fish. Aquat. Sci.* 63:2364–2376. doi:10.1139/f06-127.

Meador J, Stein J, Reichert W, Varanasi U. 1995. Bioaccumulation of polycyclic aromatic hydrocarbons by marine organisms. *Rev. Environ. Contam. Toxicol.*

143:79–165. doi:10.1007/978-1-4612-2542-3_4.

National Toxicology Program (NTP). 2016. Report on Carcinogens, fourteenth ed. Public Health Service, US Department of Health and Human Services. Research Triangle Park, NC.

Nielsen SD, Bauhaus Y, Zamaratskaia G, Junqueira MA, Blaabjerg K, Petrat-Melin B, Young JF, Rasmussen MK. 2017. Constitutive expression and activity of cytochrome P450 in conventional pigs. *Res. Vet. Sci.* 111:75–80. doi:10.1016/j.rvsc.2016.12.003.

Nilsen BM, Berg K, Goksøyr A. 1998. Induction of cytochrome P4501A (CYP1A) in fish: A biomarker for environmental pollution. In: Phillips IR, Shephard EA, editors. Cytochrome P450 Protocols. Totowa, NJ: Humana Press. p. 423–438.

Nomiyama K, Hirakawa S, Eguchi A, Kanbara C, Imaeda D, Yoo J, Kunisue T, Kim EY, Iwata H, Tanabe S. 2014. Toxicological assessment of polychlorinated biphenyls and their metabolites in the liver of Baikal seal (Pusa sibirica). *Environ. Sci. Technol.* 48:13530–13539. doi:10.1021/es5043386.

Oksanen J, Guillaume Blanchet F, Friendly M, Kindt R, Legendre P, McGlinn D, Minchin PR, O'Hara RB, Simpson GL, Solymos P. 2017. vegan: Community Ecology Package. R package version 2.4-4.

Olin JA, Beaudry M, Fisk AT, Paterson G. 2014. Age-related polychlorinated biphenyl dynamics in immature bull sharks (Carcharhinus leucas). *Environ. Toxicol. Chem.* 33:35–43. doi:10.1002/etc.2402.

Van der Oost R, Beyer J, Vermeulen NPE. 2003. Fish bioaccumulation and biomarkers

in environmental risk assessment: A review. *Environ. Toxicol. Pharmacol.* 13:57–149. doi:10.1016/S1382-6689(02)00126-6.

Pethybridge H, Cossa D, Butler EC. 2010a. Mercury in 16 demersal sharks from southeast Australia: Biotic and abiotic sources of variation and consumer health implications. *Mar. Environ. Res.* 69:18–26. doi:10.1016/j.marenvres.2009.07.006.

Pethybridge H, Daley R, Virtue P, Nichols P. 2010b. Lipid composition and partitioning of deepwater chondrichthyans: inferences of feeding ecology and distribution. *Mar. Biol.* 157:1367–1384. doi:10.1007/s00227-010-1416-6.

Pethybridge H, Daley R, Virtue P, Nichols PD. 2011. Lipid (energy) reserves, utilisation and provisioning during oocyte maturation and early embryonic development of deepwater chondrichthyans. *Mar. Biol.* 158:2741–2754. doi:10.1007/s00227-011-1773-9.

Plumlee JD, Wells RJD. 2016. Feeding ecology of three coastal shark species in the northwest Gulf of Mexico. *Mar. Ecol. Prog. Ser.* 550:163–174. doi:10.3354/meps11723.

Port of Houston Authority. 2018. Port of Houston Overview. Houston (TX, USA). [Accessed 2018-03-14]. Available from: http://porthouston.com/about-us/.

R Development Core Team. 2017. *R: A language and environment for statistical computing*. Vienna (AT): R Foundation for Statistical Computing.

Romero-Romero S, Herrero L, Fernández M, Gómara B, Acuña JL. 2017. Biomagnification of persistent organic pollutants in a deep-sea, temperate food web. *Sci. Total Environ.* 605–606:589–597. doi:10.1016/j.scitotenv.2017.06.148.

Rossouw G. 1987. Function of the liver and hepatic lipids of the lesser sand shark, Rhinobatos annulatus (Müller & Henle). *Comp. Biochem. Physiol. - B Biochem. Mol. Biol.* 86:785–790. doi:10.1016/0305-0491(87)90225-2.

Safe S. 1994. Polychlorinated biphenyls (PCBs): Environmental impact, biochemical and toxic responses, and implications for risk assessment. *Crit. Rev. Toxicol.* 24:87–149.

Santschi PH, Presley BJ, Wade TL, Garcia-Romero B, Baskaran M. 2001. Historical contamination of PAHs, PCBs, DDTs, and heavy metals in Mississippi River Delta, Galveston Bay and Tampa Bay sediment cores. *Mar. Environ. Res.* 52:51–79. doi:10.1016/S0141-1136(00)00260-9.

Sawyna JM, Spivia WR, Radecki K, Fraser DA, Lowe CG. 2017. Association between chronic organochlorine exposure and immunotoxicity in the round stingray (Urobatis halleri). *Environ. Pollut.* 223:42–50. doi: 10.1016/j.envpol.2016.12.019.

Schwacke LH, Smith CR, Townsend FI, Wells RS, Hart LB, Balmer BC, Collier TK, De Guise S, Fry MM, Guillette LJ, Lamb SV, Lane SM, McFee WE, Place NJ, Tumlin MC, Ylitalo GM, Zolman ES, Rowles TK. 2014. Health of common bottlenose dolphins (Tursiops truncatus) in Barataria Bay, Louisiana, following the Deepwater Horizon oil spill. *Environ. Sci. Technol.* 48:93–103. doi:10.1021/es403610f.

Serrano R, Fernández M, Rabanal R, Hernández M, Gonzalez MJ. 2000. Congener-specific determination of polychlorinated biphenyls in shark and grouper livers from the northwest African Atlantic Ocean. *Arch. Environ. Contam. Toxicol.* 38:217–224. doi:10.1007/s002449910029.

Snelson FF, Mulligan TJ, Williams SE. 1984. Food habits, occurrence, and population structure of the bull shark, Carcharhinus leucas, in Florida coastal lagoons. *Bull. Mar. Sci.* 34:71–80.

Solé M, Antó M, Baena M, Carrasson M, Cartes JE, Maynou F. 2010. Hepatic biomarkers of xenobiotic metabolism in eighteen marine fish from NW Mediterranean shelf and slope waters in relation to some of their biological and ecological variables. *Mar. Environ. Res.* 70:181–188. doi:10.1016/j.marenvres.2010.04.008.

Solé M, Rodriguez S, Papiol V, Maynou F, Cartes JE. 2009. Xenobiotic metabolism markers in marine fish with different trophic strategies and their relationship to ecological variables. *Comp. Biochem. Physiol. - C Toxicol. Pharmacol.* 149:83–89. doi:10.1016/j.cbpc.2008.07.008.

Steevens JA, Reiss MR, Pawlisz A V. 2005. A methodology for deriving tissue residue benchmarks for aquatic biota: A case study for fish exposed to 2,3,7,8-tetrachlorodibenzo-p-dioxin and equivalents. *Integr. Environ. Assess. Manag.* 1:142–151. doi:10.1897/IEAM_2004a-014.1.

Steichen JL, Windham R, Brinkmeyer R, Quigg A. 2012. Ecosystem under pressure: Ballast water discharge into Galveston Bay, Texas (USA) from 2005 to 2010. *Mar. Pollut. Bull.* 64:779–789. doi:10.1016/j.marpolbul.2012.01.028.

Storelli MM, Storelli A, Marcotrigiano GO. 2005. Concentrations and hazard assessment of polychlorinated biphenyls and organochlorine pesticides in shark liver from the Mediterranean Sea. *Mar. Pollut. Bull.* 50:850–855.

doi:10.1016/j.marpolbul.2005.02.023.

Suh J, Kang JS, Yang KH, Kaminski NE. 2003. Antagonism of aryl hydrocarbon receptor-dependent induction of CYP1A1 and inhibition of IgM expression by di-ortho-substituted polychlorinated biphenyls. *Toxicol. Appl. Pharmacol.* 187:11–21. doi:10.1016/S0041-008X(02)00040-6.

Sun R, Sun Y, Li QX, Zheng X, Luo X, Mai B. 2018. Polycyclic aromatic hydrocarbons in sediments and marine organisms: Implications of anthropogenic effects on the coastal environment. *Sci. Total Environ.* 640–641:264–272. doi:10.1016/j.scitotenv.2018.05.320.

Tanabe S. 2002. Contamination and toxic effects of persistent endocrine disrupters in marine mammals and birds. *Mar. Pollut. Bull.* 45:69–77. doi:10.1016/S0025-326X(02)00175-3.

U.S. Environmental Protection Agency (USEPA). 2017. Superfund National Priorities List (NPL) Sites – by State. Washington, D.C. (USA). [Accessed 2017-09-12]. Available from: https://www.epa.gov/superfund/national-priorities-list-npl-sites-state#TX.

Varanasi U, Stein JE, Nishimoto M. 1987. Chemical carcinogenesis in feral fish: Uptake, activation, and detoxication of organic xenobiotics. *Environ. Health Perspect.* Vol. 71:155–170. doi:10.1289/ehp.8771155.

Wade TL, Sweet ST, Sericano JL, DeFreitas DA, Lauenstein GG. 2014. Polychlorinated dibenzo-p-dioxins and dibenzofurans detected in bivalve samples from the NOAA National Status and Trends Program. *Mar. Pollut. Bull.* 81:317–324.

doi:10.1016/j.marpolbul.2013.09.002.

Wan Y, Jin X, Hu J, Jin F. 2007. Trophic dilution of polycyclic aromatic hydrocarbons (PAHs) in a marine food web from Bohai Bay, North China. *Environ. Sci. Technol.* 41:3109–3114. doi:10.1021/es062594x.

Whyte JJ, Jung RE, Schmitt CJ, Tillitt DE. 2000. Ethoxyresorufin-O-deethylase (EROD) activity in fish as a biomarker of chemical exposure. *Crit. Rev. Toxicol.* 30:347–570. doi:10.1080/10408440091159239.

Wilson JY, Moore MJ, Stegeman JJ. 2010. Catalytic and immunochemical detection of hepatic and extrahepatic microsomal cytochrome P450 1A1 (CYP1A1) in white-sided dolphin (Lagenorhynchus acutus). *Aquat. Toxicol.* 96:216–224. doi:10.1016/j.aquatox.2009.10.021.

Zhou H, Qu Y, Wu H, Liao C, Zheng J, Diao X, Xue Q. 2010. Molecular phylogenies and evolutionary behavior of AhR (aryl hydrocarbon receptor) pathway genes in aquatic animals: Implications for the toxicology mechanism of some persistent organic pollutants (POPs). *Chemosphere* 78:193–205. doi:10.1016/j.chemosphere.2009.09.012.

CHAPTER V

CONCLUSIONS

Predator-prey interactions are the functional subunits that fuel food web dynamics, but are often only evaluated from a single perspective. The distribution or diet of species are frequently the only methods used to characterize these relationships (Scharf et al. 2000; Preisser et al. 2005; Aragón and Sánchez-Fernández 2013), which do not take performance (mediated by morphology) into account. As the abundance of terrestrial and aquatic species decline due to thermal stress, habitat degradation, overfishing, and pollution, predators will likely be required to travel further or exert more energy to consume other types of available prey (Lotze et al. 2006; Estes et al. 2011; Beaugrand et al. 2019). Therefore, the plasticity of trophic interactions is expected to be constrained by the performance capacity of predators to capture and consume new types of prey (Ruehl and DeWitt 2007; Drymon et al. 2012; Kiszka et al. 2015). The habitat and dietary resources currently being used by species have also become increasingly contaminated (van der Oost et al. 2003; Islam and Tanaka 2004), necessitating the characterization of current routes of exposure and health status to develop risk assessments for the mitigation of individual- and population-level effects. The interdisciplinary assessment of a species' ecological role provides a comprehensive approach to understanding resource use as well as a basis to predict trophic plasticity under future ecological regimes.

This dissertation applied an integrative approach to characterizing the ecological roles of bull, blacktip, and bonnethead sharks within coastal ecosystems using feeding biomechanics, ecomorphology, and ecotoxicology. This research also characterized niche breadth, overlap, and changes in niche variability over the ontogeny of each species to directly correspond with bite force, tooth shape, and burdens of organic contaminants. The results of my research provide sufficient evidence that multiple species of carchariniform sharks exhibit two different scaling patterns of bite force over ontogeny, which show implications for dietary shifts (Chapter 2). Relationships between material properties of prey items with tooth morphology and extent of heterodonty were re-evaluated in sharks, which provided insight for ecomorphological relationships within extant and extinct elasmobranchs (Cullen and Marshall 2019; Chapter 3). Findings from my research also provided support for the susceptibility of coastal sharks to the exposure and accumulation of organic contaminants, which may be at concentrations that impair the physiology of these species (Cullen et al. 2019; Chapter 4). When synthesized together, the results of each of these lines of study provide a depiction of the ecological roles of each species and how this contributes to the resource partitioning among these co-occurring predators. This integrative approach provides a useful framework for discerning the ecological role(s) of a species, including their potential adaptability to a rapidly changing environment.

In Chapter 2, I quantified the scaling pattern of bite force over ontogeny within bull, blacktip, and bonnethead sharks and related these performance change to niche breadth and variability. My findings suggest that significant positive allometric scaling

of bite force in small bull and bonnethead sharks are associated with increased niche breadth and specialization on energy-rich prey, respectively. Positive scaling of bite force may provide juvenile bull sharks with greater opportunity to diverge in their dietary preferences by becoming ecological specialists at an individual level. This would reduce intraspecific competition when estuarine prey resources are limited (Bolnick et al. 2003; Svanbäck and Bolnick 2007; Araújo et al. 2011; Matich et al. 2011). An exponential relationship between body size in bonnethead sharks and their primary prey, blue crabs, may result in intraspecific resource partitioning where the largest crabs are only available to adult bonnetheads (Cortés et al. 1996). Additionally, it may benefit bonnetheads to rapidly grow and achieve adult body size sooner since this resource is not readily available to most competitors. A relationship between bite force scaling patterns and diet was not apparent in blacktip sharks, which may be phylogenetically-constrained in their growth (Gould 1966; Pélabon et al. 2013, 2014; Araya-Ajoy et al. 2019). Stable isotope analyses supported the characterization of bull sharks as generalists, which overlap entirely with the ecological niche of piscivorous blacktips. Bonnetheads exhibited greater levels of niche overlap with bull and blacktip sharks than was expected given their known diets, but this was likely obscured by the lack of a discriminating variable (e.g. $\delta^{34}S$; Plumlee and Wells 2016; Rossman et al. 2016). My research supports the importance of feeding performance as a driver of ontogenetic diet shifts in two of the three species studied.

In Chapter 3, I used elliptic Fourier analysis to measure the outlines of teeth in bull, blacktip, and bonnethead sharks in the assessment of heterodonty by tooth position

and over ontogeny. Previous studies have found inconclusive relationships between tooth morphology and diet in sharks, but these teeth were often tested from a single position in isolation from the jaws and were not tested in a dynamic manner (Huber et al. 2009; Whitenack and Motta 2010; Bergman et al. 2017). I did not find a functionally-relevant change in tooth morphology over ontogeny in any of the species evaluated apart from the PostLow position in bull sharks, which implies that the morphology of teeth post-parturition are suitable for consumption of most prey species. The greatest level of heterodonty was found in bull sharks, which suggests that extent of heterodonty may be directly associated with the level of dietary specialization. Although it requires further functional testing, the morphology of teeth present in each species appears best-suited for the material properties of their respective prey, as well as their respective method of prey processing (Cullen and Marshall 2019). If so, all teeth throughout the jaws could be used in a manner to maximize net energy intake through increased prey handling efficiency, which may be particularly constrained in the specialist blacktip and bonnethead sharks.

In Chapter 4, I measured burdens of PAHs and PCBs in muscle and liver tissue of bull, blacktip, and bonnethead sharks. I related these burdens to biomarkers of exposure and used them to develop a risk assessment of physiological impact. I found that PAH accumulation was similar across all three species, suggesting that species co-occurrence in addition to a relatively low capacity for PAH biotransformation resulted in comparable tissue burdens (Cullen et al. 2019). PCBs appeared to biomagnify up the food web, where tertiary consumer bull and blacktip sharks had significantly greater

burdens of this contaminant than secondary consumer bonnethead sharks. Blacktip and bonnethead sharks may occasionally exhibit significant overlap in habitat since congener profiles and total burdens of PAHs and PCBs resulting from acute exposure of these species were significantly more similar than with bull sharks. However, chronic exposure to these contaminants has resulted in significantly similar congener profiles and total burdens of PAHs and PCBs in bull and blacktip sharks compared to bonnetheads (Cullen et al. 2019). The low correlation of congener profiles in all species relative to activity of EROD and GST biomarkers suggests that other contaminants are impacting these physiological responses. This finding supports the importance of studying the effects of complex mixtures of pollutants rather than individual classes or congeners (Groten et al. 2001; van der Oost et al. 2003; Spurgeon et al. 2010). The TEQ_{PCBs} for all three shark species suggested that these sharks may be experiencing physiological toxicity compared to established thresholds for fishes and aquatic mammals (Kannan et al. 2000; Steevens et al. 2005; Cullen et al. 2019). Toxicity of these contaminants require further investigation using multiple toxic endpoints to determine the extent of these impacts.

This dissertation provides biomechanical and morphological support for ecological differences among all three species, which facilitates their co-occurrence within estuarine and coastal habitats. Although adult sharks are often capable of processing their prey of choice by virtue of their large body size and hypertrophied jaw muscles, YoY and juvenile sharks often must forage for small prey items that are more easily consumed (softer, less evasive). Due to the constraints of body size, gape, and

foraging inexperience, YoY and juvenile sharks are limited in their prey selection. To overcome these limitations, all three species display significant positive allometric scaling of bite force (Chapter 2). This mechanism may be particularly important in conferring advantages at small size classes, enabling them to partition niche-space with sympatric predators, handle prey more efficiently, consume larger prey relative to their body size, and increase overall rate of growth (Hernandez and Motta 1997; Erickson et al. 2003; Huber et al. 2005, 2006; Kolmann and Huber 2009; Habegger et al. 2012). This is especially important regarding prey handling efficiency and net energy intake with respect to material properties and evasiveness of prey (Emlen 1966; Schoener 1971; Emerson et al. 1994; Anderson et al. 2008; Kolmann et al. 2015). Regarding ontogenetic changes in ecological roles, bull sharks appear to shift from a mesopredator role as YoY to that of a top predator as an adult due to their large bite forces and body sizes, as well as possessing a tooth morphology suited to the capture and processing of high trophic level prey (e.g. large fishes, marine mammals, birds, reptiles; Cliff and Dudley 1991; Werry et al. 2011; Chapter 3). Blacktip and bonnethead sharks remain mesopredators over their ontogeny despite greater than 10-fold increases in bite force since they do not feed on increasingly higher trophic level prey and only attain moderate body sizes by comparison (Heupel et al. 2014; Chapter 2).

Additionally, differences in resource use and trophic position appear to influence the bioaccumulation of certain contaminants and therefore susceptibility to toxicity. In Galveston Bay, TX, there is a decreasing gradient in sediment concentrations of PAHs and PCBs southward from the Houston Ship Channel to the mouth of Galveston Bay

(Brooks et al. 1992; Oziolor et al. 2018). Therefore, the estuarine nursery habitat of YoY and juvenile conspecifics may provide an early source of contaminant exposure in these species. Young organisms are often more vulnerable to contaminant-induced toxicity than adults (McKim 1977; Woltering 1984; Incardona et al. 2004; Meador et al. 2006), which is exacerbated by the maternal offloading of pollutants to offspring *in utero* (Lyons et al. 2013; Mull et al. 2013; Olin et al. 2014; Weijs et al. 2015). PAHs and PCBs are lipophilic and preferably adsorb to organic material in the water column, which are consumed by filter feeders or settle to the benthos (Baumard et al. 1998; Johnson et al. 2002; Khairy et al. 2014; Apell and Gschwend 2016). Bull and blacktip sharks feed higher in the water column than bonnetheads, where both species are high trophic position predators that are vulnerable to the biomagnification of PCBs (Cullen et al. 2019; Chapter 4). The concentrations of PCBs, especially the more toxic dioxin-like PCBs, were high in both bull and blacktip sharks and indicated possible physiological impacts. Although bonnethead sharks feed at a lower trophic level than the other two species, they primarily feed on benthic prey where concentrations of organic pollutants are the greatest in aquatic habitats (Meador et al. 1995; Baumard et al. 1998; Livingstone 1998). In addition, many crustaceans are not able to rapidly biotransform contaminants such as PAHs and PCBs that are quickly metabolized by most vertebrates (Meador et al. 1995; Livingstone 1998; Hylland 2006), which makes bonnetheads particularly vulnerable to continuous pollutant exposure. Therefore, bull and blacktip sharks are susceptible to the biomagnification of toxic concentrations of PCBs due to their high

trophic positions, whereas bonnetheads are vulnerable due to the high contamination of their foraging habitat (Cullen et al. 2019).

Responses of bull, blacktip, and bonnethead sharks to changes in prey species composition will likely vary as a result of differences in fishing pressure, anthropogenic disturbance, and climate change. Compared to blacktip and bonnethead sharks, bull sharks have greater gapes and body sizes that allow them to consume larger prey sooner than the other two species. As dietary generalists that exhibit bite forces great enough to overcome the material properties of most available prey, bull sharks will likely be resilient in their response to a loss or change in available prey species. The specialist feeding strategy of blacktip sharks may not jeopardize their ability to capture prey, although this will depend on the composition and size classes of available teleost fishes. Blacktip sharks primarily feed on clupeid and sciaenid fishes over their ontogeny, which are often targets of commercial and recreational fisheries (Cooke and Cowx 2004; Lellis-Dibble et al. 2008; Figueira and Coleman 2010; Robinson et al. 2015; Geers et al. 2016; Buchheister et al. 2017). If stocks of these species become depleted then blacktip sharks may need to feed on a greater number of smaller prey to achieve the same level of net energy intake since only adults are large enough to feed on other elasmobranchs (Castro 1996; Hoffmayer and Parsons 2003). Behavioral plasticity of habitat use and prey capture will therefore dictate the success of blacktip sharks in their ability to cope with loss of primary prey species (Ruehl and DeWitt 2007; Matich et al. 2011; Rosenblatt et al. 2015; Svanbäck et al. 2015). The success of bonnethead sharks in the face of habitat degradation may be uncertain, however. Portunid crabs and penaeid

shrimp are primary prey of bonnethead sharks and these species rely on coastal marsh habitats for resources important to growth and protection from predation (Zimmerman et al. 2002; Kroetz et al. 2017). The accelerated loss of these habitats has resulted in a temporary increase in crab and shrimp production in the northern Gulf of Mexico (Zimmerman et al. 2002), but these stocks may crash following the continued exploitation and loss of larval-stage marsh habitat, as well as adult seagrass habitat (Lotze et al. 2006; Waycott et al. 2009). Therefore, bonnetheads would need to travel further to reach unimpacted habitats or compete with sympatric predators for the remaining small crustacean and cephalopod prey. Gape, bite force, tooth morphology, and stereotypy of feeding behavior could limit the resiliency of this species if they were required to compete with sympatric predators for limited resources (Wilga and Motta 2000; Mara et al. 2010; Cullen and Marshall 2019; Chapter 2). In combination with the current fate of organic contaminants and routes of exposure in these sharks, bonnetheads may experience greater stress regarding net energy intake and health status compared to bull and blacktip sharks. Sublethal effects of exposure can result in decreased fecundity or infertility (Gelsleichter et al. 2005, 2006), potentially affecting the survival rates of sharks (Gelsleichter et al. 2005; Gallagher et al. 2012; Taylor et al. 2014) and in turn may result in a tertiary stress response with detrimental population level effects (Gelsleichter and Walker 2010). In addition to mean generation time, population growth rates, and fecundity, future management plans should incorporate predictions of prey availability and contaminant bioaccumulation in the conservation of sustainable predator populations.

References

Anderson RA, Mcbrayer LD, Herrel A. 2008. Bite force in vertebrates: opportunities and caveats for use of a nonpareil whole-animal performance measure. *Biol. J. Linn. Soc.* 93:709–720. doi:10.1111/j.1095-8312.2007.00905.x.

Apell JN, Gschwend PM. 2016. In situ passive sampling of sediments in the Lower Duwamish Waterway Superfund site: Replicability, comparison with ex situ measurements, and use of data. *Environ. Pollut.* 218:95–101. doi:10.1016/j.envpol.2016.08.023.

Aragón P, Sánchez-Fernández D. 2013. Can we disentangle predator-prey interactions from species distributions at a macro-scale? A case study with a raptor species. *Oikos* 122:64–72. doi:10.1111/j.1600-0706.2012.20348.x.

Araújo MS, Bolnick DI, Layman CA. 2011. The ecological causes of individual specialisation. *Ecol. Lett.* 14:948–958. doi:10.1111/j.1461-0248.2011.01662.x.

Araya-Ajoy YG, Ranke PS, Kvalnes T, Rønning B, Holand H, Myhre AM, Pärn H, Jensen H, Ringsby TH, Sæther BE, et al. 2019. Characterizing morphological (co)variation using structural equation models: Body size, allometric relationships and evolvability in a house sparrow metapopulation. *Evolution (N. Y).* 73:452–466. doi:10.1111/evo.13668.

Baumard P, Budzinski H, Garrigues P, Sorbe J, Burgeot T, Bellocq J. 1998. Concentrations of PAHs (polycyclic aromatic hydrocarbons) in various marine organisms in relation to those in sediments and to trophic level. *Mar. Pollut. Bull.* 36:951–960. doi:10.1016/S0025-326X(98)00088-5.

Beaugrand G, Conversi A, Atkinson A, Cloern J, Chiba S, Fonda-Umani S, Kirby RR, Greene CH, Goberville E, Otto SA, et al. 2019. Prediction of unprecedented biological shifts in the global ocean. *Nat. Clim. Chang.* 9:237–243. doi:10.1038/s41558-019-0420-1.

Bergman J, Lajeunesse M, Motta P. 2017. Teeth penetration force of the tiger shark Galeocerdo cuvier and sandbar shark Carcharhinus plumbeus. *J. Fish Biol.* 91:460–472. doi:10.1111/jfb.13351.

Bolnick DI, Svanbäck R, Fordyce JA, Yang LH, Davis JM, Hulsey CD, Forister ML. 2003. The ecology of individuals: Incidence and implications of individual specialization. *Am. Nat.* 161:1–28. doi:10.1086/343878.

Brooks JM, Wade TL, Kennicut MC, Wiesenburg DA, Wilkinson D, McDonald TJ, McDonald SJ. 1992. Toxic contaminant characterization of aquatic organisms in Galveston Bay: A pilot study. GBNEP-20. Galveston Bay National Estuary Program, Webster, TX, USA.

Buchheister A, Miller TJ, Houde ED. 2017. Evaluating ecosystem-based reference points for Atlantic Menhaden. *Mar. Coast. Fish.* 9:457–478. doi:10.1080/19425120.2017.1360420.

Castro JI. 1996. Biology of the blacktip shark, Carcharhinus limbatus, off the southeastern United States. *Bull. Mar. Sci.* 59:508–522.

Cliff G, Dudley SF. 1991. Sharks caught in the protective gill nets off Natal, South Africa. 4. The bull shark Carcharhinus leucas Valenciennes. *South African J. Mar. Sci.* 10:253–270. doi:10.2989/02577619109504636.

Cooke SJ, Cowx IG. 2004. The role of recreational fishing in global fish crises. *Bioscience* 54:857–859. doi:10.1641/0006-3568(2004)054[0857:trorfi]2.0.co;2.

Cortés E, Manire CA, Hueter RE. 1996. Diet, feeding habits, and diel feeding chronology of the bonnethead shark, Sphyrna tiburo, in southwest Florida. *Bull. Mar. Sci.* 58:353–367. doi:10.1007/s00227-006-0325-1.

Cullen JA, Marshall CD. 2019. Do sharks exhibit heterodonty by tooth position and over ontogeny? A comparison using elliptic Fourier analysis. *J. Morphol.* 280:687–700. doi:10.1002/jmor.20975.

Cullen JA, Marshall CD, Hala D. 2019. Integration of multi-tissue PAH and PCB burdens with biomarker activity in three coastal shark species from the northwestern Gulf of Mexico. *Sci. Total Environ.* 650:1158–1172. doi:10.1016/j.scitotenv.2018.09.128.

Drymon JM, Powers SP, Carmichael RH. 2012. Trophic plasticity in the Atlantic sharpnose shark (Rhizoprionodon terraenovae) from the north central Gulf of Mexico. *Environ. Biol. Fishes* 95:21–35. doi:10.1007/s10641-011-9922-z.

Emerson SB, Greene HW, Charnov EL. 1994. Allometric aspects of predator-prey interactions. In: Ecological Morphology: Integrative Organismal Biology. Chicago: University of Chicago Press. p. 123–139.

Emlen J. 1966. The role of time and energy in food preference. *Am. Nat.* 100:611–617.

Erickson GM, Lappin AK, Vliet KA. 2003. The ontogeny of bite-force performance in American alligator (Alligator mississippiensis). *J. Zool.* 260-:317–327. doi:10.1017/S0952836903003819.

Estes JA, Terborgh J, Brashares JS, Power ME, Berger J, Bond WJ, Carpenter SR, Essington TE, Holt RD, Jackson JBC, et al. 2011. Trophic downgrading of planet earth. *Science* 333:301–306. doi:10.1126/science.1205106.

Figueira WF, Coleman FC. 2010. Comparing landings of United States recreational fishery sectors. *Bull. Mar. Sci.* 86:499–514.

Gallagher A, Kyne P, Hammerschlag N. 2012. Ecological risk assessment and its application to elasmobranch conservation and management. *J. Fish Biol.* 80:1727–48. doi:10.1111/j.1095-8649.2012.03235.x.

Geers TM, Pikitch EK, Frisk MG. 2016. An original model of the northern Gulf of Mexico using Ecopath with Ecosim and its implications for the effects of fishing on ecosystem structure and maturity. *Deep. Res. Part II Top. Stud. Oceanogr.* 129:319–331. doi:10.1016/j.dsr2.2014.01.009.

Gelsleichter J, Manire CA, Szabo NJ, Cortés E, Carlson J, Lombardi-Carlson L. 2005. Organochlorine concentrations in bonnethead sharks (Sphyrna tiburo) from four Florida estuaries. *Arch. Environ. Contam. Toxicol.* 48:474–483. doi:10.1007/s00244-003-0275-2.

Gelsleichter J, Walker CJ. 2010. Pollutant exposure and effects in sharks and their relatives. In: Carrier J, Musick J, Heithaus M, editors. Sharks And Their Relatives II: Biodiversity, Adaptive Physiology, And Conservation. Boca Raton: CRC Press. p. 491–537.

Gelsleichter J, Walsh CJ, Szabo NJ, Rasmussen LEL. 2006. Organochlorine concentrations, reproductive physiology, and immune function in unique

populations of freshwater Atlantic stingrays (Dasyatis sabina) from Florida's St. Johns River. *Chemosphere* 63:1506–1522. doi:10.1016/j.chemosphere.2005.09.011.

Gould SJ. 1966. Allometry and size in ontogeny and phylogeny. *Biol. Rev.* 41:587–640.

Groten JP, Feron VJ, Sühnel J. 2001. Toxicology of simple and complex mixtures. *Trends Pharmacol. Sci.* 22:316–322.

Habegger ML, Motta PJ, Huber DR, Dean MN. 2012. Feeding biomechanics and theoretical calculations of bite force in bull sharks (Carcharhinus leucas) during ontogeny. *Zoology* 115:354–364. doi:10.1016/j.zool.2012.04.007.

Hernandez LP, Motta PJ. 1997. Trophic consequences of differential performance: ontogeny of oral jaw-crushing performance in the sheepshead, Archosargus probatocephalus (Teleostei, Sparidae). *J. Zool.* 243:737–756. doi:10.1111/j.1469-7998.1997.tb01973.x.

Heupel M, Knip D, Simpfendorfer C, Dulvy N. 2014. Sizing up the ecological role of sharks as predators. *Mar. Ecol. Prog. Ser.* 495:291–298. doi:10.3354/meps10597.

Hoffmayer ER, Parsons GR. 2003. Food habits of three shark species from the Mississippi Sound in the northern Gulf of Mexico. *Southeast. Nat.* 2:271–280. doi:10.1656/1528-7092(2003)002[0271:fhotss]2.0.co;2.

Huber DR, Claes JM, Mallefet J, Herrel A. 2009. Is extreme bite performance associated with extreme morphologies in sharks? *Physiol. Biochem. Zool.* 82:20–28. doi:10.1086/588177.

Huber DR, Eason TG, Hueter RE, Motta PJ. 2005. Analysis of the bite force and mechanical design of the feeding mechanism of the durophagous horn shark

Heterodontus francisci. *J. Exp. Biol.* 208:3553–3571. doi:10.1242/jeb.01816.

Huber DR, Weggelaar CL, Motta PJ. 2006. Scaling of bite force in the blacktip shark Carcharhinus limbatus. *Zoology* 109:109–119. doi:10.1016/j.zool.2005.12.002.

Hylland K. 2006. Polycyclic aromatic hydrocarbon (PAH) ecotoxicology in marine ecosystems. *J. Toxicol. Environ. Heal. Part A* 69:109–123. doi:10.1080/15287390500259327.

Incardona JP, Collier TK, Scholz NL. 2004. Defects in cardiac function precede morphological abnormalities in fish embryos exposed to polycyclic aromatic hydrocarbons. *Toxicol. Appl. Pharmacol.* 196:191–205. doi:10.1016/j.taap.2003.11.026.

Islam MS, Tanaka M. 2004. Impacts of pollution on coastal and marine ecosystems including coastal and marine fisheries and approach for management: A review and synthesis. *Mar. Pollut. Bull.* 48:624–649. doi:10.1016/j.marpolbul.2003.12.004.

Johnson LL, Collier TK, Stein JE. 2002. An analysis in support of sediment quality thresholds for polycyclic aromatic hydrocarbons (PAHs) to protect estuarine fish. *Aquat. Conserv. Mar. Freshw. Ecosyst.* 12:517–538. doi:10.1002/aqc.522.

Kannan K, Blankenship AL, Jones PD, Giesy JP. 2000. Toxicity reference values for the toxic effects of polychlorinated biphenyls to aquatic mammals. *Hum. Ecol. Risk Assess.* 6:181–201. doi:10.1080/10807030091124491.

Khairy MA, Weinstein MP, Lohmann R. 2014. Trophodynamic behavior of hydrophobic organic contaminants in the aquatic food web of a tidal river. *Environ. Sci. Technol.* 48:12533–12542. doi:10.1021/es502886n.

Kiszka JJ, Aubail A, Hussey NE, Heithaus MR, Caurant F, Bustamante P. 2015. Plasticity of trophic interactions among sharks from the oceanic south-western Indian Ocean revealed by stable isotope and mercury analyses. *Deep Sea Res. Part I Oceanogr. Res. Pap.* 96:49–58. doi:10.1016/j.dsr.2014.11.006.

Kolmann MA, Huber DR. 2009. Scaling of feeding biomechanics in the horn shark Heterodontus francisci: ontogenetic constraints on durophagy. *Zoology* 112:351–361. doi:10.1016/j.zool.2008.11.002.

Kolmann MA, Huber DR, Motta PJ, Grubbs RD. 2015. Feeding biomechanics of the cownose ray, Rhinoptera bonasus, over ontogeny. *J. Anat.* 227:341–351. doi:10.1111/joa.12342.

Kroetz AM, Drymon JM, Powers SP. 2017. Comparative dietary diversity and trophic ecology of two estuarine mesopredators. *Estuaries and Coasts* 40:1171–1182. doi:10.1007/s12237-016-0188-8.

Lellis-Dibble KA, McGlynn KE, Bigford TE. 2008. Estuarine fish and shellfish species in U.S. commercial and recreational fisheries: Economic value as an incentive to protect and restore estuarine habitat. U.S. Dep. Commerce, NOAA Tech. Memo. NMFS-F/SPO-90.

Livingstone DR. 1998. The fate of organic xenobiotics in aquatic ecosystems: quantitative and qualitative differences in biotransformation by invertebrates and fish. *Comp. Biochem. Physiol. - A Mol. Integr. Physiol.* 120:43–49. doi:10.1016/S1095-6433(98)10008-9.

Lotze HK, Lenihan HS, Bourque BJ, Bradbury RH, Cooke RG, Kay MC, Kidwell SM,

Kirby MX, Peterson CH, Jackson JBC. 2006. Depletion, degradation, and recovery potential of estuaries and coastal seas. *Science* 312:1806–1809. doi:10.1126/science.1128035.

Lyons K, Carlisle A, Preti A, Mull C, Blasius M, O'Sullivan J, Winkler C, Lowe CG. 2013. Effects of trophic ecology and habitat use on maternal transfer of contaminants in four species of young of the year lamniform sharks. *Mar. Environ. Res.* 90:27–38. doi:10.1016/j.marenvres.2013.05.009.

Mara KR, Motta PJ, Huber DR. 2010. Bite force and performance in the durophagous bonnethead shark, Sphyrna tiburo. *J. Exp. Zool. Part A Ecol. Genet. Physiol.* 313:95–105. doi:10.1002/jez.576.

Matich P, Heithaus MR, Layman CA. 2011. Contrasting patterns of individual specialization and trophic coupling in two marine apex predators. *J. Anim. Ecol.* 80:294–305. doi:10.1111/j.1365-2656.2010.01753.x.

McKim JM. 1977. Evaluation of tests with early life stages of fish for predicting long-term toxicity. *J. Fish. Board Canada* 34:1148–1154.

Meador J, Sommers F, Ylitalo G, Sloan C. 2006. Altered growth and related physiological responses in juvenile Chinook salmon (Oncorhynchus tshawytscha) from dietary exposure to polycyclic aromatic hydrocarbons (PAHs). *Can. J. Fish. Aquat. Sci.* 63:2364–2376. doi:10.1139/f06-127.

Meador J, Stein J, Reichert W, Varanasi U. 1995. Bioaccumulation of polycyclic aromatic hydrocarbons by marine organisms. *Rev. Environ. Contam. Toxicol.* 143:79–165. doi:10.1007/978-1-4612-2542-3_4.

Mull CG, Lyons K, Blasius ME, Winkler C, O'Sullivan JB, Lowe CG. 2013. Evidence of maternal offloading of organic contaminants in white sharks (Carcharodon carcharias). *PLoS One* 8:e62886. doi:10.1371/journal.pone.0062886.

Olin JA, Beaudry M, Fisk AT, Paterson G. 2014. Age-related polychlorinated biphenyl dynamics in immature bull sharks (Carcharhinus leucas). *Environ. Toxicol. Chem.* 33:35–43. doi:10.1002/etc.2402.

van der Oost R, Beyer J, Vermeulen NPE. 2003. Fish bioaccumulation and biomarkers in environmental risk assessment: A review. *Environ. Toxicol. Pharmacol.* 13:57–149. doi:10.1016/S1382-6689(02)00126-6.

Oziolor EM, Apell JN, Win ZC, Back JA, Usenko S, Matson CW. 2018. Polychlorinated biphenyl (PCB) contamination in Galveston Bay, Texas: Comparing concentrations and profiles in sediments, passive samplers, and fish. *Environ. Pollut.* 236:609–618. doi:10.1016/j.envpol.2018.01.086.

Pélabon C, Bolstad GH, Egset CK, Cheverud JM, Pavlicev M, Rosenqvist G. 2013. On the relationship between ontogenetic and static allometry. *Am. Nat.* 181:195–212. doi:10.1086/668820.

Pélabon C, Firmat C, Bolstad GH, Voje KL, Houle D, Cassara J, Rouzic A Le, Hansen TF. 2014. Evolution of morphological allometry. *Ann. N. Y. Acad. Sci.* 1320:58–75. doi:10.1111/nyas.12470.

Plumlee JD, Wells RD. 2016. Feeding ecology of three coastal shark species in the northwest Gulf of Mexico. *Mar. Ecol. Prog. Ser.* 550:163–174. doi:10.3354/meps11723.

Preisser EL, Bolnick DI, Benard ME. 2005. Scared to death? The effects of intimidation and consumption in predator-prey interactions. *Ecology* 86:501–509.

Robinson KL, Ruzicka JJ, Hernandez FJ, Graham WM, Decker MB, Brodeur RD, Sutor M. 2015. Evaluating energy flows through jellyfish and gulf menhaden (Brevoortia patronus) and the effects of fishing on the northern Gulf of Mexico ecosystem. *ICES J. Mar. Sci.* 72:2301–2312.

Rosenblatt AE, Nifong JC, Heithaus MR, Mazzotti FJ, Cherkiss MS, Jeffery BM, Elsey RM, Decker RA, Silliman BR, Guillette LJ, et al. 2015. Factors affecting individual foraging specialization and temporal diet stability across the range of a large "generalist" apex predator. *Oecologia* 178:5–16. doi:10.1007/s00442-014-3201-6.

Rossman S, Ostrom PH, Gordon F, Zipkin EF. 2016. Beyond carbon and nitrogen: guidelines for estimating three-dimensional isotopic niche space. *Ecol. Evol.* 6:2405–2413. doi:10.1002/ece3.2013.

Ruehl CB, DeWitt TJ. 2007. Trophic plasticity and foraging performance in red drum, Sciaenops ocellatus (Linnaeus). *J. Exp. Mar. Bio. Ecol.* 349:284–294. doi:10.1016/j.jembe.2007.05.017.

Scharf FS, Juanes F, Rountree RA. 2000. Predator size - prey size relationships of marine fish predators: Interspecific variation and effects of ontogeny and body size on trophic-niche breadth. *Mar. Ecol. Prog. Ser.* 208:229–248. doi:10.3354/meps208229.

Schoener TW. 1971. Theory of feeding strategies. *Annu. Rev. Ecol. Syst.* 2:369–404.

Spurgeon DJ, Jones OAH, Dorne JLCM, Svendsen C, Swain S, Stürzenbaum SR. 2010.

Systems toxicology approaches for understanding the joint effects of environmental chemical mixtures. *Sci. Total Environ.* 408:3725–3734. doi:10.1016/j.scitotenv.2010.02.038.

Steevens JA, Reiss MR, Pawlisz A V. 2005. A methodology for deriving tissue residue benchmarks for aquatic biota: A case study for fish exposed to 2,3,7,8-tetrachlorodibenzo-p-dioxin and equivalents. *Integr. Environ. Assess. Manag.* 1:142–151. doi:10.1897/IEAM_2004a-014.1.

Svanbäck R, Bolnick DI. 2007. Intraspecific competition drives increased resource use diversity within a natural population. *Proc. R. Soc. B Biol. Sci.* 274:839–844. doi:10.1098/rspb.2006.0198.

Svanbäck R, Quevedo M, Olsson J, Eklöv P. 2015. Individuals in food webs: the relationships between trophic position, omnivory and among-individual diet variation. *Oecologia* 178:103–114. doi:10.1007/s00442-014-3203-4.

Taylor DL, Kutil NJ, Malek AJ, Collie JS. 2014. Mercury bioaccumulation in cartilaginous fishes from Southern New England coastal waters: Contamination from a trophic ecology and human health perspective. *Mar. Environ. Res.* 99:20–33. doi:10.1016/j.marenvres.2014.05.009.

Waycott M, Duarte CM, Carruthers TJB, Orth RJ, Dennison WC, Olyarnik S, Calladine A, Fourqurean JW, Heck KL, Hughes AR, et al. 2009. Accelerating loss of seagrasses across the globe threatens coastal ecosystems. *Proc. Natl. Acad. Sci.* 106:12377–12381. doi:10.1073/pnas.0905620106.

Weijs L, Briels N, Adams DH, Lepoint G, Das K, Blust R, Covaci A. 2015. Maternal

transfer of organohalogenated compounds in sharks and stingrays. *Mar. Pollut. Bull.* 92:59–68. doi:10.1016/j.envres.2014.12.022.

Werry J, Lee S, Otway N, Hu Y, Sumpton W. 2011. A multi-faceted approach for quantifying the estuarine-nearshore transition in the life cycle of the bull shark, Carcharhinus leucas. *Mar. Freshw. Res.* 62:1421–1431. doi:10.1071/MF11136.

Whitenack L, Motta P. 2010. Performance of shark teeth during puncture and draw: implications for the mechanics of cutting. *Biol. J. Linn. Soc.* 100:271–286.

Wilga C, Motta P. 2000. Durophagy in sharks: feeding mechanics of the hammerhead Sphyrna tiburo. *J. Exp. Biol.* 203:2781–2796.

Woltering DM. 1984. The growth response in fish chronic and early life stage toxicity tests: A critical review. *Aquat. Toxicol.* 5:1–21. doi:10.1016/0166-445X(84)90028-6.

Zimmerman RJ, Minello TJ, Rozas LP. 2002. Salt marsh linkages to productivity of penaeid shrimps and blue crabs in the northern Gulf of Mexico. In: Weinstein M, Kreeger D, editors. Concepts and Controversies in Tidal Marsh Ecology. Dordrecht: Springer. p. 293–314.